

MASTER
NEUROBIOLOGY

EEG mapping of brain activity resulting from stimulation with brand logos

Diogo Filipe Prada da Silva

M

2020



UNIVERSIDADE DO PORTO

FACULDADE DE MEDICINA

Dissertação de candidatura ao grau de Mestre em Neurobiologia

Orientador: Doutor José Paulo Marques dos Santos

EEG MAPPING OF BRAIN ACTIVITY RESULTING
FROM SIMULATION WITH BRAND LOGOS

DIOGO FILIPE PRADA DA SILVA

2020

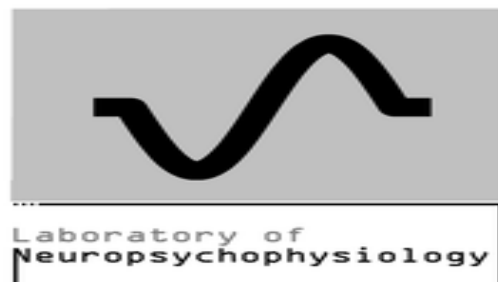


Table of Contents

<i>Agradecimientos</i>	9
<i>Preamble</i>	13
<i>Abstract</i>	16
<i>Introduction</i>	19
1. Scientific questions	20
2. Perception of human faces	21
a. The N170 ERP	22
b. The Fusiform gyrus	24
3. Perception of brand logos and symbols	26
4. Recollection and familiarity related to a visual stimulus	27
5. The cognitive process of preference	29
<i>Objectives</i>	33
Part A	34
Part B	35
<i>Material and Methods</i>	36
1. Part A	37
1.1. Visual stimuli set definition	37
1.2. Stimulus presentation.....	39
1.3. Participants selection.....	39
1.4. Ethical procedures.....	40
2. Part B	41
2.1. Study structure	41
2.1.1. First session - Subjects screening	41
2.1.2. Stimuli selection	41
2.1.3. Stimulus presentation.....	42
2.1.4. Second session - EEG data collection.....	43
2.2. Subjects	43
2.3. Ethical procedures.....	44
2.4. EEG data analysis	44
2.5. Global field potential and global dissimilarity calculations.....	45
2.6. EEG source localization.....	46

2.7. Statistical analysis	47
Results	48
1. Analysis of the activity in the Regions of Interest	49
2. Analysis of the event-related potentials	55
2.1. The N100 ERP	55
2.2. The N200 / P300 ERPs	61
2.3. The LPP ERP	67
3. Analysis of neural sources of brand valuation	73
Discussion	92
1. Event-related potentials associated with the expression of preference	93
2. Source of the brain activity related to the expression of preference	96
Conclusions and Future Perspectives	98
References	101
Appendix A – Visual stimuli	107
Part A	108
Known Brand Logos	108
Unknown Brand Logos	113
Known faces	118
Unknown Faces	123
Known objects	128
Unknown objects	134
Part B	139
Brand logos	139
Appendix B – Statistical Analysis	153
Statistical analysis of the lorGFP elicited in IC2 and IC7	154
Statistical analysis of the GFP	157
Appendix C – IC2 coordinates	169
Appendix D - IC7 coordinates	174
Appendix E – Hydrocel Geodesic Sensor Net 128 Channel Map	178

Table of figures

Figure 1 Table containing the ERPs related to face perception 21

Figure 2 Anatomical location of the fusiform gyrus. 24

Figure 3 Scheme of stimulus presentation. 39

Figure 4 Scheme of stimulus presentation. 43

Figure 5 Average lorGFP values of preferred and indifferent brands, in IC2 49

Figure 6 Average lorGFP values of preferred and fictitious brands, in IC2..... 50

Figure 7 Average lorGFP values of indifferent and fictitious brands, in IC2..... 51

Figure 8 Average lorGFP values of preferred and indifferent brands, in IC7 52

Figure 9 Average lorGFP values of preferred and fictitious brands, in IC7..... 53

Figure 10 lorGFP values of indifferent and fictitious brands, in IC7..... 54

Figure 11 Average potential measured, for the preferred and indifferent categories, in the E70..... 55

Figure 12 Average potential measured, for the preferred and fictitious categories, in the E70 electrode 55

Figure 13 Average potential measured, for the indifferent and fictitious categories, in the E70 electrode 56

Figure 14 Average potential measured, for the preferred and indifferent categories, in the E75 electrode 57

Figure 15 Average potential measured, for the preferred and fictitious categories, in the E75 electrode 57

Figure 16 Average potential measured, for the indifferent and fictitious categories, in the E75 electrode 58

Figure 17 Average potential measured, for the preferred and indifferent categories, in the E83 electrode 59

Figure 18 Average potential measured, for the preferred and fictitious categories, in the E83 electrode 59

Figure 19 Average potential measured, for the indifferent and fictitious categories, in the E83 electrode 60

Figure 20 Average potential measured, for the preferred and indifferent categories, in the E24 electrode 61

Figure 21 Average potential measured, for the preferred and fictitious categories, in the E24 electrode 61

Figure 22 Average potential measured, for the indifferent and fictitious categories, in the E24 electrode 62

Figure 23 Average potential measured, for the preferred and indifferent categories, in the E11 electrode 63

Figure 24 Average potential measured, for the preferred and fictitious categories, in the E11 electrode 63

Figure 25 Average potential measured, for the indifferent and fictitious categories, in the E11 electrode ... 64

Figure 26 Average potential measured, for the preferred and indifferent categories, in the E124 electrode .. 65

Figure 27 Average potential measured, for the preferred and fictitious categories, in the E124 electrode..... 65

Figure 28 Average potential measured, for the indifferent and fictitious categories, in the E124 electrode .. 66

Figure 29 Average potential measured, for the preferred and indifferent categories, in the P3 electrode 67

Figure 30 Average potential measured, for the preferred and fictitious categories, in the E52 electrode 67

Figure 31 Average potential measured, for the indifferent and fictitious categories, in the E52 electrode 68

Figure 32 Average potential measured, for the preferred and indifferent categories, in the E62 electrode 69

Figure 33 Average potential measured, for the preferred and fictitious categories, in the E62 electrode 69

Figure 34 Average potential measured, for the indifferent and fictitious categories, in the E62 electrode 70

Figure 35 Average potential measured, for the preferred and indifferent categories, in the E92 electrode 71

Figure 36 Average potential measured, for the preferred and fictitious categories, in the E92 electrode 71

Figure 37 Average potential measured, for the indifferent and fictitious categories, in the E92 electrode 72

Figure 38 Average GFP for the preferred and indifferent categories..... 73

Figure 39 Average eLORETA image of neural source for preferred brand logos at 28 ms..... 73

Figure 40 Average eLORETA image of the brain source for preferred brand logos at 30 ms..... 74

Figure 41 Average eLORETA image of the brain source for preferred brand logos at 32 ms..... 74

Figure 42 Average eLORETA image of neural source for indifferent brand logos at 28 ms..... 74

Figure 43 Average eLORETA image of the brain source for indifferent brand logos at 30 ms..... 75

Figure 44 Average eLORETA image of the brain source for indifferent brand logos at 32 ms..... 75

Figure 45 Average potential registered in the occipital electrodes for the “preferred” brand logos, from 0 ms to 100 ms of latency. 76

Figure 46 Average potential registered in the occipital electrodes for the “indifferent” brand logos, from 0 ms to 100 ms of latency. 76

Figure 47 Average potential registered in the occipital electrodes for the “fictitious” brand logos, from 0 ms to 100 ms of latency. 77

Figure 48 Average GFP for the preferred and fictitious categories 78

Figure 49 Average eLORETA image of the brain source for preferred brand logos at 376 ms..... 78

Figure 50 Average eLORETA image of the brain source for preferred brand logos at 378 ms. 79

Figure 51 Average eLORETA image of the brain source for preferred brand logos at 380 ms..... 79

Figure 52 Average eLORETA image of the brain source for fictitious brand logos at 376 ms. 79

Figure 53 Average eLORETA image of the brain source for fictitious brand logos at 378 ms. 80

Figure 54 Average eLORETA image of the brain source for fictitious brand logos at 380 ms.	80
Figure 55 Average GFP for the indifferent and fictitious categories	81
Figure 56 Average eLORETA image of the brain source for indifferent brand logos at 370 ms.....	81
Figure 57 Average eLORETA image of the brain source for indifferent brand logos at 372 ms.....	82
Figure 58 Average eLORETA image of the brain source for indifferent brand logos at 374 ms.....	82
Figure 59 Average eLORETA image of the brain source for fictitious brand logos at 370 ms.	82
Figure 60 Average eLORETA image of the brain source for fictitious brand logos at 372 ms.	83
Figure 61 Average eLORETA image of the brain source for fictitious brand logos at 374 ms.	83
Figure 62 Average potential registered in the occipital electrodes for the “preferred” brand logos from 300 ms to 400 ms of latency.	84
Figure 63 Average potential registered in the occipital electrodes for the “indifferent” brand logos from 300 ms to 400 ms of latency.	84
Figure 64 Average potential registered in the occipital electrodes for the “fictitious” brand logos from 300 ms to 400 ms of latency.	85
Figure 65 Global dissimilarity values for the preferred and the indifferent categories.....	86
Figure 66 Brain topographic map at 220 ms (max. DISS), for the preferred and for the indifferent categories	86
Figure 67 Brain topographic map at 140 ms (min. DISS), for the preferred and for the indifferent categories	87
Figure 68 Brain topographic map at 30 ms (max. statistical effect), for the preferred and for the indifferent categories	87
Figure 69 Global dissimilarity values for the preferred and the fictitious categories	88
Figure 70 Brain topographic map at 228 ms (max. DISS), for the preferred and for the fictitious categories	88
Figure 71 Brain topographic map at 160 ms (min. DISS), for the preferred and for the fictitious categories	89
Figure 72 Brain topographic map at 378 ms (max. statistical effect), for the preferred and for the fictitious categories	89
Figure 73 Global dissimilarity values for the indifferent and the fictitious categories	90
Figure 74 Brain topographic map at 224 ms (max. DISS), for the indifferent and for the fictitious categories	90
Figure 75 Brain topographic map at 154 ms (min. DISS), for the indifferent and for the fictitious categories	91
Figure 76 Brain topographic map at 372 ms (max. statistical DISS), for the indifferent and for the fictitious categories	91
Figure 77 Paired t-test results for the statistical analysis of lorGFP elicited by the “preferred” brand logos versus the lorGFP elicited by the “indifferent” brand logos in region of IC2.	154
Figure 78 Paired t-test results for the statistical analysis of lorGFP elicited by the “preferred” brand logos versus the lorGFP elicited by the “fictitious” brand logos in region of IC2.....	154
Figure 79 Paired t-test results for the statistical analysis of lorGFP elicited by the “indifferent” brand logos versus the lorGFP elicited by the “fictitious” brand logos in region of IC2. The value of α was set to 0,05.	155
Figure 80 Paired t-test results for the lorGFP elicited by the “preferred” brand logos versus the lorGFP elicited by the “indifferent” brand logos in the region of IC7.	155
Figure 81 Paired t-test results for the lorGFP elicited by the “preferred” brand logos versus the lorGFP elicited by the “fictitious” brand logos in the region of IC7.....	156
Figure 82 Paired t-test results for the lorGFP elicited by the “indifferent” brand logos versus the lorGFP elicited by the “fictitious” brand logos in the region of IC7.....	156
Figure 83 Paired t-test results for the GFP elicited by the “preferred” brands versus the GFP elicited by the “indifferent” brands.	157
Figure 84 Paired t-test results for the GFP elicited by the “preferred” brands versus the GFP elicited by the “fictitious” brands.....	157
Figure 85 Paired t-test results for the GFP elicited by the “indifferent” brands versus the GFP elicited by the “fictitious” brands.....	158
Figure 86 Paired t-test map produced in eLORETA for “Preferred vs Indifferent” at 30 ms. t-value (left inferior occipital gyrus) = -0,246.	159
Figure 87 Paired t-test map produced in eLORETA for “Preferred vs Indifferent” at 28 ms. t-value (left inferior occipital gyrus) = -0,596.	159
Figure 88 Paired t-test map produced in eLORETA for “Preferred vs Indifferent” at 32 ms. t-value (left middle temporal gyrus) = 0,915.	159

Figure 89 Paired t-test map produced in eLORETA for “Preferred vs Indifferent” at 32 ms. t-value (left middle temporal gyrus) = -0,0702.....	160
Figure 90 Paired t-test map produced in eLORETA for “Preferred vs Indifferent” at 28 ms. The maximum t-value was 2,98 at the superior parietal lobule.....	161
Figure 91 Paired t-test map produced in eLORETA for “Preferred vs Indifferent” at 30 ms. The maximum t-value was -2,39 at the inferior temporal gyrus.....	161
Figure 92 Paired t-test map produced in eLORETA for “Preferred vs Indifferent” at 32 ms. The maximum t-value was 2,13 at the superior parietal lobule.....	161
Figure 93 Paired t-test map produced in eLORETA for “Preferred vs Fictitious” at 378 ms. t-value (left inferior occipital gyrus) = 0,686.....	162
Figure 94 Paired t-test map produced in eLORETA for “Preferred vs Fictitious” at 376 ms. t-value (left inferior occipital gyrus) = 1,360.....	162
Figure 95 Paired t-test map produced in eLORETA for “Preferred vs Fictitious” at 380 ms. t-value (left inferior occipital gyrus) = -0,522.....	162
Figure 96 Paired t-test map produced in eLORETA for “Preferred vs Fictitious” at 376 ms. The maximum t-value was 5,09 at the superior frontal gyrus.....	163
Figure 97 Paired t-test map produced in eLORETA for “Preferred vs Fictitious” at 378 ms. The maximum t-value was 2,56 at the inferior parietal lobule.....	163
Figure 98 Paired t-test map produced in eLORETA for “Preferred vs Fictitious” at 380 ms. The maximum t-value was -3,96 at the superior temporal gyrus.....	163
Figure 99 Paired t-test map produced in eLORETA for “Indifferent vs Fictitious” at 370 ms. t-value (left inferior occipital gyrus) = -1,00.....	164
Figure 100 Paired t-test map produced in eLORETA for “Indifferent vs Fictitious” at 370 ms. t-value (left inferior occipital gyrus) = -1,89.....	164
Figure 101 Paired t-test map produced in eLORETA for “Indifferent vs Fictitious” at 372 ms. t-value (left inferior occipital gyrus) = -1,61.....	164
Figure 102 Paired t-test map produced in eLORETA software for “Indifferent vs Fictitious” at 372 ms. t-value (left cuneus) = -1,67.....	165
Figure 103 Paired t-test map produced in eLORETA for “Indifferent vs Fictitious” at 374 ms. t-value (left inferior occipital gyrus) = 0,549.....	165
Figure 104 Paired t-test map produced in eLORETA for “Indifferent vs Fictitious” at 374 ms. t-value (left lingual gyrus) = 0,121.....	165
Figure 106 Paired t-test map produced in eLORETA for “Indifferent vs Fictitious” at 370 ms. The maximum t-value was - 4,40 at the right inferior temporal gyrus.....	166
Figure 105 Paired t-test map produced in eLORETA for “Indifferent vs Fictitious” at 372 ms. Maximum t-value was -4,50 at tight fusiform gyrus.....	166
Figure 107 Paired t-test map produced in eLORETA for “Indifferent vs Fictitious” at 374 ms. The maximum t-value was 2,98 at the superior frontal gyrus.....	166
Figure 108 Paired t-test results for the statistical analysis of the potential registered in occipital electrodes when comparing the “preferred” brand logos brain activity with the “indifferent” brand logos brain activity, between 0 and 100 ms.....	167
Figure 109 Paired t-test results for the statistical analysis of the potential registered in occipital electrodes when comparing the “preferred” brand logos brain activity with the “fictitious” brand logos brain activity, between 300 and 400 ms.....	167
Figure 110 Paired t-test results for the statistical analysis of the potential registered in occipital electrodes when comparing the “indifferent” brand logos brain activity with the “fictitious” brand logos brain activity, between 300 and 400 ms.....	168
Figure 111 Topographic map highlighting the electrodes, circled in red, that presented significant statistical effect between preferred and indifferent brand logos, starting at 24 ms and ending at 36 ms.....	168
Figure 112 IC2 region retrieved from Marques dos Santos, Moutinho, and Castelo-Branco (2014). Axial cut (z = -12).....	173
Figure 113 IC7 region retrieved from Marques dos Santos et al. (2014). Axial cut (z = -12).....	177

List of abbreviations

- PAD – Pleasure-Arousal-Dominance
- SAM – Self-Assessment Manikin
- IC – Independent Component
- fmri – functional magnetic resonance imaging
- EEG – Electroencephalography
- ERP – Event-related potential
- LPC – Late parietal component
- vmPFC – Ventromedial prefrontal cortex
- LPP – Late positive potential
- MoCA – Montreal Cognitive Assessment
- GFP – Global Field Power
- lorGFP – Loreta Global Field Power
- DISS – Global dissimilarity
- eLoreta – Exact low-resolution brain electromagnetic tomography

Agradecimientos

Existe sempre o momento indicado para fazer os devidos agradecimentos a todos os que marcaram presença neste percurso. Aqui se segue o meu.

Aos meus pais, as minhas pedras basilares, não só neste momento, mas durante toda a minha Vida. Graças aos seus sacrifícios foi-me dada a oportunidade de avançar na minha formação, marcando sempre presença neste percurso, no qual, por várias vezes, deram-me os melhores conselhos quando tinha importantes decisões a tomar. Tendo sido um projeto abalado por inúmeras contrariedades, a sua presença, as suas palavras, a sua serenidade e o seu carinho fizeram com que os contratempos fossem sempre ultrapassados, fazendo com que estes não fossem suficientemente desmotivadores para me levar a tomar uma decisão mais radical relativamente ao meu futuro. Nunca me faltaram com nada, conto com eles todos os dias, e eles comigo, como assim espero, para que, em conjunto, consigamos todos alcançar a melhor Vida possível. Para eles não existem nem palavras, nem extensos textos para simbolizar o valor que têm na minha Vida. Ser-lhes-ei eternamente grato por tudo o que sou e tenho. Agradeço!

Ao meu orientador, Doutor José Paulo Marques dos Santos, pelo seu papel fundamental na orientação na minha dissertação de mestrado. Perante o desafio enorme que todo este projeto constituiu, nunca nos arredamos do desafio até ele estar devidamente concluído. Perante adversidades, seja quando confrontados pelas questões da Comissão de Ética, como também com a introdução titubeante do novo RGPD na comunidade científica, como, por fim, termos sido todos atingidos pela calamidade social e sanitária do COVID-19, o projeto teve de sofrer diversas modificações, umas mais significativas que outras, mas que, em conjunto, com maior serenidade e experiência partilhada, foi possível chegar ao final com o trabalho realizado. Pode não ter sido fácil conciliar a nossa ação, em determinados momentos, mas o essencial foi atingido no final, e por isso estou-lhe profundamente agradecido, por toda a ajuda, compreensão, e mentoria durante todo este percurso. Desejo-lhe os maiores sucessos, tanto pessoais como profissionais. Aproveito também para agradecer à Diana Correia pela contribuição essencial que teve para este projeto.

A todos os membros do Laboratório de Neuropsicofisiologia, com o devido destaque ao Professor Doutor Fernando Barbosa, ao Tiago Paiva, à Rita Pasion e à Andreia Azeredo, por me terem recebido, da melhor forma possível, no laboratório, mostrando-se

sempre disponíveis para me auxiliarem, tanto na execução das tarefas laboratoriais, como nas importantes elucidações relativamente a diferentes conceitos tanto práticos, como teóricos. Ao Professor Doutor Fernando Barbosa, pela sua pronta disponibilização em acolher o meu projeto no Laboratório de Neuropsicofisiologia, e pela retidão com que nos foi colocando a par de todas as alterações inevitáveis que a situação do Covid-19 veio trazer ao funcionamento do laboratório. Ao Tiago Paiva, por ter sido uma presença fundamental neste projeto, tanto a nível académico como a nível pessoal. Pela total disponibilidade em me acompanhar na construção do projeto, e com a sugestão de importantes alterações. Pela ajuda prestada ao ensinar-me as diferentes técnicas que teria de executar no laboratório. Pela palavra amiga em todos os momentos de maior pressão durante as diferentes peripécias do projeto. Pela orientação em importantes momentos de tomada de decisão. No fundo, por todo o companheirismo e apoio que me mantiveram à tona durante todo este projeto. Ficar-te-ei sempre grato, e estarei disponível para te auxiliar sempre que precisares de mim. Desejo-te os maiores sucessos tanto a nível pessoal, como ao nível profissional. À Rita Pasion, por me ter acolhido da melhor possível, permitindo-me acompanhar, de perto, os seus projetos para que eu pudesse desenvolver a minha aptidão em diferentes técnicas laboratoriais. Pelas suas palavras atenciosas, que me deixaram sempre à vontade de transmitir as dúvidas que foram surgindo ao longo de todo processo. Desejo-te igualmente os maiores sucessos pessoais e profissionais possíveis. À Andreia Azeredo, pela pronta disponibilidade para me ajudar a administrar os testes psicológicos previstos no projeto. Uma palavra final de agradecimento a todos os elementos com que me cruzei no Laboratório de Neuropsicofisiologia, pela excelente experiência vivida, desejando-lhes os maiores sucessos para as suas vidas.

Ao Doutor Carlos Reguenga, que no seu papel institucional como diretor do mestrado de Neurobiologia, ao qual pertença, e para o qual agora presto provas, por sempre se ter mostrado disponível para acolher as minhas reservas e preocupações, fornecendo-me conselhos e orientações para que pudesse tomar as melhores decisões possíveis ao longo de todo este percurso. Agradeço-lhe por tudo isto e deixo aqui expresso o meu desejo dos melhores sucessos, tanto para a nível pessoal, como a nível profissional.

Aos meus amigos mais próximos, Ana Marques, Beatriz Silva, Francisco Lopes, Filipa Curinha, João Ribeiro, Marta Almeida, Néilson Carvalho, Patrícia Oliveira, Raquel Pinto, Sofia Santos, Telma Costa, Telma Filipa, Tiago Almeida e Tiago Gonçalves. Todos

marcam a minha Vida, do seu modo especial, e todos participaram neste projeto comigo, seja através das suas perguntas e curiosidades, que me colocaram durante os nossos diferentes encontros, seja por me emprestarem a sua atenção e amizade nos momentos em que mais precisei do seu apoio. E, no fundo, para que o projeto pudesse correr da melhor forma possível, a presença de todos foi essencial. Mais uma vez, palavras valem de pouco para representar o valor que todos trazem à minha Vida. Maiores sucessos para todos vocês, é o que eu vos desejo.

Aos meus colegas de mestrado, com os quais pude partilhar excelentes momentos durante todo este mestrado, e a quem desejo a maior das fortunas, para que o futuro lhes possa trazer, tanto a nível pessoal, como a nível profissional, os maiores sucessos.

Ao resto da minha família, que sempre se manteve atenta ao meu estado de espírito, incentivando-me, nos momentos mais complicados, para que continuasse e concluísse, com sucesso, este patamar no meu percurso académico. Que continue a poder contar com eles, da mesma forma que eles podem contar comigo para os desafios na Vida.

Ao meu psicólogo, Doutor José Ferreira, por me ter acompanhado durante uma parte significativa deste meu projeto, auxiliando-me na gestão de expectativas, na gestão de stress e na minha resiliência emocional, para que, no final, pudesse concluir este projeto da melhor forma possível.

Preamble

The scientific project that supports my master's thesis has suffered significant changes since the first draft, which was scrutinized, and evaluated, at the end of the first year of the master's. That should be considered as a natural development of the master's thesis, since early results may suggest more adequate approaches for the project. However, this particular master's thesis went through several challenges that led to an important decision. In the early stages of the project, it was necessary to submit it to the revision by the Comissão de Ética para a Saúde do Centro Hospitalar de São João / Faculdade de Medicina da Universidade do Porto. Several reviews were needed until the project was fully accepted and authorized by the Comissão de Ética and by the board of the Faculdade de Medicina. This process took a few months, putting the project on hold until its completion. After this one, a new challenge emerged. Taking into account that the initial project requested the participation of volunteers, it was necessary the evaluation by Unidade de Proteção de Dados da Universidade do Porto, to verify the proper fulfillment of the recently implemented Regulamento Geral sobre a Proteção de Dados (RGPD). Since this regulation had been recently updated, new procedures were added, and a formal meeting was requested to further scrutinize the project. After that meeting, an additional email exchange was necessary to conclude the process. This procedure took a few months from the project, and lead to several changes on it. In the few time that remained until the master's thesis delivery deadline, several other practical issues emerged and the time that remained wasn't enough to present a well-done master's thesis. So, I made the decision and added a new year to my master's degree. We took this opportunity to make several changes that we considered advantageous, after several analysis of the literature on the topics covered and started preparing the new approach. However, when everything was ready and we were about to start recruiting volunteers to carry out the first phase of the project, dedicated to improving the protocol used, all the uncertainty surrounding the Covid-19 pandemic began. After a short time, the expected occurred and the national quarantine was decreed and the entire project was suspended, with no expected resumption date. Considering all the impact that the situation of Covid had on this year's calendar, a new important decision was made. Seeing that we couldn't perform the data collections, since the Laboratório de Neuropsicofisiologia had its operation reduced to the minimum, I needed to find an alternative for my master's thesis. With the guidance of my adviser, Doutor José Paulo Marques dos Santos, I oriented my thesis in a different direction. José

Santos had collected data, obtained during a previous master's thesis, belonging to the student Diana Correia, that had not yet been analyzed. Since my master's thesis project was on a similar line of investigation as Diana's project, we decided that I should move forward with this data, analyzing it and extracting the respective results to conclude my master's thesis.

However, all the work that I prepared before the forced stop provoked by the Covid-19 pandemic shouldn't be absent from this master's thesis. Thus, for this decision to be harmoniously integrated into this document, and to facilitate the reading and interpretation of its content, it was decided that all the work done under my original master's thesis project would be identified with the tag "Part A" and all the work done related to Diana's project would be identified with the tag "Part B".

It is expected that this editorial decision will be understood in the face of everything that happened during the entire process described during this preamble.

Abstract

Preference is the result of a cognitive process that allows a subject to discriminate between two or more options that are made available for him to choose from. For Neurobiology and Cognitive Neuroscience, studying the preference mechanism helps to better comprehend the foundations of decision-making mechanisms. Studies that aimed to comprehend the impact of preference on consumer behaviour have founded two models for decision making: the behavioral theory, which emphasizes the intrinsic properties of the stimulus itself, properties that create specific cognitive responses in the subject, shaping his decision; the utility theory, which emphasizes the internal cognitive states of the subject which allows him to determine the value of novel/old stimuli before making a decision. Diverse neural sources have been pointed out, among which stands out the ventromedial prefrontal cortex, a brain structure that is associated with elaborate cognitive processes, thus setting the timing for this valuation process to the later stages of stimulus processing, more specifically, at the moment of its semantic comprehension. However, a recent study created an alternative hypothesis that rooted the individual's discriminatory capacity, guided by his preference, in structures that are known as visual and visual-associative areas of the brain, such as the fusiform gyrus. To strengthen the evidence in favor of this new hypothesis, this experiment was set to determine the timing of this discriminatory process and the involvement of the visual areas in it.

An EEG protocol was built using brand logos as the target stimulus. From a pool of 200 brand logos, 70 were individually picked by each subject. These were divided into two categories: preferred and indifferent. To close the stimuli set, 35 fictitious brand logos were added. The EEG data was used to verify specific event-related potentials and to calculate the GFP. To determine the neural sources of the discrimination between the three categories, electrophysiological data was introduced into eLORETA software.

Activity in both independent components, IC2 and IC7, demonstrated statistically significant differences between all experimental conditions. In line with these results, the main neural source retrieved for the different categories, at statistically significant moments, was the left inferior occipital gyrus. The latency in which statistically significant differences between categories varied between comparison groups. While the difference between the GFP elicited by preferred and indifferent brand logos occurred before 100 ms, this difference between preferred and fictitious, and indifferent and fictitious occurred after 300 ms.

The results obtained in this experiment corroborate the hypothesis set at the start, since neural sources pointed out the role of visual processing structures in the valuation of brand logos. Another conclusion, obtained through time analysis of GFP for preferred and indifferent brand logos, is that the discrimination based on preference may occur at early stages of cognition, contrary to what is generally described, which is that decision making processes at later stages of cognition.

Keywords: brand valuation; brand logos; preference; fusiform; EEG

Introduction

1. Scientific questions

A scientific question emerged from Marques dos Santos et al. (2014) study, where subjects were asked to passively visualize while performing functional magnetic resonance imaging (fMRI), three categories of visual stimuli: human faces, objects, and brand logos, all with a caption associated. The “brand logo” category was the focus of this study. So, before the fMRI session, subjects were asked to participate in a preliminary session where the investigator requested the subjects to evaluate a set of 200 logs using the Pleasure – Arousal – Dominance scale (PAD) (J. Russell & A. Mehrabian, 1977) and the Self Assessment Manikin (SAM) (Morris, 1995). This individual evaluation resulted in the constitution of two subclasses of brand logos: preferred and indifferent. The logos that were classified as highly arousing and highly pleasurable, by the subject, were attributed to the preferred brand logo subclass. The logos that were classified with lower arousal values and having null pleasure value (pleasure value = 0, in a scale that goes from -2 to 2) were attributed to the indifferent brand logo subclass. The fMRI data were analyzed, and several regions of interest, involved in the task, were determined. Then an Independent Component Analysis was made, and it outputted 173 independent components. These 173 independent components were used to build a matrix that was then imputed to an Artificial Neural Network (ANN) built with 6 nodes. The ANN was then used to perform a classification task where it classified the input data into the same four categories presented to the subject: human faces, preferred brand logo, indifferent brand logo, and objects. From the 6 nodes that constituted the ANN, 2 demonstrated results that could, alone, discriminate the input between these 4 classes. From these two nodes, it was possible to determine the independent components (ICs) that mostly contributed to the ability of the ANN to classify the input. These ICs presented visual and visual associative brain areas as the most participating brain regions on the discrimination task. Yet, the detailed spatial information presented more relevant information. In both ICs, one of the major active structures was the fusiform gyrus, a visual associative brain structure, to which diverse visual categorization capacities are attributed to. The fusiform gyrus counts with different known areas, such as the fusiform face area, known for face cognition (N. Kanwisher, J. McDermott, & M. M. Chun, 1997), and the parahippocampal gyrus, known for topographic integration (Epstein, Harris, Stanley, & Kanwisher, 1999).

Assuming these cognitive capacities for visual discrimination, the results from Marques dos Santos et al. (2014), corroborated by Hanson, Matsuka, and Haxby (2004) study, give rise to the scientific questions that support this research project: Does the fusiform gyrus take part on the cognitive process of brand valuation and categorization? And, since the areas highlighted in the mentioned study belong to visual cognition structures, does the categorization process start in early stages of stimulus processing, instead of being characterized by high level cognitive processing that occur at later stages?

2. Perception of human faces

As a social animal, humans needed to develop specific cognitive processes to easily recognize other members of their kind. The study of human faces has been a relevant topic in neuroscience, producing a wide variety of results that seek to explain what cognitive processes are involved at the moment when the individual observes a face. In studies using the EEG technique and ERP analysis as the method, several important markers were described in association with different cognitive processes involved with face characterization, discrimination, and recognition. They are well summarized in the following table, taken from Olivares et al. (2015).

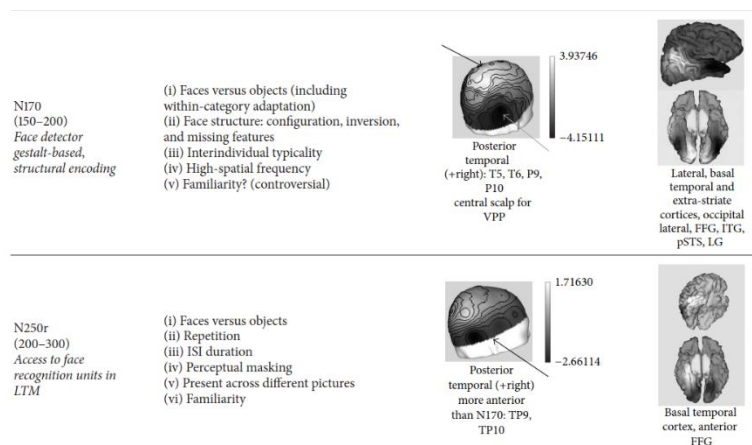


Figure 1 Table containing the ERPs related to face perception

Source: Olivares, Iglesias, Saavedra, Trujillo-Barreto, and Valdés-Sosa (2015)

The earlier ERPs are inherently linked to sensory processes, that is, in the initial processing of any type of external stimulus which, in this case, deals with the detection and understanding of the visual stimulus as being a human face. While the ERPs with higher latencies generally translate semantic evaluation of faces. Despite the abundance of relevant markers, for our study, we give all the relevance to the N170 since it is an ERP that has already demonstrated its modulation when tests were performed that opposed human faces and objects, and whose topography determines the presence of activity in the area of the fusiform gyrus, a cortex region that has relevant importance to our study. These two elements will be explored in greater detail below.

a. The N170 ERP

The N170 is a negative occipitotemporal potential that occurs between 100 to 200 ms after stimulus onset and which was first described in Bentin, Allison, Puce, Perez, and McCarthy (1996). In this study, the N170 was elicited when subjects were asked to perform a visual target detection task with the visual stimuli set being constituted by unfamiliar human faces, scrambled faces, cars, and butterflies. The results obtained in this experiment showed that the unfamiliar human faces elicited the N170, while the other stimuli (scrambled faces, cars, and butterflies) did not. These results led to the major conclusion of this study, which declared the N170 as a face-sensitive ERP. This study also tried to identify the possible neural source of N170, attributing it to the fusiform gyrus. Recently, in Gao, Conte, Richards, Xie, and Hanayik (2019), this localization was not only confirmed but even complemented. Through the combination of structural magnetic resonance imaging, functional magnetic resonance imaging, and high-density ERP, the neural source of N170 was pinpointed in the fusiform gyrus, more specifically in the middle and posterior fusiform gyrus.

In Bentin et al. (1996) other properties of the N170 were studied through different experiments. To determine if the N170 was face-specific to human faces and not an ERP evoked when a subject observed a familiar human body part, another visual target detection task was made but this time using a visual stimuli set constituted by human faces, animal faces, human hands, cars, and furniture. The results showed that N170 was significantly larger in human faces when compared to all other visual stimuli category. The

major conclusion of this experiment was that the N170 was elicited by viewing the human face and not by viewing familiar human body parts. This was later confirmed in the Thierry et al. (2006) experiment, where it was demonstrated that a different ERP, the N190, was elicited when a subject performed observed images of human bodies, with the face removed, in contrast with other visual stimuli like human faces and silhouettes.

Another property of N170 studied in Bentin et al. (1996) was the effect of inversion in the visual stimuli. They grouped upright human faces, inverted human faces, upright cars, inverted cars, and butterflies in a new visual target detection task. The results verified that only the upright and the inverted human faces elicited the N170, while the remaining visual stimuli did not elicit. The difference in the ERP elicited by the inverted human faces in comparison with the ERP of the upright human faces was the delay for the inverted human faces. This concluded that the N170 was the mechanism that allowed the brain to classify a visual stimulus as “face”. Later, Eimer (2000) confirmed these results and added that the delay of the N170 ERP, verified for the inverted human faces, also occurred when subjects observed upright human faces without some internal features, such as eyes and nose, or without external features, such as hair and neck.

In one last experiment, Bentin et al. (1996) tried to determine if the N170 ERP was elicited by human faces or for the presence of the features that complete the human face. For that, another visual target detection task was made now using human faces, butterflies, and then isolated face elements such as eyes, lips, and noses. The results determined that N170 ERP that was elicited by the isolated eyes was similar to the ERP elicited by the human faces. The other two face features, the isolated nose, and lips elicited a delayed N170 ERP in comparison with the human face N170 ERP. These results took, as conclusion, that the eyes are the most salient feature of the human face, being the major contributor for the elicitation of the N170. Itier, Latinus, and Taylor (2006) have confirmed this conclusion and added that the N170 did not change significantly when inverted isolated eyes were presented to subjects.

b. The Fusiform gyrus

The fusiform gyrus is a large spindle-shaped gyrus that spans across the basal surface of the temporal and occipital lobes of both cerebral hemispheres, as represented in Figure 2.

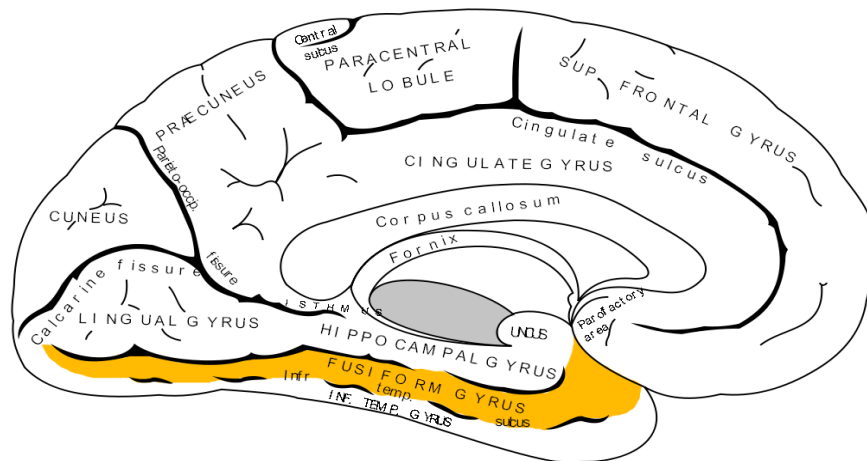


Figure 2 Anatomical location of the fusiform gyrus.

Original Source: Gray (1918)

It was first described in Huschke (1854). The fusiform gyrus is the major anatomical structure of the ventral temporal cortex and the major contributor to the high-visual cortex activity (Weiner & Zilles, 2016). Several cognitive functions have already been associated with this brain region. The fusiform gyrus is associated with the visual processing of color, as studied in Gonzalez, Relova, Prieto, Peleteiro, and Romero (2006). In this study, a contralateral response in the fusiform gyrus was elicited when a group of red, blue, and green dots was presented to a subject. When a group of white dots was presented to the same subject, there was no recorded activity in the fusiform gyrus. This led to the conclusion that the fusiform gyrus should be involved in the processing of color in visual stimuli. Another recognized cognitive function that elicits the activity of the fusiform gyrus in the process of shape recognition.

The existence of a specific region of the brain enabling humans to interpret certain visual stimuli as a “face” was an important contribution to resolve a question that neuroscientist and psychologist had for a long time, and that still stands: are certain cognitive functions domain-specific, this is, are they restricted to the activity of a limited

brain region or are the cognitive processes more dependent of the connectivity between different areas of the brain. The answer that the fusiform face area (FFA) brought to this question was its exclusivity in the identification of faces. The fusiform face area was first identified in Nancy Kanwisher, Josh McDermott, and Marvin M. Chun (1997), during a passive visual task, where the subjects observed images of human faces mixed with images of common objects. The result, in most of the subjects, was a stronger activation in the right fusiform gyrus while they viewed human faces when compared with the activation during the visualization of common objects. In this same experiment, they performed several manipulations to the pictures of human faces and tested them in a similar visual task. The results of these experiments led to the conclusion that the activity in the right fusiform gyrus, which they after nominated as FFA, was present only with the visualization of faces and it was also independent of the presence/absence of the low-level visual features in the pictures. The laterality of this human cognitive function was confirmed in the recent study of Jonas et al. (2015). In this study, when the region of the FFA was electrically stimulated through intracerebral stimulation, transient prosopagnosia, which is defined as the loss of the ability to recognize or identify human faces while still being able to visualize them (Bodamer, 1947), occurred. Since only the stimulation of this particular area impaired the subject capacity to identify human faces and not the stimulation of other brain regions, a conclusion was drawn that the anterior right fusiform gyrus, also known as FFA, was essential to this cognitive function.

However, this specificity attributed to this brain region was put to a test when the FFA was involved in visual expertise. The expertise theory demonstrates that when a subject is an expert relatively to a certain visual stimuli category, the FFA is elicited when a novel visual stimulus is presented. However, this only happens when that visual stimulus belongs to the category that the subject is an expert in. This expertise was demonstrated in studies like Tanaka and Curran (2001) and Gauthier, Skudlarski, Gore, and Anderson (2000). In both studies, the subjects were because of their expertise in birds and dogs, for the first one, and birds and cars, for the second one. In both studies results, the activation of the FFA was higher for the experts vs the novices when their specific expertise category was presented. In the Gauthier et al. (2000) another interesting conclusion was offered when the activation of the FFA, when the subjects looked into pictures of their expertise category, was compared to the activation of the FFA when these subjects looked into faces.

For the faces, the activity in the FFA was always higher. This led to the possible conclusion that while someone can resort to their FFA to “exercise” their expertise relative to a specific non-face visual category, they will constantly have more experience seeing faces when compared to seeing cars/birds, taking the example of this particular study case, leading always to higher activation of the FFA with the presentation of faces.

3. Perception of brand logos and symbols

Assuming that brand logos are symbols that carry the meaning and value of the brand that it represents, often being the most identifiable element of it, among the general population, the scientific studies that try to compare them with images of objects can find several issues since the start. However, it is possible to assume, by common sense, that almost everyone can distinguish between a symbol, such as brand logos, and an object, even if this one has a particular connection with the brand itself since both have different physical properties. While the object is a material thing, that can be seen and touched, a symbol has an abstract existence, and this difference makes it possible to ponder scientific studies using both visual stimuli.

Studies done with brand logos, using an EEG/ERP approach, generally respond to the great interest that the area of Marketing has, in its continuous search to develop new tools to empower brand creators in the creation of their product/service (Plassmann, Ramsøy, & Milosavljevic, 2012). However, the cognitive process involved in the perception of brands, and its logos, may be similar to the ones involved in the perception of letters or words (Camarrone & Van Hulle, 2019), since both are important vehicles of meaning.

The most common specific ERPs modulated in the processing of symbols are the N170, P200, N300, and N400 (Lu & Hou, 2019). The first one, N170, when related to symbol perception, is generally interpreted as a cognitive marker for visual expertise effect involved in activities such as reading (Maurer, Brandeis, & McCandliss, 2005; Maurer, Zevin, & McCandliss, 2008) (Wong, Gauthier, Woroch, Debuse, & Curran, 2005). The P200 is a letter recognition neuronal marker independent of priming effects (Petit, Midgley, Holcomb, & Grainger, 2006). Both N300 and N400 are related to the semantic

processing of words and contextual integration (Coch & Mitra, 2010; Franklin, Dien, Neely, Huber, & Waterson, 2007; Hamm, Johnson, & Kirk, 2002; Molinaro, Conrad, Barber, & Carreiras, 2010). The N170, the N300, and N400 may be the most interesting ones to use as references. The first because brand logos have become one visual stimulus on which it is easy to develop the visual expertise effect nowadays. The second and the third because they access the main property of a brand logo, which is meaning.

4. Recollection and familiarity related to a visual stimulus

To recognize or to be familiar with the elements of the surrounding environment is essential for a successful day to day life of a person. The definition of recognizing is sometimes mistaken with the definition of familiarity. As stated in Wixted (2007), familiarity is a distinct mental process of recollection. While familiarity is a fast cognitive process, it should only contain information about specific intra-stimulus information, such for example, the physical properties of an object. On the other hand, recollection is a slower cognitive process that, not only retrieves intra-stimulus information, even if sometimes incomplete, but also retrieves context information, retrieving environment information present at the moment of the first contact between a person and a particular visual stimulus. However, the debate around the importance of familiarity is not yet finished, since there are competing theoretical models trying to establish its mechanism. In Wixted (2007), there is a well-documented review of this debate, which declares a strong competition between the signal-detection theory and the dual-process signal detection. Only this second theory recognizes the contribution of familiarity, which, associated with the recollection process, seems to produce the associative memory of a given stimulus. Familiarity seems to enter this process as a parallel process to recollection (Evans & Wilding, 2012; Mickes, Wais, & Wixted, 2009). When the signal produced by the visual stimulus does not reach a specific threshold that could lead to a perfect recollection, and to a prompt affirmation of its recognition, by the individual, familiarity processing is introduced so that the individual can estimate his knowledge concerning the stimulus. Therefore, saying that something is known is stronger than saying that something is familiar to us. The importance of distinguishing these two subcomponents of associative memory led to several studies.

Several ERPs studies have been conducted to verify if there is a real distinction between the two cognitive processes. There are two that have been pointed out as potential markers. For the familiarity cognitive process, several studies have indicated the FN400 as the most probable marker. Its topography shows a significant negativity difference, between 300 – 500 ms after onset, at frontal sources of the cortex (Stróžak, Abedzadeh, & Curran, 2016), when a subject is perceiving a “new” visual stimulus when compared with the perception of an “old” visual stimulus, as noted in Speer and Curran (2007), possibly indicating that the lower activation is associated with less excitability caused by a stimulus already familiar to the observer. However, this electrophysiological marker does not bring together the consensus of the scientific community as a specific marker for familiarity. There is also a hypothesis that this FN400 is the same as the N400, which is associated with semantic priming (when an item is faster and more easily identified when preceded by a semantically related item (called the prime). For example, the word “cat” will be more easily identified when is preceded by the word “dog” than when preceded by the word “smartphone”), (Voss & Federmeier, 2011). Nonetheless, although they may coincide in the temporal window, the topography may be the decisive factor that separates the N400 and FN400, as shown in Bridger, Bader, Kriukova, Unger, and Mecklinger (2012). These results are also present in Leynes, Bruett, Krizan, and Veloso (2017), although this study raises the question of whether this ERP is a good marker for the cognitive phenomenon of familiarity or is related to the phenomenon of conceptual memory, which seeks to continually complement the information it has about a specific concrete stimulus.

Related to the recollection cognitive process, the ERP that is considered its specific marker is the left parietal component (LPC), as described in Allan, L. Wilding, and Rugg (1998), where it was described that when a subject is asked to distinguish between “new” and “old” items, a positive deflection in the activity of parietal sites occur, around 400-600 ms, even presenting laterality, since the referred deflection shows higher magnitude in the left hemisphere than the right hemisphere. In terms of magnitude, the LPC is higher when an “old” item is perceived than when a “new” item (Friedman & Johnson Jr, 2000). The recollection process is also involved in the debate surrounding familiarity and semantic priming (Li, Wang, Gao, & Guo, 2016), as explained above.

The attributes of the recollection cognitive process can be an interesting basis for studying the impact of brand logos on the valuation process of brands, since it is known that preferred brands tend to elicit positive memorized information about the brand (Feng et al., 2019) and, since the logo is an extension of the brand, its impact on the recollection process may be an alternative method to access the cognitive process of brand valuation.

5. The cognitive process of preference

The comprehension of the process involved in developing preference about something or someone is one of the scientific topics that brings more interest to disciplines such as Marketing since it would be important to comprehend how certain brands take favour next to the population, unlike other competitors. Nowadays, two theories address the cognitive process preference construction. They are the utility theory (Chatterjee & Heath, 1996) and the behavioral theory (Swait & Adamowicz, 2001). The first theory, most associated with value-based decision type, in which the central factor of preference construction is the known outcome of an available option (O'Hora, Dale, Piironen, & Connolly, 2013) defines preference as a stable and complete i.e. the options are always evaluated the same way through time (Warren, McGraw, & Van Boven, 2010). The important argument for this theory resides in the fact that, for an individual to make a value-based decision, it needs to know all the options or minimal information about them, so it could internalize all of them and proceed with the internal valuation process. This internal valuation process is defined by the individual values scales that an individual constructs when interacting with the options (Vlaev, Chater, Stewart, & Brown, 2011). In contrast, the second theory, most associated with perceptual-based decision type, in which the stimulus characteristics are the essential elements of the decision (Ratcliff, Philiastides, & Sajda, 2009), making the preferences neither stable nor complete (Warren et al., 2010). These differences between the theories are related to several factors, which are context, experience, and cognitive constraints. The first factor shows two different components: goal-orientation and framing. About the first, the decision-maker has specific objectives that create bias in its favorite choices, i.e in its preferences. Therefore, given that the individual creates new goals as he achieves the previous ones, the preferred options should also change so that the decision-maker can reach his new objective, thus contributing to the instability of preferences

(Warren et al., 2010). The second component links the instability of preferred options to the way that they are presented to the decision-makers, being possible to determine the influence of a given decision made just before the studied decision (Chang, Kim, & Cho, 2017). Another factor that supports the behavioral theory is the effect of cognitive constraints, such as time pressure, state of depletion, in preference construction. Reduced periods for decision-making or the existence of simultaneous competing tasks and leads to reduced processing for preference construction (Warren et al., 2010). The last factor, experience, divides its support for the two theories presented earlier. Experience is directly related to memory and learning process, considering that these processes are essential for linking a given decision taken in the past and the respective outcome. This argument relates experience with the utility theory, however, as described in Wimmer and Shohamy (2012) the simultaneous activation of the hippocampus and visual associative brain areas could suggest that stimulus characteristics could influence the decision process when know options are in cause, thus supporting the behavioral theory. Considering all the arguments presented, preference construction theories need more development to be optimized.

As debated in Lin, Cross, Jones, and Childers (2018), there is an emerging tendency for companies to invest more attention and resources in neuroscientific tools to provide better information on how consumers interact with your brand and develop strategies to enhance your value with them. For this reason, the fundamentals of the phenomenon of preference present themselves as one of the most important topics in this area.

One of the essential first steps to discover more about a cognitive process is to determine its neural origin. In McClure et al. (2004), they could conclude that preference can vary its neural origin depending on the information provided to the subject. When they compared the blind tasting (the subjects did not know which brand they were drinking at the time of the experiment) of Coke[®] and Pepsi[®], they observed that the variance of activity on the ventromedial prefrontal cortex (vmPFC) provides enough information to determine the subjects' preferences. When the brand information was added to the tasting experiment, the hippocampus, the dorsolateral prefrontal cortex, and the midbrain had their activity modulated by the subjects' preferences. This study allows the conclusion that the subject's valuation of a given brand is independent of the current experience with the product/service provided by the brand, being rather dependent on previous knowledge/contact with the brand. These results were confirmed by the lesion study of

Koenigs and Tranel (2008), where subjects with lesions on the vmPFC were asked to perform the same tasks as the subjects in McClure et al. (2004). The most important result of this lesion study was that, when the vmPFC is injured, even when brand information is added into the tasting task between the two brands of drinks mentioned before, the predetermined preference did not impact the decision after the tasting task. In Deppe, Schwindt, Kugel, Plassmann, and Kenning (2005), when subjects were asked to rank between different brands of beer and different brands of coffee, the brands that have been classified as preferred (displayed as the first choice) elicited higher activation in cortex areas associated with episodic memory, working memory and emotion modulation. However, considering the target of our experiment, a specific result was described by the higher activation was elicited on the right supermarginal gyrus, when the preferred brand was presented to the subjects. It is important to refer that the right supermarginal gyrus has been associated with the integration of sensory characteristics present in symbols related to the brands, such as logos (Jonathan Downar, Crawley, Mikulis, & Davis, 2001; J. Downar, Crawley, Mikulis, & Davis, 2002), thus indicating that specific characteristics of visual stimuli related to brands take its amount of importance when a subject expresses preference for a particular brand. Another important result provided by Deppe et al. (2005) was the important contributions of emotions for the construction of specific preferences, with influence future choices.

Although fMRI was the most prevalent technique at the beginning of the neuromarketing area of study, recently the EEG technique started to capture the interest of researchers, since it has its technical and cost benefits when compared with other neuroscientific techniques, but mainly because of the recent improvements made to improve its spatial resolution.

Studies focusing on the modulation of ERPs have brought interesting results, centering the discussion around four possible cognitive markers: the N100, N200, P300, and the Late Positive Potential (LPP).

In a recent study, Nazari et al. (2019) have reported that the occipital N100 may be modulated by individual preference. When comparing culturally known brand logos with unknown brand logos (artificially created for the experiment), and with the verbal confirmation of subjects' preferences, the N100 was determined in both categories, with

higher neural activity being registered in the right occipital cortex. However, it was in the latency and amplitude that differences between both categories were found. The results demonstrated that the know/preferred brand logos had a shorter latency and a higher amplitude than the unknown brand logos.

The N200 seems to have an important influence on preference when it is established by social pressures. In Q. Ma, Abdeljelil, and Hu (2019), the modulation of the N200 ERP presents the cultural/ethnic influence over brand evaluation. In this study, the N200 amplitude was lower when the subject was observing a brand logo that was recommended by other subjects of their own ethnic group, commonly referred to as in-group influence, than when observing a recommended logo from subjects from another ethnic group, commonly known as out-group influence. This evidence can contribute to potential differences in the value of a brand in different regions of the world, leading to the development of different preferences for the same brands in different parts of the world.

Both Khushaba, Greenacre, Al-Timemy, and Al-Jumaily (2015) and Gajewski, Drizinsky, Zülch, and Falkenstein (2016) studies have demonstrated that the P300 ERP has a role in the cognition of preference. In the first one, it was demonstrated that, when preferred actions were expressed instead of non-preferred ones, a P300 with higher amplitude was produced at frontal and parietal regions, demonstrating a possible association of this ERP component with the construction of preference. In the second one, a forced counter-intuitive purchase option resulted in lower amplitudes for the P300, demonstrating that when a personal beliefs/preference related to a certain brand/product are challenged, the properties of this ERP is influenced.

In Bosshard, Bourke, Kunaharan, Koller, and Walla (2016) the LPP was directly related to the valuation of brands through the presentation of brand names, whose individual valuation of each subject was assessed through a questionnaire performed before the EEG session. The LPP modulation demonstrated differences between the observation of a liked brand name and an unliked one, being that the LPP amplitude was higher for liked brands. The topography of the LPP in this study, which was significantly lateralized in favor of the right hemisphere, reinforces the theory that what generates the preference for a brand is the influence on the motivational cognitive process of a subject, which are more correlated with the right hemisphere (Cacioppo, Crites, & Gardner, 1996).

Objectives

Part A

Considering the results of studies such as Puce, Allison, Asgari, Gore, and McCarthy (1996) and Nancy Kanwisher et al. (1997), where human faces elicited a higher activation in the fusiform gyrus when compared with objects and written words, results such as the ones presented in Marques dos Santos et al. (2014) creates doubt around the cognitive specificity of the structure. So, to further comprehend the cognitive process involved, this study had the following objectives:

- Verify possible differences or similarities in the role of the fusiform gyrus in the visual perception of the three different categories of visual stimuli used in the experiment: human faces, objects, and brand logos.

- Investigate if familiarity and/or the expertise effect occur between the two subcategories defined, known and unknown, for the three categories of visual stimuli used by analyzing the ERPs evoked during the task.

Part B

Taking into account the interesting results provided by the work of Marques dos Santos et al. (2014), further clarification is needed to better understand the cognitive process of brand logos valuation, looking to overcome the time-defining limitations present in this fMRI study.

So, this scientific research project was based on two major hypotheses:

- Regarding the neural source of the discrimination process involved in preference, regarding brand logos, the function of visual and visual-associative areas of the brain may present a hierarchically superior role in the construction of preference than the deliberative areas of the brain.
- Considering the higher activity detected in visual and visual-associative areas of the brain, during brand logos discrimination according to personal preference, the cognitive process of brand valuation may occur at early stages of stimulus processing, contrasting with the currently most accepted model, in which this cognitive process occurs in later stages during semantic processing of the stimulus.

To test these two hypotheses, the following objectives were outlined for this project:

- Analyze the temporal profile of the discriminatory process involved in brand valuation.
- Determine the role of visual areas of the brain, and in particular, the function of the fusiform gyrus, identified in Marques dos Santos et al. (2014), in the brand valuation process.

Material and Methods

1. Part A

1.1. Visual stimuli set definition

The complete set of visual stimuli available for the experiment is presented in Appendix A, Part A. The initial set is formed by 240 images, equally split by three different categories:

- Human faces
- Objects
- Brand logos.

Then each one of these categories was divided into two subcategories:

- Known
- Unknown

Each one of these subcategories described had 40 images attributed to. The images used as the “Known Brand Logos” were gathered in a previous experiment. The images used as the “Unknown Brand Logos” were specifically designed for the experience, since they do not represent any real brand. The images used as the “Known Human Faces” were not retrieved from any specific database, since there was no open database already built that was designed for the Portuguese community. The images were then gathered online by the experimenter. The selected images were chosen to be balanced with the images from the “Unknown Human Faces”. The images used as the “Unknown Human Faces” were gathered from D. S. Ma, Correll, and Wittenbrink (2015). The images used as the “Known Objects” were retrieved from Bradley and Lang (2017) database. The images used as “Unknown Objects” were retrieved from Horst and Hout (2016) database.

From the starting forty images gathered for each category/subcategory, only thirty images were about to be used in the behavioral data collection procedure. To select the final thirty images a validation process was performed. An online form was created, through the Survey Monkey platform, where the forty starting images were presented, followed by these four questions:

1st Question: “How agreeable is this face/object/brand logo?”¹

2nd Question: “How aroused does this face/object/brand logo leaves you?”²

3rd Question: “Do you know this face/object/ brand logo?”³

4th Question: “In which context do you know it?”⁴

To construct the 1st and 2nd questions, the PAD emotional state model (J. A. Russell and A. Mehrabian (1977); Mehrabian (1995)) and the Self-Assessment Manikin (SAM) (Morris, 1995) were used. Since the Dominance property was not fundamental to the study it was excluded from the questionnaire. So, the answers made available for these two questions used the PAD scale, ranging from 1 to 5, 1 being the lowest level of attraction/activation, and 5 being the highest level of attraction/activation. In the 3rd question, the answers made available to the participants were “I know it” and “I don’t know it”. The 4th question was used as confirmation of the previous one, assessing the real knowledge of the participant on the image presented. For this question, no predefined answers were presented, and the participant was asked to write his answer.

The thirty best matching images with its category/subcategory, previously assigned by the investigator were selected to construct the final stimuli set. All the images that did not achieve the 70% match with their specific category/subcategory were going to be excluded. If there was any type of draw, the researcher would choose the ones with higher values in the answers to question 1 and 2.

¹ “O quão agradável é esta face/objeto/ logotipo?”

² “O quão ativa/o te deixou esta/e face/objeto/logotipo?”

³ “Conhece esta face/objeto/ logotipo?”

⁴ “De que contexto a/o conhece?”

1.2. Stimulus presentation

The final set of visual stimuli established was loaded into the E-Prime 2.0 software (Psychology Software Tools, Pittsburgh, PA)⁵ to be presented electronically to the participants. The stimulus presentation was randomized, and followed this scheme:

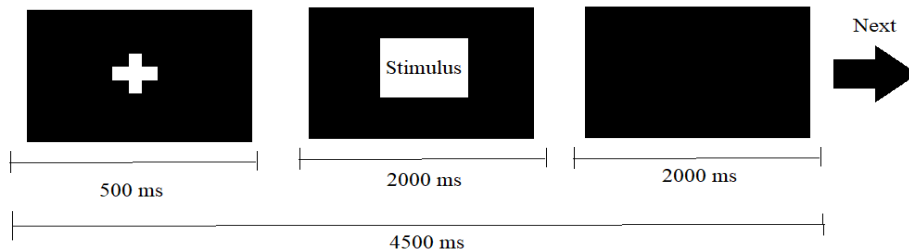


Figure 3 Scheme of stimulus presentation.

1.3. Participants selection

To enter into the experiment, volunteers needed to fulfill the following selection criteria: be over 18 years of age, be a Portuguese native, be right-handed, have the minimum education level (that is, have completed the 12th year of school), could not be taking psychotropic drugs or any other medication that causes behavioral changes, could not have any type of connection with the area of Marketing, either through an academic degree or through professional experience. For the female volunteers, an extra criterion was stipulated, they could not be pregnant or breastfeeding.

After all these criteria were met, two additional tests were administered in the first session of the experiment: the Montreal Cognitive Assessment (MoCA) and the Edinburgh Handedness Inventory. MoCA was intended to be used as a selection criterion since all volunteers who obtained a result below the threshold, which was a test score inferior to 26 points, out of 30 possible, would be considered as excluded from the experiment. The Edinburgh Handedness Inventory was intended to be used as a selection criterion since only right-handed volunteers (left hemisphere dominant) were included in the experiment. Both tests would be administered by a certified professional psychologist.

⁵ <https://pstnet.com/products/e-prime/>

1.4. Ethical procedures

This experiment was evaluated and validated by the Comissão de Ética para a Saúde do Centro Hospitalar de São João / Faculdade de Medicina da Universidade do Porto. Since this experiment involved sensible human data, an additional evaluation, related with the treatment of personal information of the participant, was requested from the Unidade de Proteção de Dados da Universidade do Porto.

2. Part B

2.1. Study structure

The study had two sessions. The first one comprehended the subjects screening and stimuli selection. The second one had the EEG data acquisition.

2.1.1. First session - Subjects screening

In the first session, all the subjects were screened for their demographic information, to record their demographic data and to verify that they met all the inclusion criteria of the experience that were: be over 18 years of age, be a Portuguese native, be right-handed, have the minimum education level (that is, have completed the 12th year of school), could not be taking psychotropic drugs or any other medication that causes behavioral changes, and, for the female participants, could not be pregnant or breastfeeding.

Then all subjects were asked to complete the Edinburgh Handedness Inventory and the MoCA. The performance of the subjects on these two assessments was also an inclusion/exclusion criteria, since only right-handed subjects (left hemisphere dominant) with a final scored, in MoCA, higher than 26 points, out of the 30 possible points, were admitted to the experiment.

2.1.2. Stimuli selection

After completing all the screening, it was necessary to create a personalized stimulus set for each of the subjects because each participant has his/her brand preferences. This final set was made up of 35 preferred brands' logos, plus 35 indifferent logos, which had to be selected by each one of the subjects. For such purpose, the subjects were individually asked to assess a set of 200 commercial brands' logos, which is presented in Appendix A, Part B. All the brands' logos were gathered in a previous experiment. This set contained brands' logos from different product/service segments (e.g. food and beverages,

apparel, banks, cars, etc). The subjects assessed the stimulus using the PAD scale (J. A. Russell and A. Mehrabian (1977); Mehrabian (1995) and the SAM (Morris, 1995), to sort each one of the brands' logos in relation to Pleasure and Arousal, taking into account that the values of the Pleasure dimension ranged from -2 to +2 (-2 being the lowest level of pleasure, indicating unpleasant evaluation of the brand's logo and +2 being the highest level of pleasure, indicating a pleasant evaluation of the brand's logo) and the values of the Arousal dimension ranged from 1 to 5 (1 being the lowest level of arousal, indicating total lack of arousal in the evaluation of the brand's logo and 5 being the highest level of pleasure, indicating a complete arousal in the evaluation of the brand's logo). The brands' logos and both PAD and SAM were presented through a laptop, using SuperLab 5 software⁶.

The results of the assessments were processed to define which brands' logos were preferred and which ones were indifferent to each of the subjects. The criteria used for this classification were: preferred brands' logos were the ones who had the Pleasure ratings of +1 and +2 and the Arousal ratings of 3, 4, or 5. Indifferent brands' logos were the ones who had the Pleasure rating of 0 and the Arousal ratings of 1, 2, or 3. To complete the individual set of stimuli, 35 fictitious brands' logos were added. To continue the experiment, the subject had to guarantee a final set of 35 + 35 + 35 brands' logos.

2.1.3. Stimulus presentation

The final set of visual stimuli established was loaded into the E-Prime 2.0 software (Psychology Software Tools, Pittsburgh, PA) to be presented electronically to the participants. The subject received the following instructions, which were tested before the EEG data collection, in a training exercise: After visualizing the stimulus the subject had to press the keys 1, 2, 3, and 4 of a keyboard to match the following possible answers "like", "don't like", "indifferent" and "don't know". The keyboard setup was customized so that the subject did not have to move his head to check the keys, thus avoiding harmful artifacts

⁶ <https://cedrus.com/superlab/update/v5/index.html>

for the EEG data collection. The subject could submit its answer until the complete dark screen appeared, as introduced by the following schematic Figure 4:

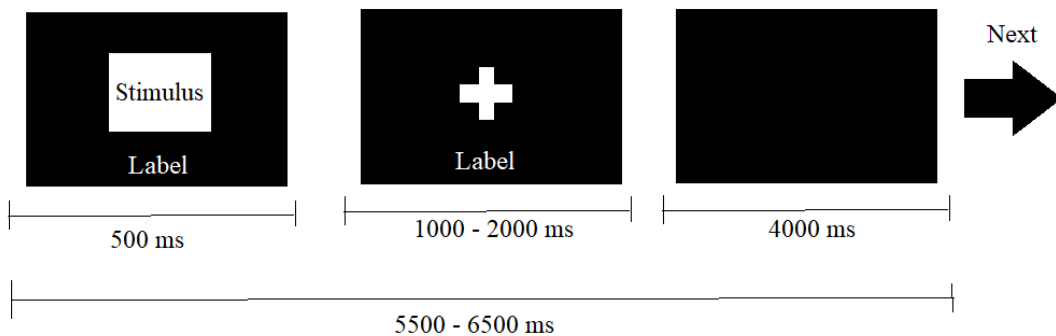


Figure 4 Scheme of stimulus presentation.

The label identified in the figure contained the following answers, from the left to the right of the screen: "Like", "Don't like", "Indifferent" and "Don't know".

2.1.4. Second session - EEG data collection

As reported before, the response was triggered using E-prime V2.0 (2011, Psychology Software Tools Inc., Pennsylvania, USA)⁷ synchronized with the EEG acquisition software NetStation V4.5.2 (2008, Electrical Geodesics Inc., Oregon, USA)⁸. EEG data were recorded using a 128-electrode Hydrocel Geodesic Sensor Net with a Net Amps 300 amplifier (Electrical Geodesics Inc., EGI, Eugene, EUA)⁸. All impedances were kept below 5 k Ω , as Net Amps is a high input impedance amplifier. All electrodes were referenced to the vertex (Cz) and re-referenced offline to the average reference. The digitizing rate was 500 Hz.

2.2. Subjects

65 right-handed adults (29 males, 36 females; mean age = 27.4, SD = 8.16) with no history of neurological disorder participated in this experiment. From the initial 65 subjects, 45 were excluded. The reasons for these exclusions were: incompleteness of their

⁷ <https://pstnet.com/products/e-prime/>

⁸ <https://www.egi.com/>

brand logos stimulus set; did not reach the minimum results established for the MoCA and the Edinburgh Handedness Inventory; the electrophysiological (EEG) recordings presented issues and it was not possible to repeat the acquisition; did not attend all sessions of the experience; presented clinical artifacts on their anatomical magnetic resonance image. The final sample of subjects had 20 right-handed adults (9 males, 11 females; mean age = 24.9, SD = 5.83). All subjects were recruited through different means such as personal invitation, posters posted publicly at different colleges, through different public platforms of the Laboratório de Neuropsicofisiologia, and through dynamic emailing.

2.3. Ethical procedures

This experiment was evaluated and validated by the Comissão de Ética para a Saúde do Centro Hospitalar de São João / Faculdade de Medicina da Universidade do Porto.

2.4. EEG data analysis

The files containing the electrophysiological activity collected for each one of the subjects was uploaded to the EEGLAB software (Delorme & Makeig, 2004)⁹. Using this software, the raw data file was analyzed and treated. First, the channel locations were updated and verified. Then the data was filtered using two different filters. One for low frequencies, under 0.1 Hz, and the other for high frequencies, over 40 Hz. After that, the ICA computation was made to identify components that could be removed, such as malfunctioning channels and artifacts such as blinks, head movement, saccades, and heart rate. The next step was the epoch extraction associated with the removal of baseline. As a last step of treatment, data interpolation was made, and all data were re-referenced to the average reference.

The file that resulted of the EEGLab treatment was then loaded into the ERPLAB, to create an event-list which assigned different bins to different events, which were the following: preferred, indifferent, and fictitious. Then we proceed to the creation of bin-based epochs and thus updating the files into a different ERPset for each one of the subjects.

⁹ <https://sccn.ucsd.edu/eeglab/index.php>

After loading all the final ERPsets, from all 20 subjects, to the EEGLab, the grand average was calculated, creating an ERPset containing the average amplitude, in microvolts (μV), for each time point, in milliseconds (ms), and for each one of the electrodes used. This grand average ERPset had also the three bins described above.

2.5. Global field potential and global dissimilarity calculations

To calculate the global field potential (GFP) (Murray, Brunet, & Michel, 2008; Skrandies, 1990) for each time point, for each specific experimental condition, the following formula was used:

$$GFP_u = \sqrt{\frac{1}{n} \cdot \sum_{i=1}^n u_i^2} \quad (\mu\text{V})$$

- “u” stands for the experimental condition analysed.
- “n” stands for the total number of electrodes used.
- “ u_i ” stands for the average potential registered in a specific electrode, for one experimental condition, at a specific time point.

This last variable is obtained through the following formula:

$$u_i = U_i - \bar{u} \quad (\mu\text{V})$$

- “ U_i ” stands for the measured potential of a specific electrode, for one experimental condition, in a specific time point
- “ \bar{u} ” is the mean value of all “ U_i ”, for that experimental condition.

To calculate the global dissimilarity (DISS) (Skrandies, 1990) (Murray et al., 2008), for each time point, the following formula was used:

$$DISS_{u,v} = \sqrt{\frac{1}{n} \cdot \sum_{i=1}^n \left(\frac{u_i}{GFP_u} - \frac{v_i}{GFP_v} \right)^2}$$

- “u” stands for the first experimental condition
- “v” stands for the second experimental condition

- “n” stands for the total number of electrodes used
- “ u_i ” and “ v_i ” stand for the average potential registered in a specific electrode, for both experimental conditions, in a specific time point
- “ GFP_u ” and “ GFP_v ” correspond to the global field power, for condition “u” and “v” respectively, for each time point

Global dissimilarity (DISS) is an index that defines topographical configurations from two different electrical fields, so it is a property without a specific unit.

All the formulas described above were retrieved from Murray et al. (2008).

2.6. EEG source localization

To perform the source localization of brain activity, the exact low-resolution brain electromagnetic tomography, better known as eLORETA (R. Pascual-Marqui, 2007). The LORETA software (R. D. Pascual-Marqui, Michel, & Lehmann, 1994) makes use of the three-shell spherical head model registered to the Talairach human brain atlas (Talairach & Tournoux, 1988), available as a digitized MRI from the Brain Imaging Centre, Montreal Neurologic Institute. Registration between spherical and realistic head geometry used EEG electrode coordinates reported by Towle et al. (1993). The solution space is restricted to cortical gray matter and hippocampus, as determined by the corresponding digitized Probability Atlas also available from the Brain Imaging Centre, Montreal Neurologic Institute.

To accomplish the source localization of brain activity, it is necessary to provide to the LORETA software the coordinates of all the electrodes used to record it. For that, the exact three-dimensional cartesian coordinates for the 129 electrodes used in the EEG procedure were registered using EGI’s GPS technology. Since some issues arose during the capture of the electrode coordinates, it was only possible to obtain exact coordinates for 14 of the 20 subjects that participated, and to define the electrode coordinates for the remaining subjects, a global model provided by the EEG system was used.

To study the participation of the Regions of Interest IC2 and IC7 (regions that were defined in Marques dos Santos et al. (2014), whose three-dimensional cartesian

coordinates are registered in Appendix C and D, respectively), we used the tool “SLoreta to ROI” in the LORETA software.

2.7. Statistical analysis

The statistical analyses of the potentials registered in the electrodes, for the different experimental conditions and for the statistical analyses of the GFP for each one of the experimental conditions, was carried in R (version 4.0.2) with the RStudio interface (version 1.3.1903) (R Development Core Team, 2010). Paired sample t-tests were performed, setting the value of α to 0.05. The results obtained in the statistical analyses are described in Appendix B. The pairs analysed were “Preferred vs Indifferent”, “Preferred vs Fictitious” and “Indifferent vs Fictitious”.

For the statistical analysis of the source localization results, paired group t-tests were performed using the eLORETA files produced for the different experimental conditions (Nichols & Holmes, 2002). The experimental pairs used on the statistical analysis were “Preferred vs Indifferent”, “Preferred vs Fictitious” and “Indifferent vs Fictitious”. A subject-wise normalization was performed into the data. The statistical analysis was performed for all time frames registered. For statistical analysis of current source density, eLORETA applies a statistical nonparametric mapping method (SnPM) (Holmes, Blair, Watson, & Ford, 1996). We assessed the difference of cortical source localization between groups in each frequency band with voxel-by-voxel independent F-ratio-tests, based upon eLORETA log-transformed current source density power. In the resulting three-dimensional statistical mapping, cortical voxels with significant differences were identified employing a nonparametric permutation/randomization procedure (i.e., based on the Fisher’s permutation method, with the threshold set at the 5% probability level), comparing the mean source power in each voxel and the distribution in the permuted values. eLORETA used 5000 data randomizations to determine the critical probability threshold values with correction for multiple comparisons across all voxels.

Results

1. Analysis of the activity in the Regions of Interest

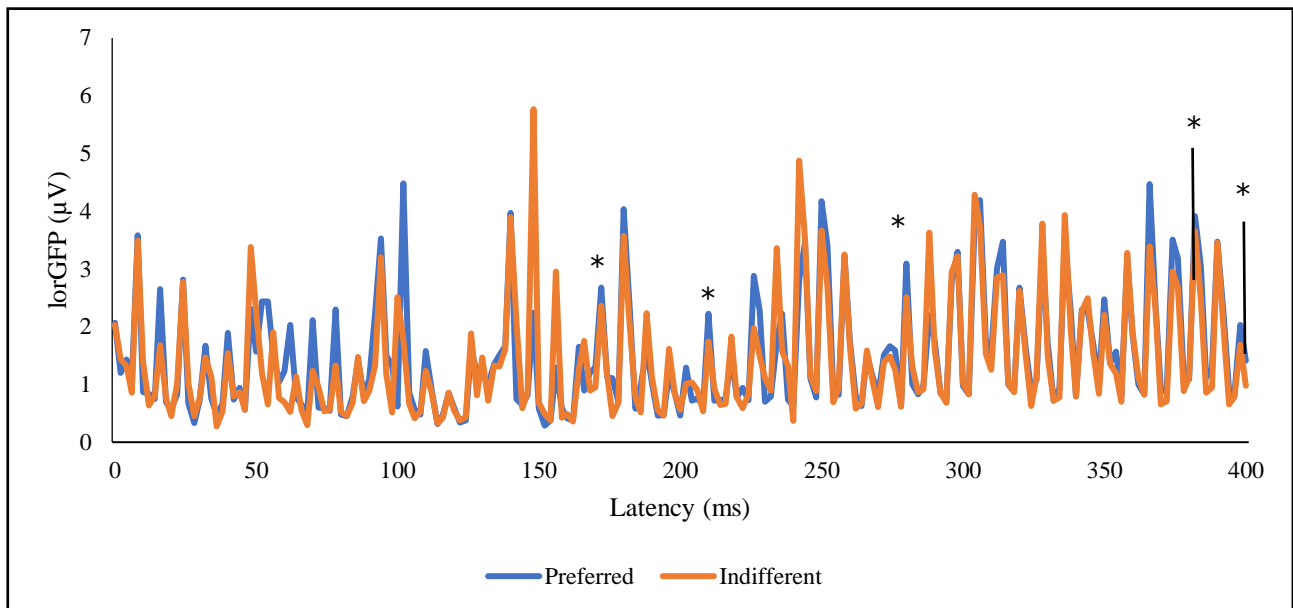


Figure 5 Average lorGFP values of preferred and indifferent brands, in IC2

The significant statistical effect between the GFP elicited by preferred and indifferent brands, in the IC2 region, was verified at the following latencies: at 166 ms ($t = -2,137$, $df = 19$; two tailed; $p = 0,046$); at 196 ms ($t = -2,588$; $df = 19$; two tailed; $p = 0,018$); at 280 ms ($t = 2,194$; $df = 19$; two tailed; $p = 0,041$); at 384 ms ($t = 2,420$; $df = 19$; two tailed; $p = 0,026$); and at 400 ms ($t = 2,095$; $df = 19$; two tailed; $p = 0,050$).

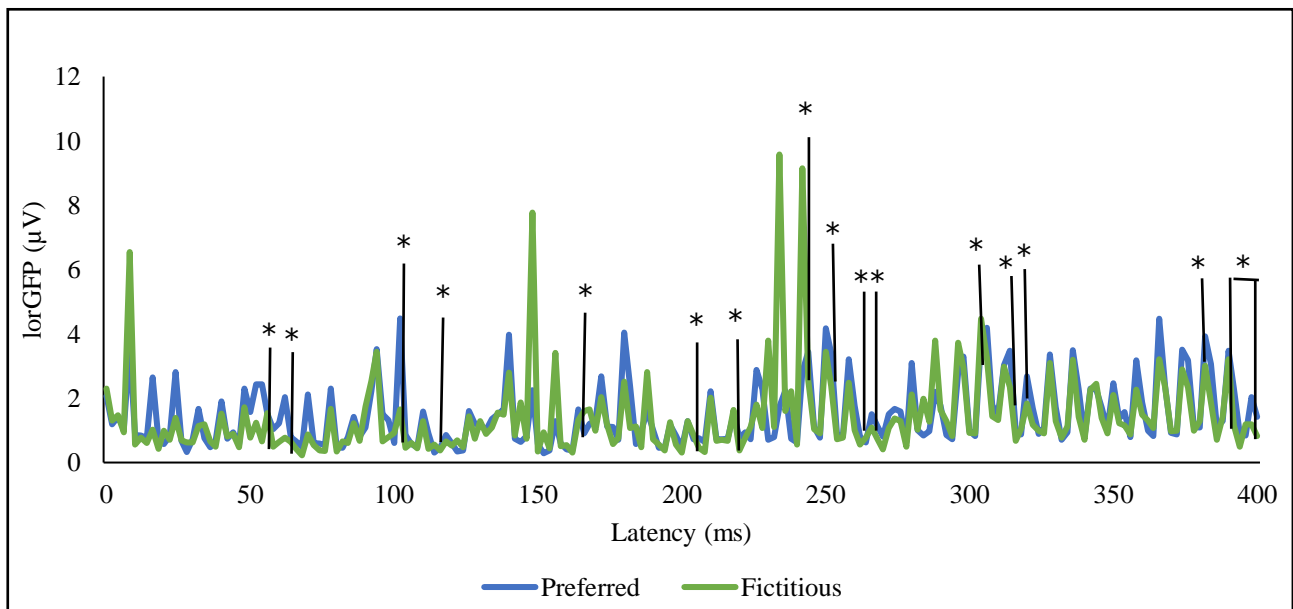


Figure 6 Average lorGFP values of preferred and fictitious brands, in IC2

The significant statistical effect between the GFP elicited by preferred and fictitious brands, in the IC2 region, was verified at the following latencies: at 58 ms ($t = 2,126$, $df = 19$; two tailed; $p = 0,047$); at 68 ms ($t = 2,572$; $df = 19$; two tailed; $p = 0,019$); at 104 ms ($t = 2,276$; $df = 19$; two tailed; $p = 0,035$); at 122 ms ($t = -3,195$; $df = 19$; two tailed; $p = 0,048$); at 166 ms ($t = -2,556$; $df = 19$; two tailed; $p = 0,019$); at 206 ms ($t = 2,153$; $df = 19$; two tailed; $p = 0,044$); at 220 ms ($t = 3,220$; $df = 19$; two tailed; $p = 0,005$); at 244 ms ($t = 2,438$; $df = 19$; two tailed; $p = 0,025$); at 252 ms ($t = 2,331$; $df = 19$; two tailed; $p = 0,031$); at 260 ms ($t = 3,397$; $df = 19$; two tailed; $p = 0,003$); at 266 ms ($t = 2,204$; $df = 19$; two tailed; $p = 0,040$); at 306 ms ($t = 2,304$; $df = 19$; two tailed; $p = 0,033$); at 314 ms ($t = 2,644$; $df = 19$; two tailed; $p = 0,016$); ; at 316 ms ($t = 2,316$; $df = 19$; two tailed; $p = 0,032$); at 320 ms ($t = 2,675$; $df = 19$; two tailed; $p = 0,015$); at 382 ms ($t = 2,125$; $df = 19$; two tailed; $p = 0,047$); at 384 ms ($t = 2,330$; $df = 19$; two tailed; $p = 0,030$); at 392 ms ($t = 3,809$; $df = 19$; two tailed; $p = 0,001$); at 394 ms ($t = 2,222$; $df = 19$; two tailed; $p = 0,039$); at 398 ms ($t = 2,812$; $df = 19$; two tailed; $p = 0,011$); and at 400 ms ($t = 2,733$; $df = 19$; two tailed; $p = 0,013$);

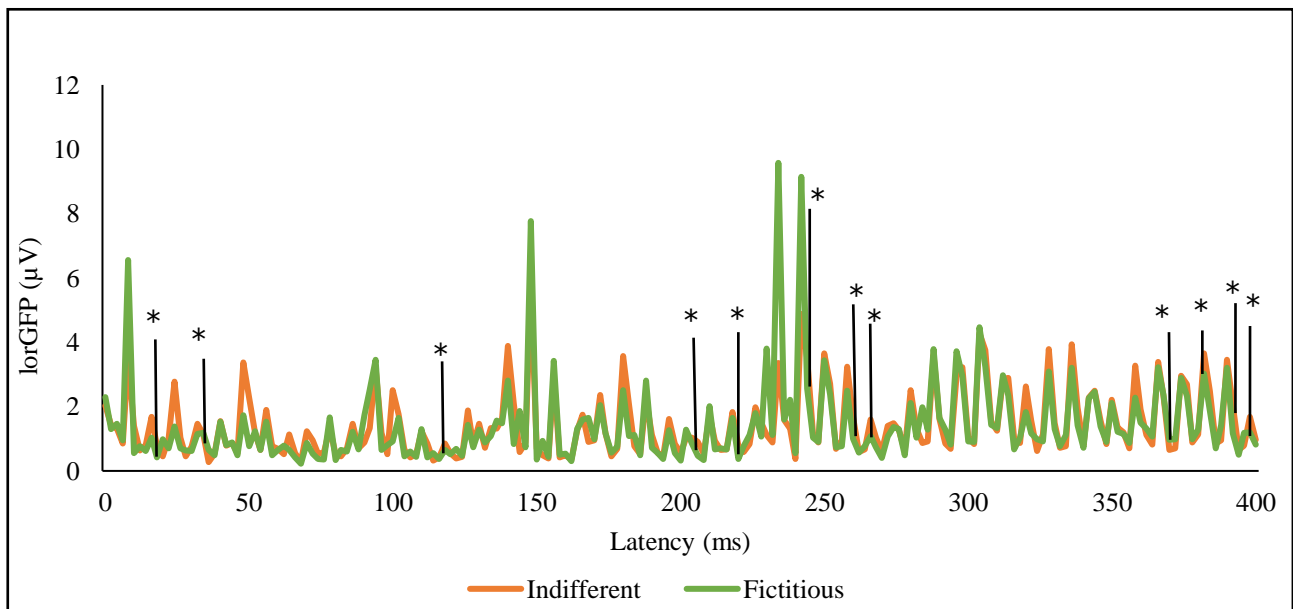


Figure 7 Average lorGFP values of indifferent and fictitious brands, in IC2

The significant statistical effect between the GFP elicited by indifferent and fictitious brands, in the IC2 region, was verified at the following latencies: at 18 ms ($t = 2,349$; $df = 19$; two tailed; $p = 0,030$); at 20 ms ($t = -2,283$; $df = 19$; two tailed; $p = 0,034$); at 36 ms ($t = -3,645$; $df = 19$; two tailed; $p = 0,002$); at 122 ms ($t = -2,755$; $df = 19$; two tailed; $p = 0,013$); at 206 ms ($t = 2,587$; $df = 19$; two tailed; $p = 0,018$); at 220 ms ($t = 2,804$; $df = 19$; two tailed; $p = 0,011$); at 244 ms ($t = 2,526$; $df = 19$; two tailed; $p = 0,021$); at 260 ms ($t = 2,396$; $df = 19$; two tailed; $p = 0,027$); at 266 ms ($t = 2,705$; $df = 19$; two tailed; $p = 0,014$); at 370 ms ($t = -2,256$; $df = 19$; two tailed; $p = 0,036$); at 382 ms ($t = 2,269$; $df = 19$; two tailed; $p = 0,035$); at 392 ms ($t = 2,776$; $df = 19$; two tailed; $p = 0,012$); and at 398 ms ($t = 2,980$; $df = 19$; two tailed; $p = 0,008$);

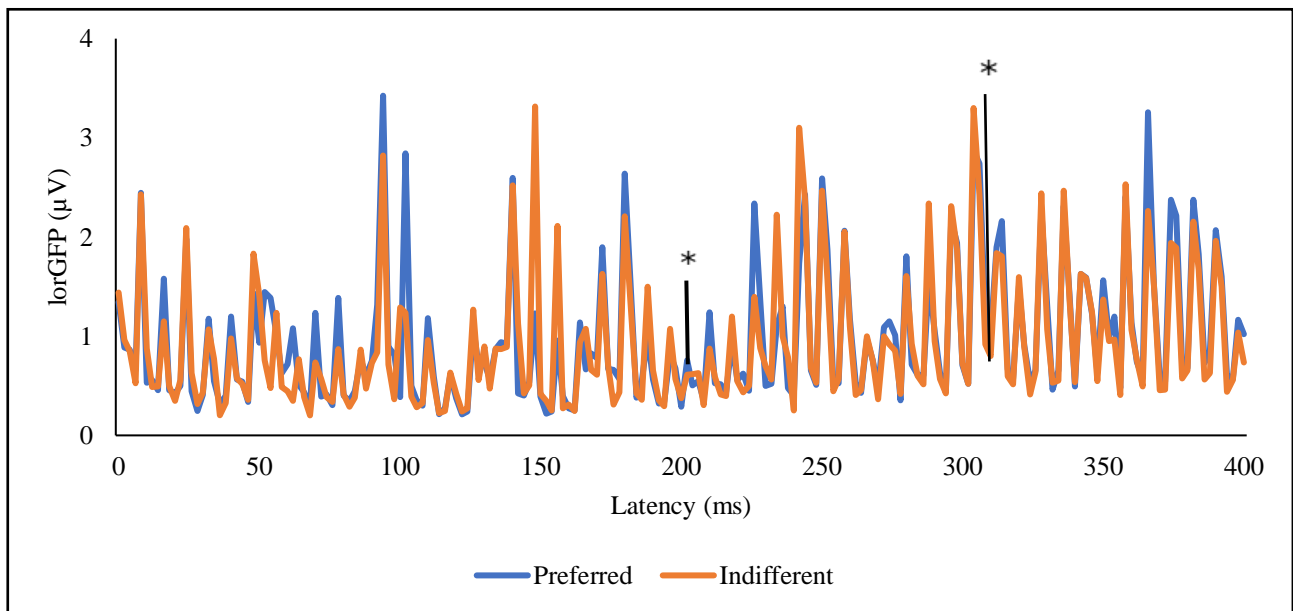


Figure 8 Average lorGFP values of preferred and indifferent brands, in IC7

The significant statistical effect between the GFP elicited by preferred and indifferent brands, in the IC7 region, was verified at the following latencies: at 196 ms ($t = -2,649$; $df = 19$; two tailed; $p = 0,016$) and 308 ms ($t = 3,094$; $df = 19$; two tailed; $p = 0,006$).

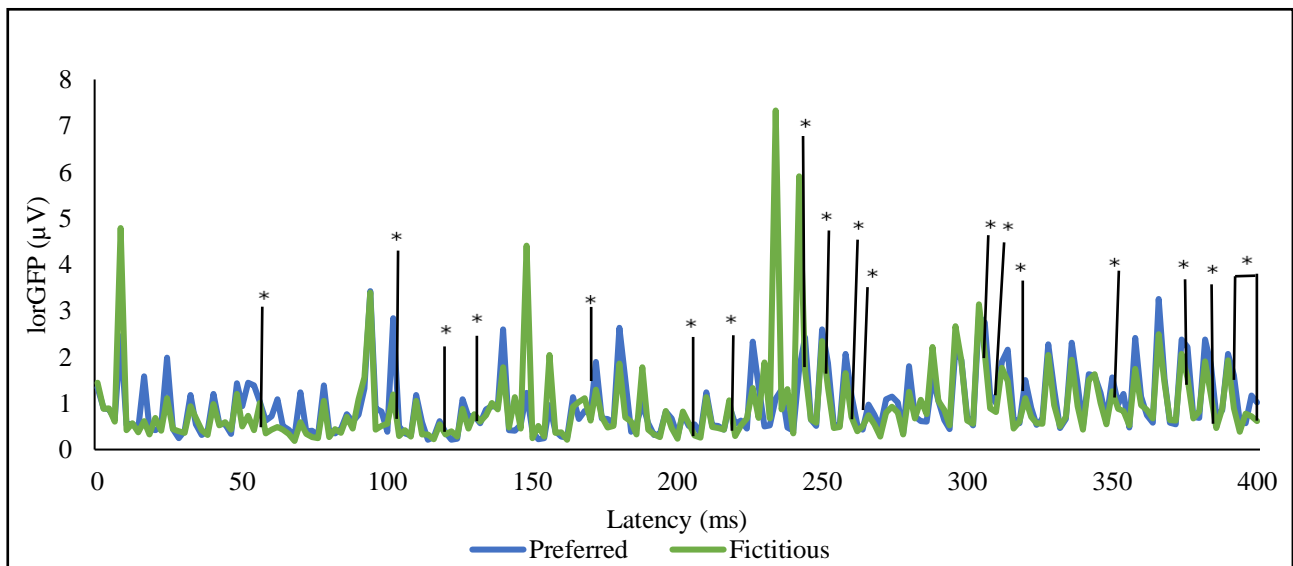


Figure 9 Average lorGFP values of preferred and fictitious brands, in IC7

The significant statistical effect between the GFP elicited by preferred and fictitious brands, in the IC7 region, was verified at the following latencies: at 58 ms ($t = 2,259$; $df = 19$; two tailed; $p = 0,036$); 104 ms ($t = 2,403$; $df = 19$; two tailed; $p = 0,027$); at 122 ms ($t = -3,714$; $df = 19$; two tailed; $p = 0,001$); at 128 ms ($t = 2,164$; $df = 19$; two tailed; $p = 0,043$); at 172 ms ($t = 2,760$; $df = 19$; two tailed; $p = 0,012$); at 206 ms ($t = 2,589$; $df = 19$; two tailed; $p = 0,018$); at 220 ms ($t = 2,933$; $df = 19$; two tailed; $p = 0,009$); at 244 ms ($t = 2,804$; $df = 19$; two tailed; $p = 0,011$); at 252 ms ($t = 2,393$; $df = 19$; two tailed; $p = 0,027$); at 260 ms ($t = 3,897$; $df = 19$; two tailed; $p = 0,001$); at 266 ms ($t = 2,514$; $df = 19$; two tailed; $p = 0,021$); at 306 ms ($t = 2,662$; $df = 19$; two tailed; $p = 0,015$); at 308 ms ($t = 2,279$; $df = 19$; two tailed; $p = 0,034$); at 314 ms ($t = 2,827$; $df = 19$; two tailed; $p = 0,011$); at 316 ms ($t = 2,625$; $df = 19$; two tailed; $p = 0,017$); at 320 ms ($t = 2,784$; $df = 19$; two tailed; $p = 0,012$); at 354 ms ($t = 2,121$; $df = 19$; two tailed; $p = 0,047$); at 376 ms ($t = 2,165$; $df = 19$; two tailed; $p = 0,043$); at 384 ms ($t = 2,542$; $df = 19$; two tailed; $p = 0,020$); at 386 ms ($t = 2,232$; $df = 19$; two tailed; $p = 0,038$); at 392 ms ($t = 3,620$; $df = 19$; two tailed; $p = 0,002$); at 396ms ($t = 3,350$; $df = 19$; two tailed; $p = 0,031$); and at 398 ms ($t = 3,350$; $df = 19$; two tailed; $p = 0,003$); and at 400 ms ($t = 2,611$; $df = 19$; two tailed; $p = 0,017$).

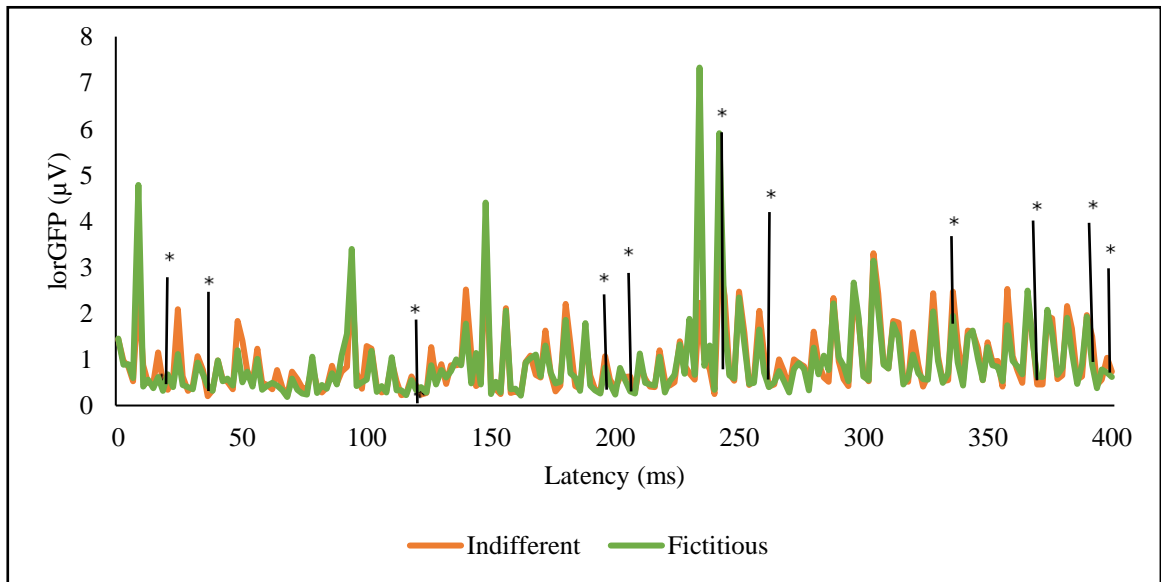


Figure 10 lorGFP values of indifferent and fictitious brands, in IC7

The significant statistical effect between the GFP elicited by indifferent and fictitious brands, in the IC7 region, was verified at the following latencies: at 18 ms ($t = 2,304$; $df = 19$; two tailed; $p = 0,032$); at 20 ms ($t = -2,146$; $df = 19$; two tailed; $p = 0,045$); at 36 ms ($t = -3,981$; $df = 19$; two tailed; $p = 0,001$); at 122 ms ($t = -2,696$; $df = 19$; two tailed; $p = 0,014$); at 196 ms ($t = 2,351$; $df = 19$; two tailed; $p = 0,030$); at 206 ms ($t = 2,473$; $df = 19$; two tailed; $p = 0,023$); at 220 ms ($t = 2,665$; $df = 19$; two tailed; $p = 0,015$); at 244 ms ($t = 2,543$; $df = 19$; two tailed; $p = 0,020$); at 260 ms ($t = 2,884$; $df = 19$; two tailed; $p = 0,010$); at 336 ms ($t = 2,399$; $df = 19$; two tailed; $p = 0,027$); at 370 ms ($t = -2,467$; $df = 19$; two tailed; $p = 0,023$); at 392 ms ($t = 3,175$; $df = 19$; two tailed; $p = 0,005$); and at 398 ms ($t = 3,218$; $df = 19$; two tailed; $p = 0,004$);

2. Analysis of the event-related potentials

2.1. The N100 ERP

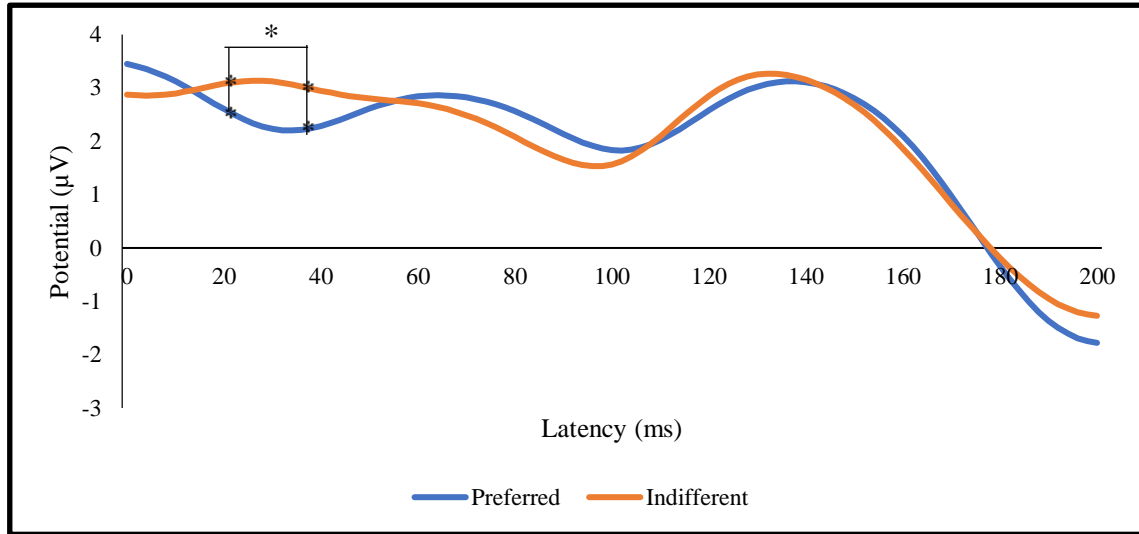


Figure 11 Average potential measured, for the preferred and indifferent categories, in the E70

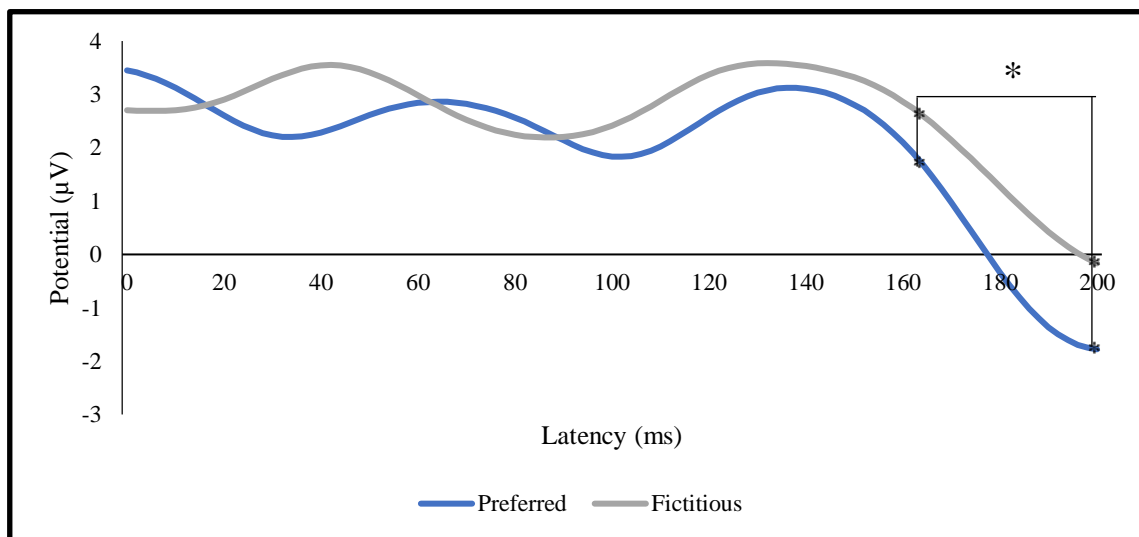


Figure 12 Average potential measured, for the preferred and fictitious categories, in the E70 electrode

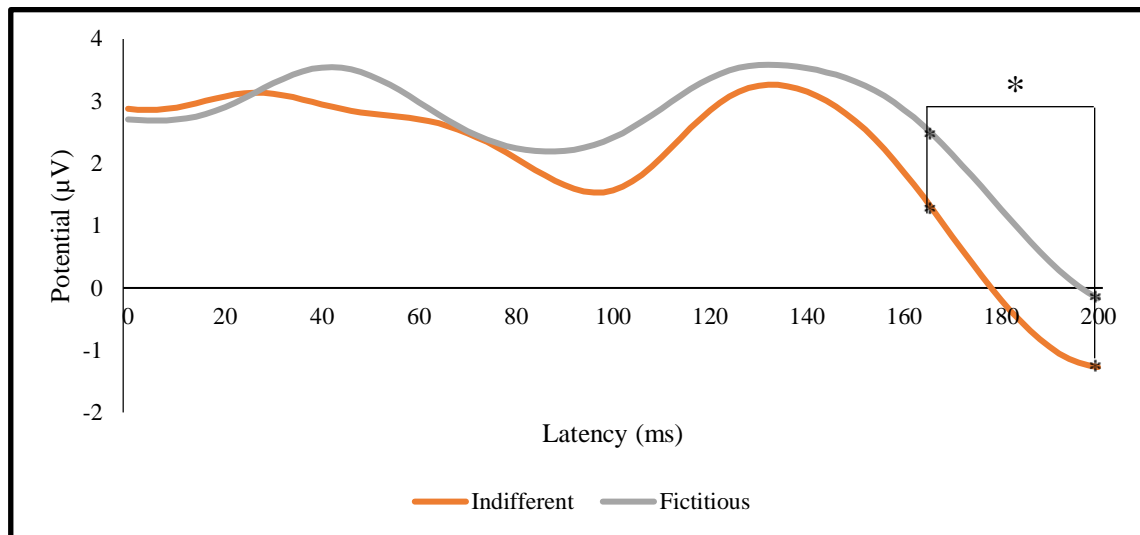


Figure 13 Average potential measured, for the indifferent and fictitious categories, in the E70 electrode

The significant statistical effect between the potential elicited by preferred and indifferent brands in the E70 electrode occurred between 22 ms ($t = -2,102$; $df = 19$; two tailed; $p = 0,049$) and 38 ms ($t = -2,236$; $df = 19$; two tailed; $p = 0,038$). The statistical effect achieved maximum value at 28 ms ($t = -3,026$; $df = 19$; two tailed ; $p = 0,007$)

In the same electrode, the significant statistical effect between the potential elicited by preferred and fictitious brands occurred between 164 ms ($t = -2,344$; $df = 19$; two tailed, $p = 0,030$) and 200 ms ($t = -3,234$; $df = 19$; two tailed; $p = 0,004$). The maximum statistical effect occurred at 180 ms ($t = -3,573$; $df = 19$; two tailed; $p = 0,002$).

For the statistical effect, in the same electrode, of the indifferent and fictitious brands, the interval started at 166 ms ($t = -2,197$; $df = 19$; two tailed; $p = 0,041$) and 200 ms ($t = -3,224$; $df = 19$; two tailed; $p = 0,004$). Maximal statistical effect between these experimental conditions occurred at 200 ms.

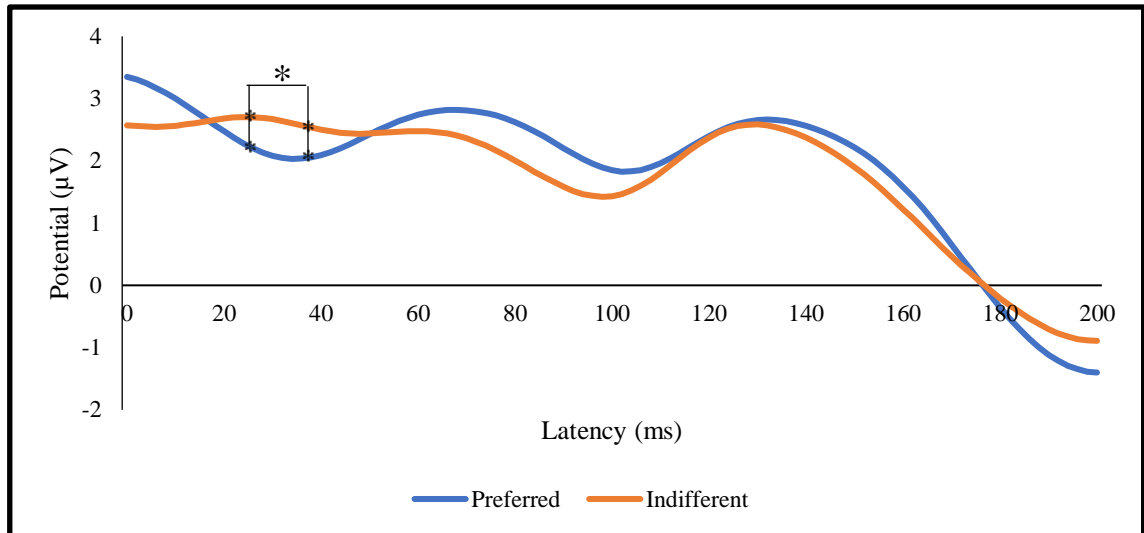


Figure 14 Average potential measured, for the preferred and indifferent categories, in the E75 electrode

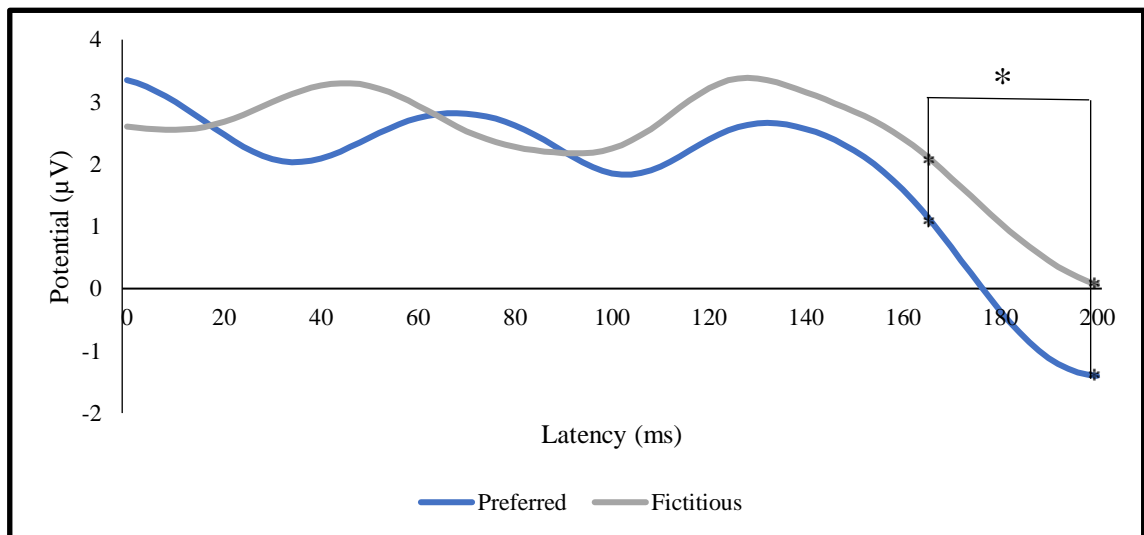


Figure 15 Average potential measured, for the preferred and fictitious categories, in the E75 electrode

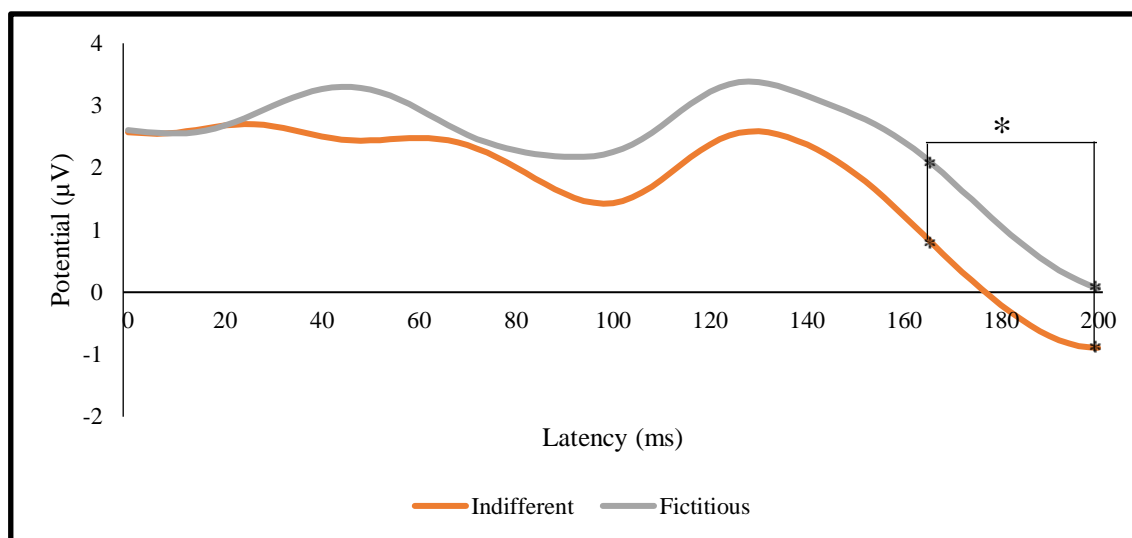


Figure 16 Average potential measured, for the indifferent and fictitious categories, in the E75 electrode

The significant statistical effect between the potential elicited by preferred and indifferent brands in the E75 electrode occurred between 26 ms ($t = -2,404$; $df = 19$; two tailed; $p = 0,027$) and 38 ms ($t = -2,140$; $df = 19$; two tailed; $p = 0,046$). The statistical effect achieved maximum value at 30 ms ($t = -2,658$; $df = 19$; two tailed; $p = 0,016$)

In the same electrode, the significant statistical effect between the potential elicited by preferred and fictitious brands occurred between 166 ms ($t = -2,109$; $df = 19$; two tailed, $p = 0,048$) and 200 ms ($t = -3,343$; $df = 19$; two tailed; $p = 0,0034$). The maximum statistical effect occurred at 198 ms ($t = -3,352$; $df = 19$; two tailed; $p = 0,0033$).

The statistical effect, in the same electrode, of the indifferent and fictitious brands, occurred in the interval starting at 166 ms ($t = -2,148$; $df = 19$; two tailed; $p = 0,045$) and 200 ms ($t = -2,810$; $df = 19$; two tailed; $p = 0,011$). Maximal statistical effect between these experimental conditions occurred at 200 ms ($t = -2,856$; $df = 19$; two tailed; $p = 0,0010$).

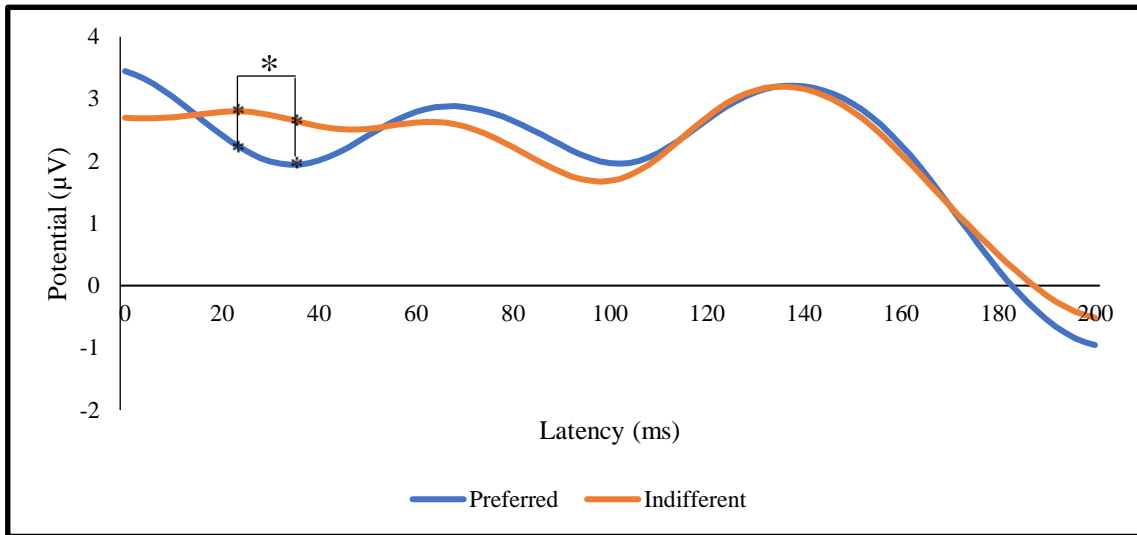


Figure 17 Average potential measured, for the preferred and indifferent categories, in the E83 electrode

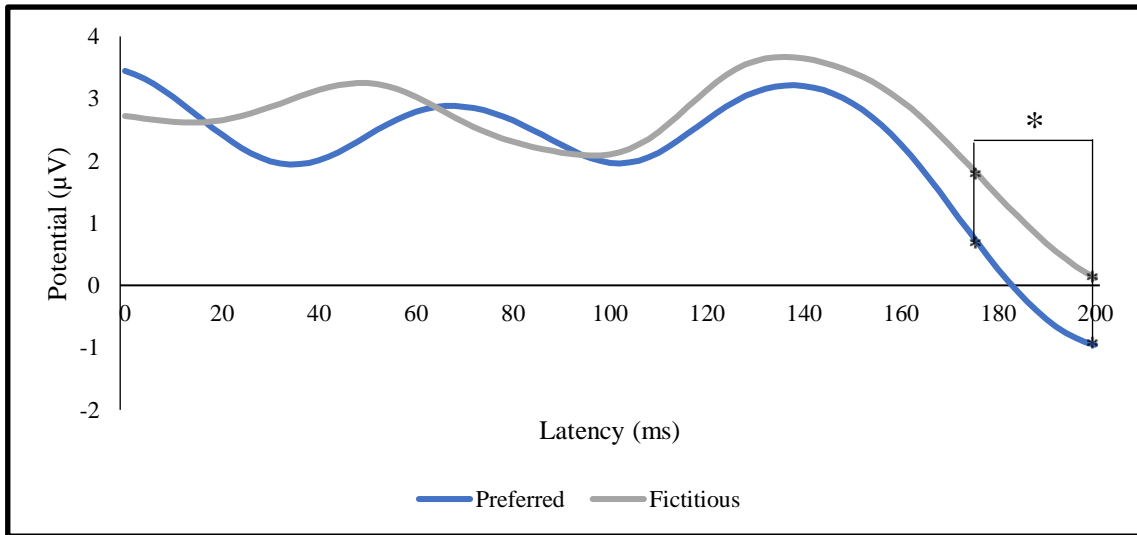


Figure 18 Average potential measured, for the preferred and fictitious categories, in the E83 electrode

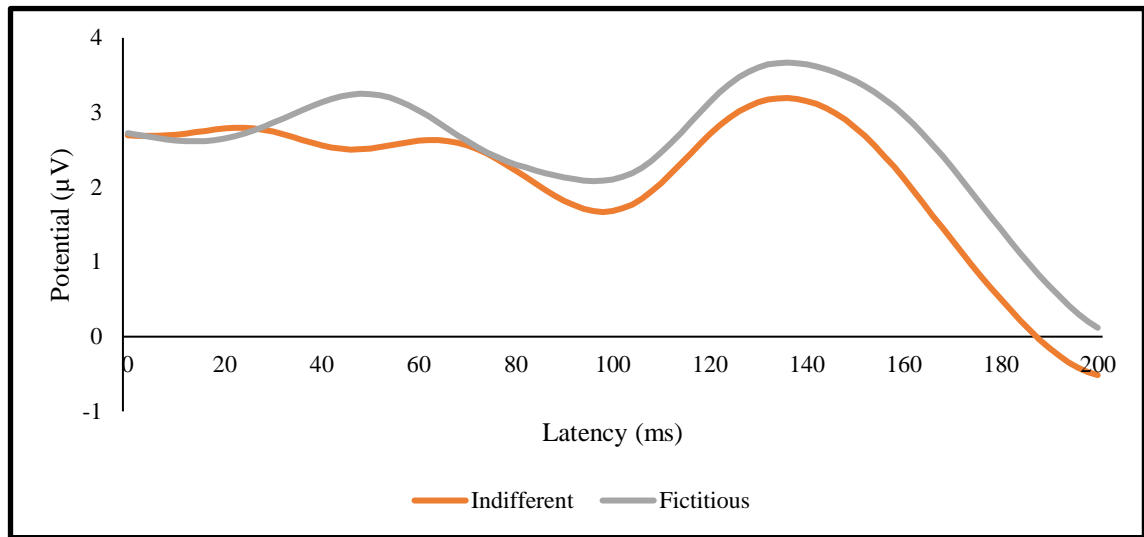


Figure 19 Average potential measured, for the indifferent and fictitious categories, in the E83 electrode

The significant statistical effect between the potential elicited by preferred and indifferent brands in the E83 electrode occurred between 24 ms ($t = -2,120$; $df = 19$; two tailed; $p = 0,047$) and 36 ms ($t = -2,200$; $df = 19$; two tailed; $p = 0,040$). The statistical effect achieved maximum value at 30 ms ($t = -2,415$; $df = 19$; two tailed; $p = 0,026$)

In the same electrode, the significant statistical effect between the potential elicited by preferred and fictitious brands occurred between 176 ms ($t = -2,097$; $df = 19$; two tailed, $p = 0,050$) and 200 ms ($t = -2,203$; $df = 19$; two tailed; $p = 0,040$). The maximum statistical effect occurred at 190 ms ($t = -2,234$; $df = 19$; two tailed; $p = 0,037$).

No statistical effect occurred between the potentials elicited by indifferent and fictitious brands in the E83 electrode.

2.2. The N200 / P300 ERPs

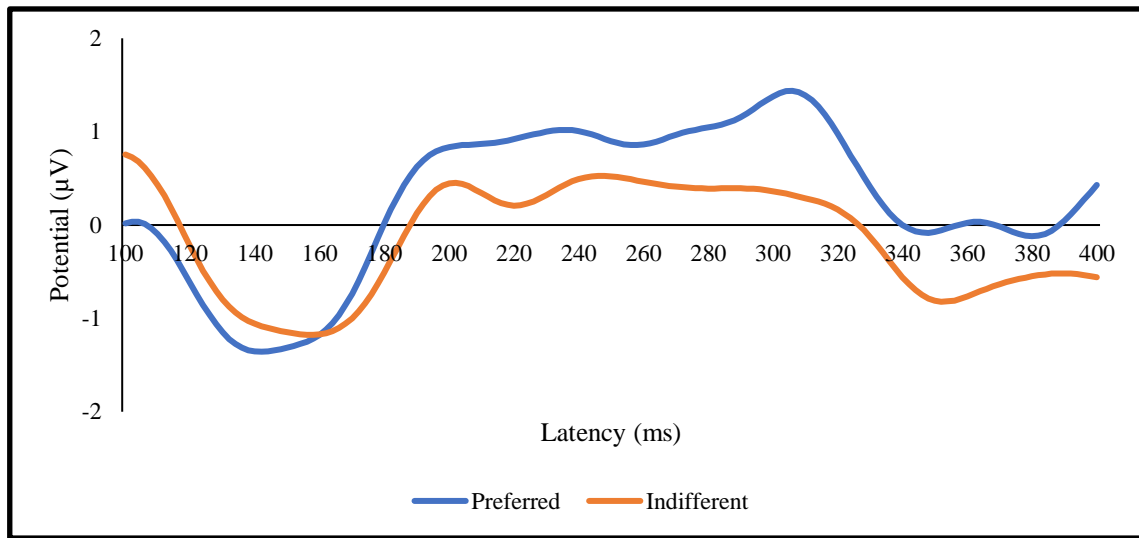


Figure 20 Average potential measured, for the preferred and indifferent categories, in the E24 electrode

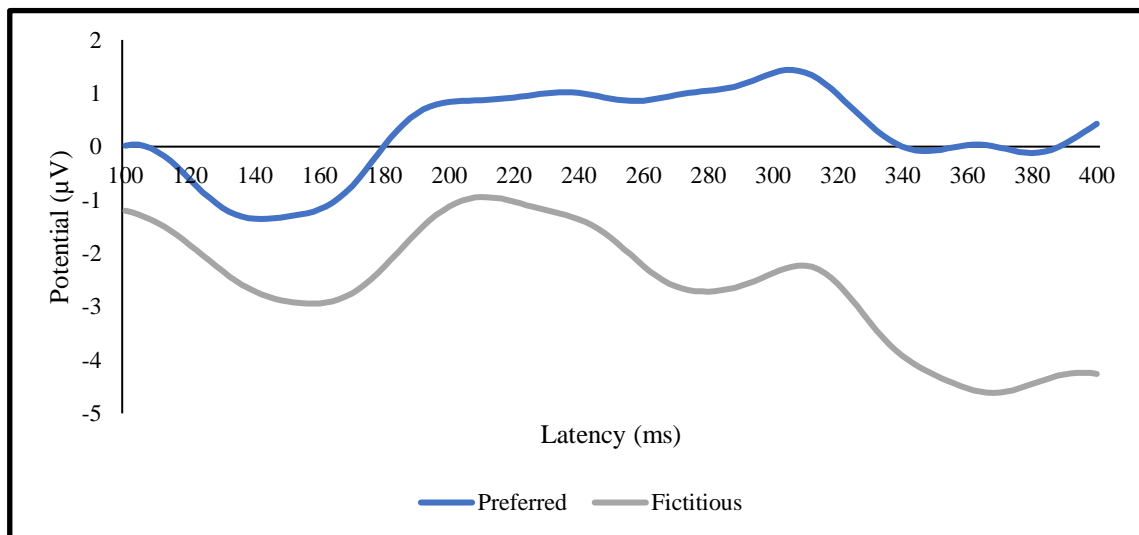


Figure 21 Average potential measured, for the preferred and fictitious categories, in the E24 electrode

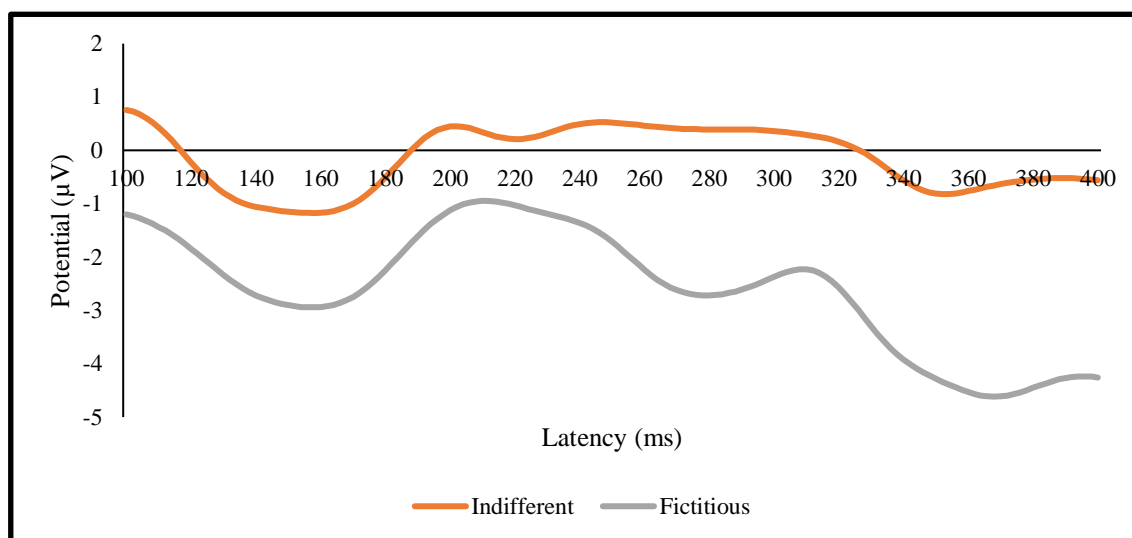


Figure 22 Average potential measured, for the indifferent and fictitious categories, in the E24 electrode

No statistical effect was observed for all condition pairs in the E24 electrode.

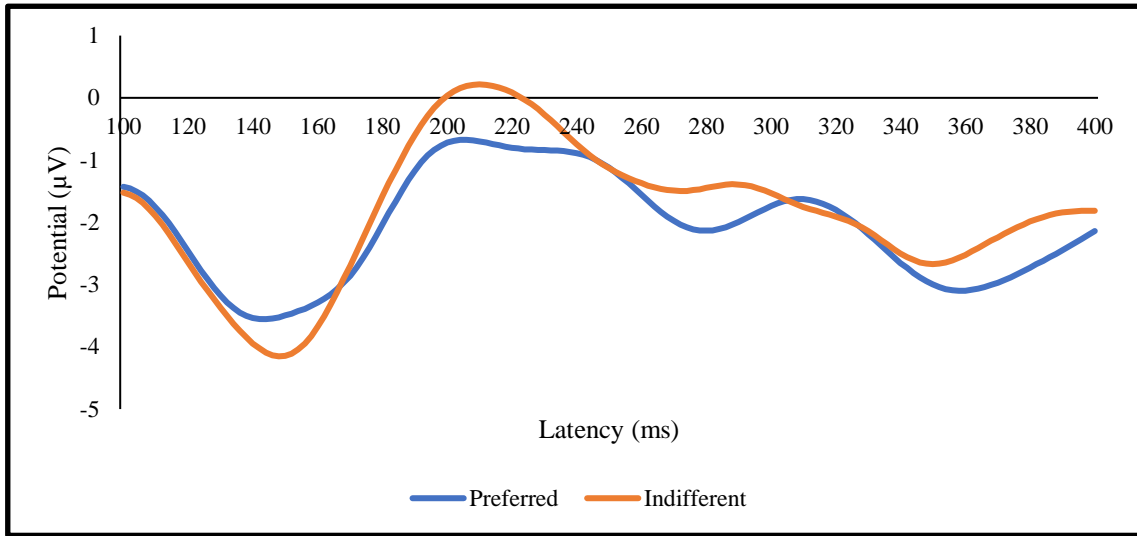


Figure 23 Average potential measured, for the preferred and indifferent categories, in the E11 electrode

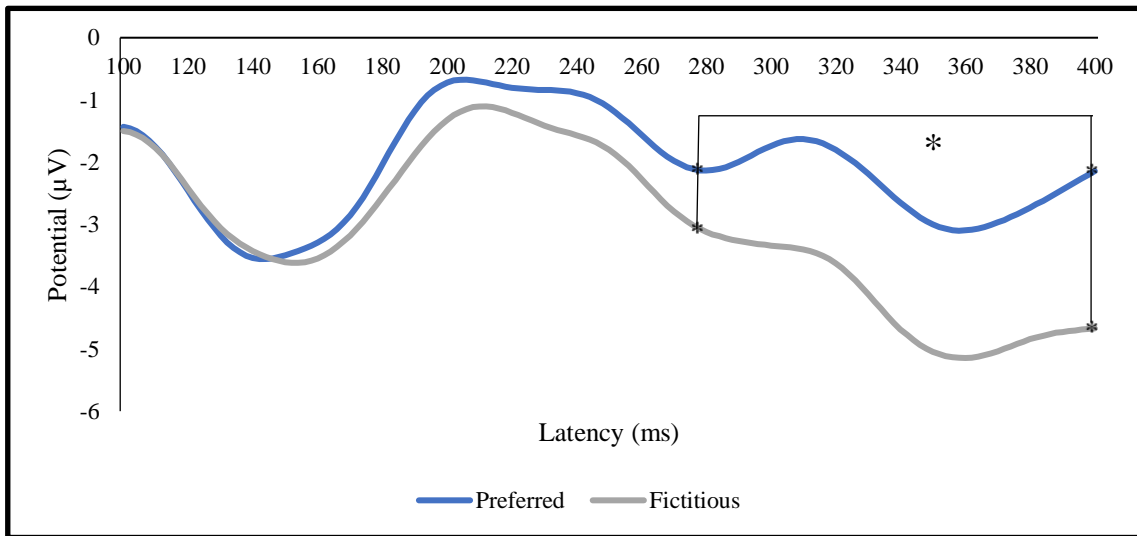


Figure 24 Average potential measured, for the preferred and fictitious categories, in the E11 electrode

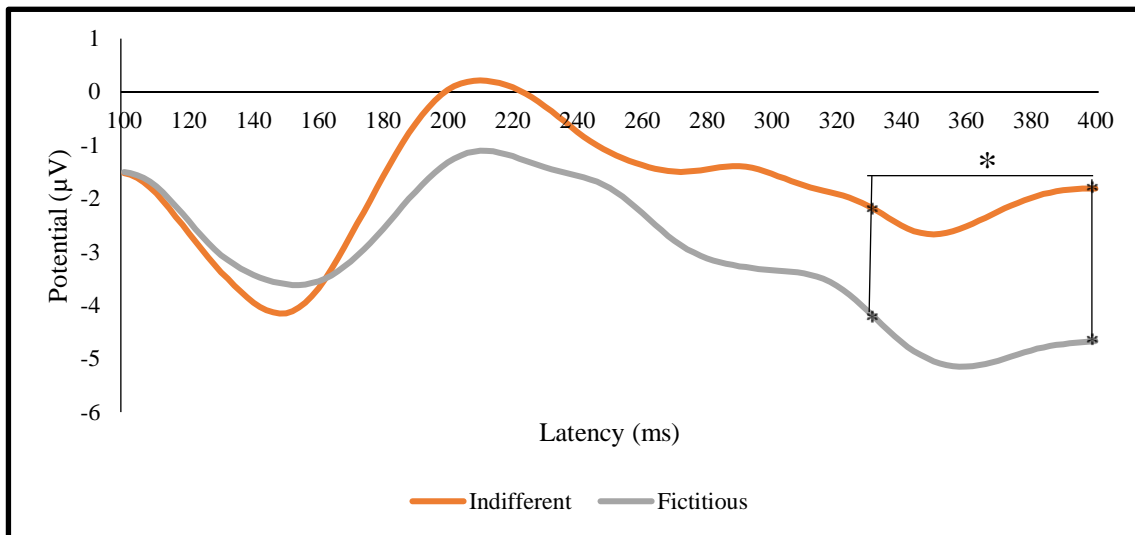


Figure 25 Average potential measured, for the indifferent and fictitious categories, in the E11 electrode

No statistical effect was determined, in the E11 electrode, between preferred and indifferent brands.

For the preferred and fictitious brands, at E11 electrode site, the statistical effect started at 278 ms ($t = 2,120$; $df = 19$; two tailed; $p = 0,047$) until 400 ms ($t = 2,822$; $df = 19$; two tailed; $p = 0,047$). Maximum statistical effect occurred at 302 ms ($t = 3,427$; $df = 19$; two tailed; $p = 0,003$).

Between indifferent and fictitious brands, at E11 electrode site, the statistical effect started at 332 ms ($t = 2,110$; $df = 19$; two tailed; $p = 0,048$) and went until 400 ms ($t = 2,886$; $df = 19$; two tailed; $p = 0,010$). The maximal statistical effect occurred at 382 ms ($t = 3,333$; $df = 19$; two tailed; $p = 0,004$).

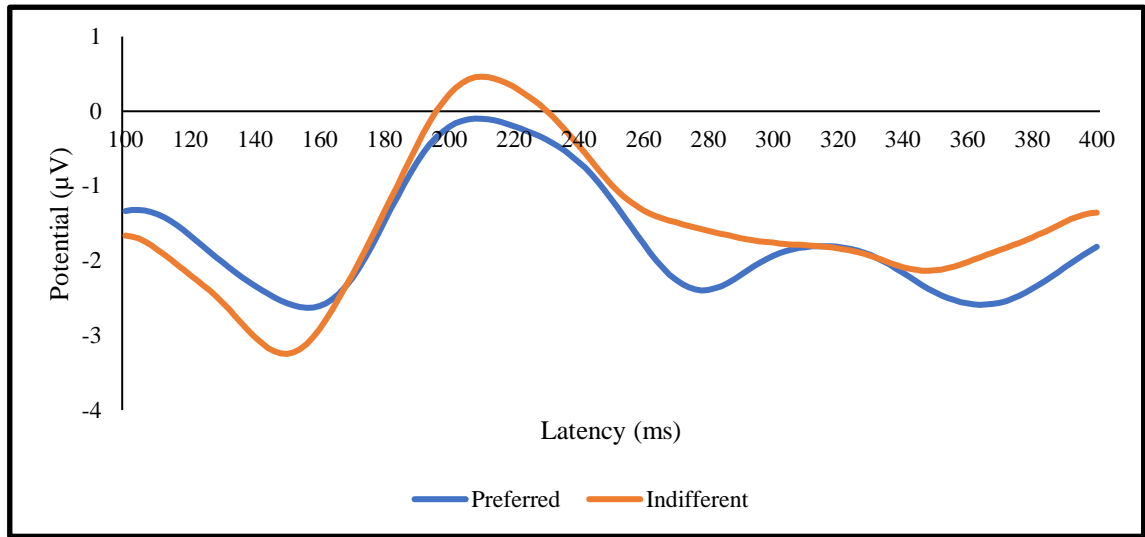


Figure 26 Average potential measured, for the preferred and indifferent categories, in the E124 electrode

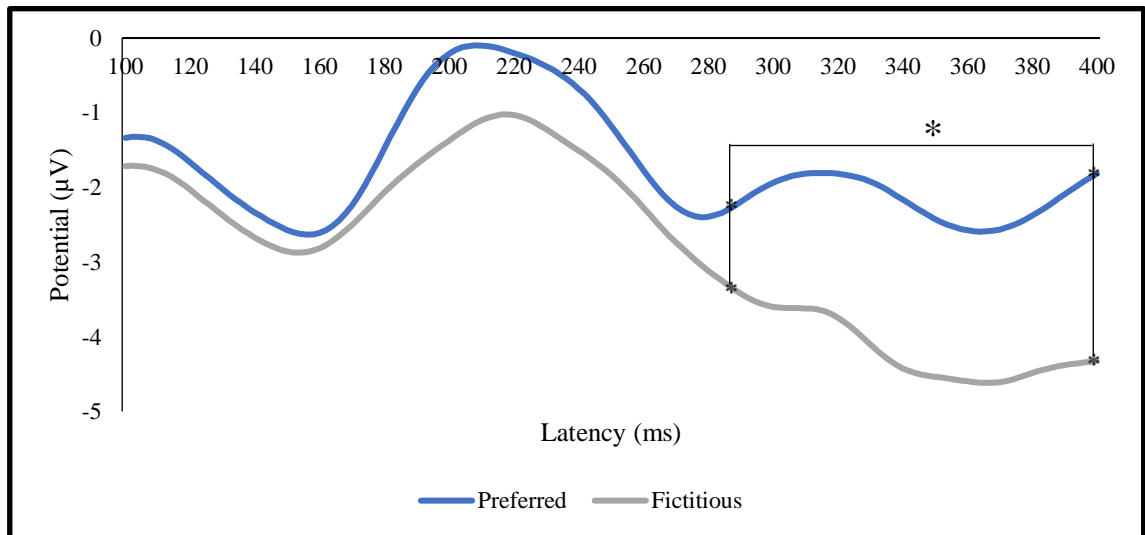


Figure 27 Average potential measured, for the preferred and fictitious categories, in the E124 electrode

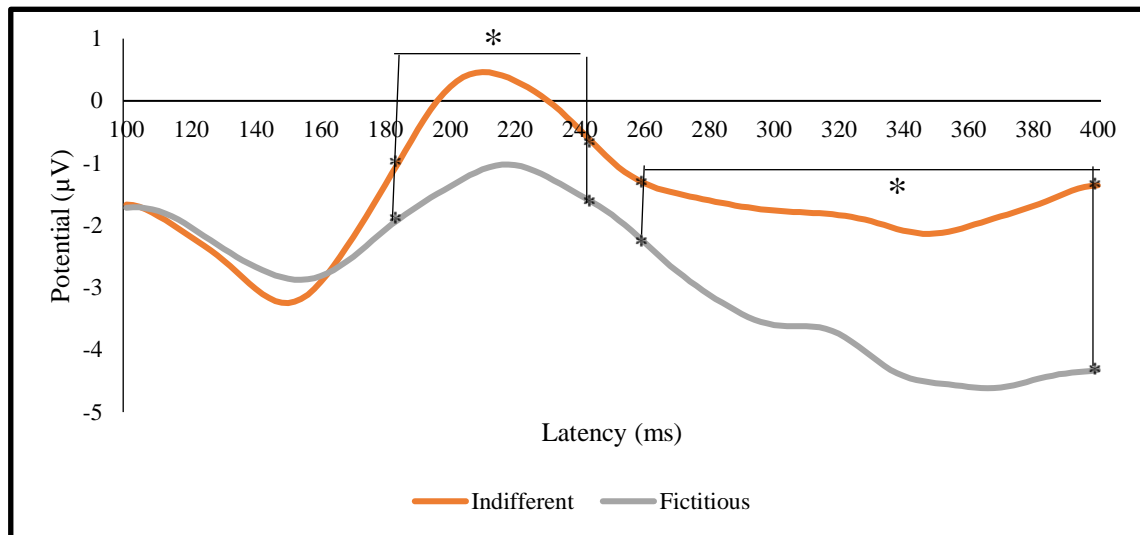


Figure 28 Average potential measured, for the indifferent and fictitious categories, in the E124 electrode

No statistical effect was obtained between preferred and indifferent brand logos in the E124 electrode.

For the preferred and fictitious brands, in the E124 electrode, the statistical effect occurred at 288 ms ($t = 2,104$; $df = 19$; two tailed; $p = 0,049$) until 400 ms ($t = 4,575$; $df = 19$; two tailed; $p = 0,0002$). The maximum statistical effect occurred at 392 ms ($t = 4,680$; $df = 19$; two tailed; $p = 0,00016$).

For the indifferent and fictitious brands, at E124 electrode site, the statistical effect started occurred at two different latency intervals. The earlier one started at 184 ms ($t = 2,291$; $df = 19$; two tailed; $p = 0,034$) until 244 ms ($t = 4,310$; $df = 19$; two tailed; $p = 0,048$). Maximum statistical effect occurred at 212 ms ($t = 2,291$; $df = 19$; two tailed; $p = 0,0004$). The second interval with statistical effect started at 260 ms ($t = 2,180$; $df = 19$; two tailed; $p = 0,0004$) and ended at 400 ms ($t = 6,395$; $df = 19$; two tailed; $p = 0,0001$). The maximal statistical effect in this second interval occurred at 384 ms ($t = 5,097$; $df = 19$; two tailed; $p = 0,0000004$).

2.3. The LPP ERP

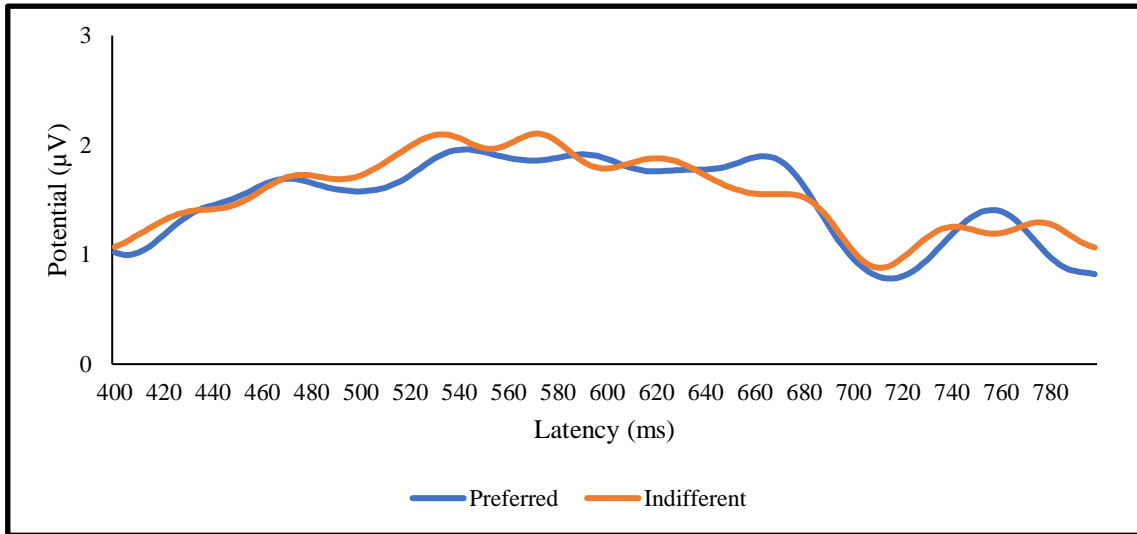


Figure 29 Average potential measured, for the preferred and indifferent categories, in the P3 electrode

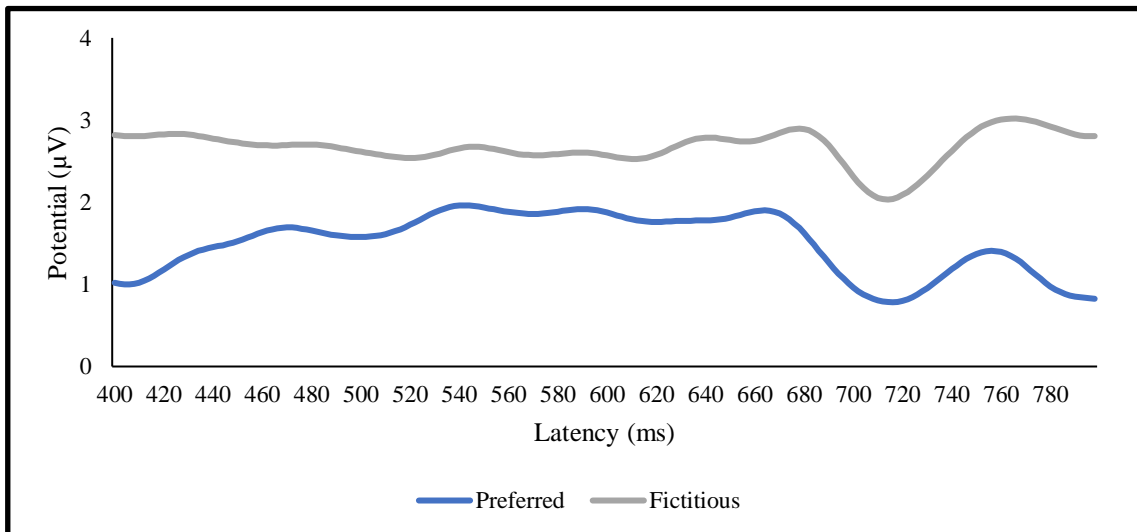


Figure 30 Average potential measured, for the preferred and fictitious categories, in the E52 electrode

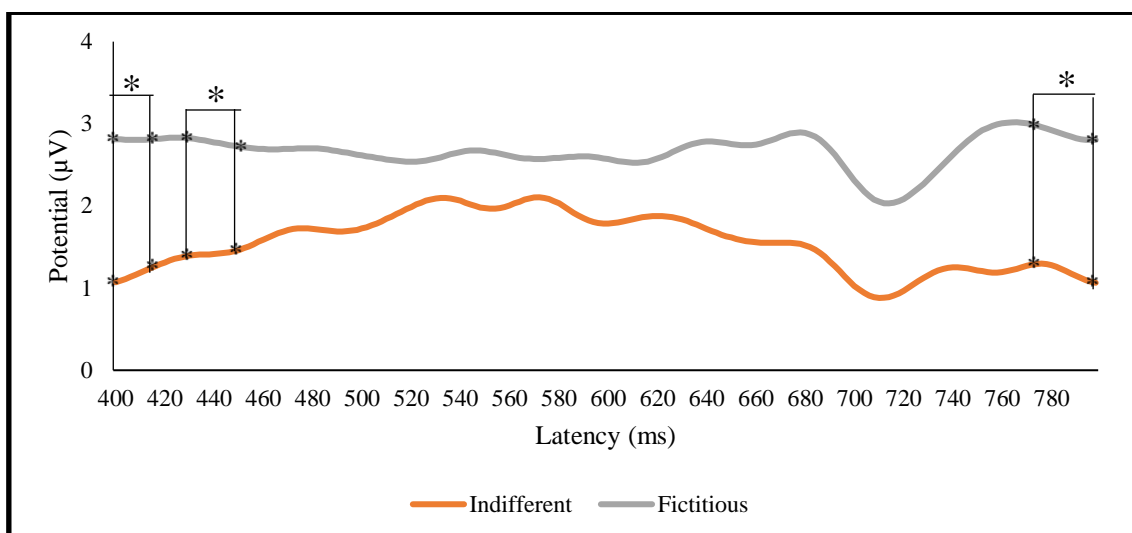


Figure 31 Average potential measured, for the indifferent and fictitious categories, in the E52 electrode

No statistical effect was obtained between preferred and indifferent brands, and between preferred and fictitious brands in the E52 electrode.

For the indifferent and fictitious brands, at E52 electrode site, the statistical effect started occurred at three different latency intervals. The earlier one started at 400 ms ($t = -2,779$; $df = 19$; two tailed; $p = 0,012$) until 418 ms ($t = -2,110$; $df = 19$; two tailed; $p = 0,048$). Maximum statistical effect occurred at 400 ms ($t = 2,291$; $df = 19$; two tailed; $p = 0,0004$). The middle interval with statistical effect started at 424 ms ($t = -2,109$; $df = 19$; two tailed; $p = 0,048$) and ended at 452 ms ($t = -2,104$; $df = 19$; two tailed; $p = 0,049$). The maximal statistical effect in this second interval occurred at 440 ms ($t = -2,555$; $df = 19$; two tailed; $p = 0,019$). The last interval with statistical effect occurred between 774 ms ($t = -2,108$; $df = 19$; two tailed; $p = 0,048$) and 798 ms ($t = -2,281$; $df = 19$; two tailed; $p = 0,034$). The maximal statistical effect in this interval occurred at 798 ms.

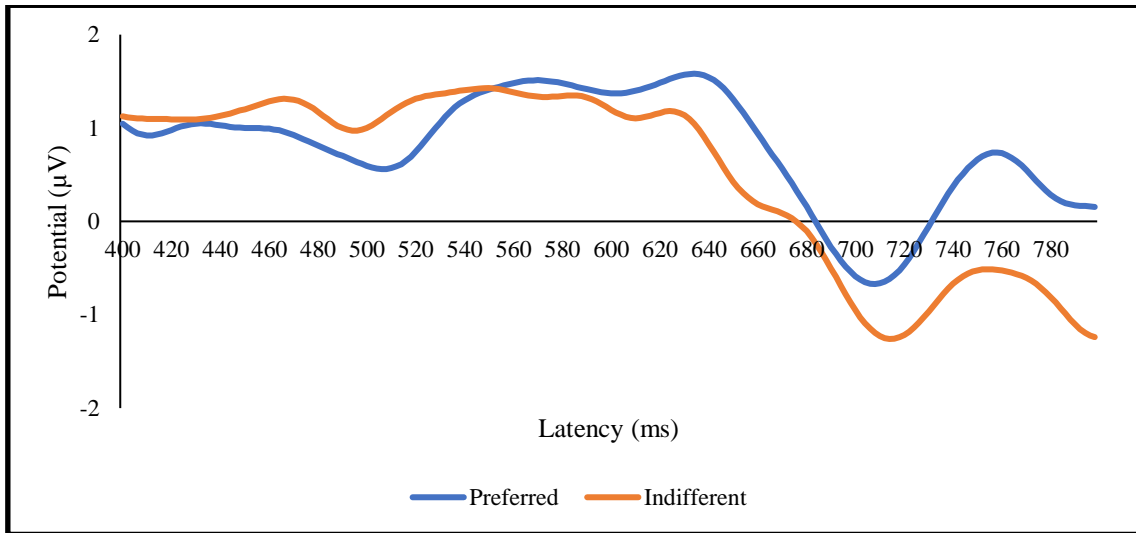


Figure 32 Average potential measured, for the preferred and indifferent categories, in the E62 electrode

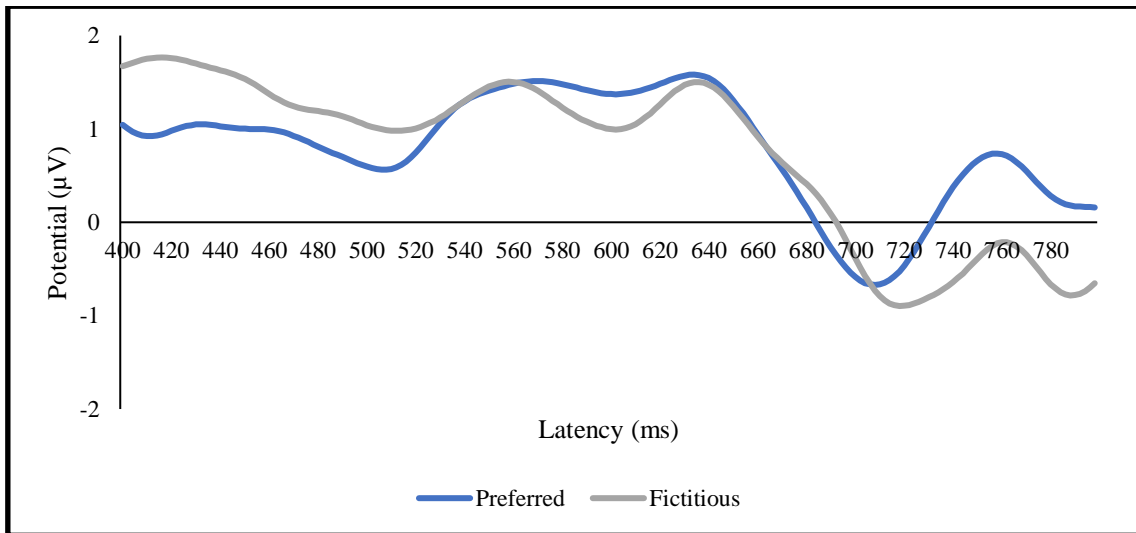


Figure 33 Average potential measured, for the preferred and fictitious categories, in the E62 electrode

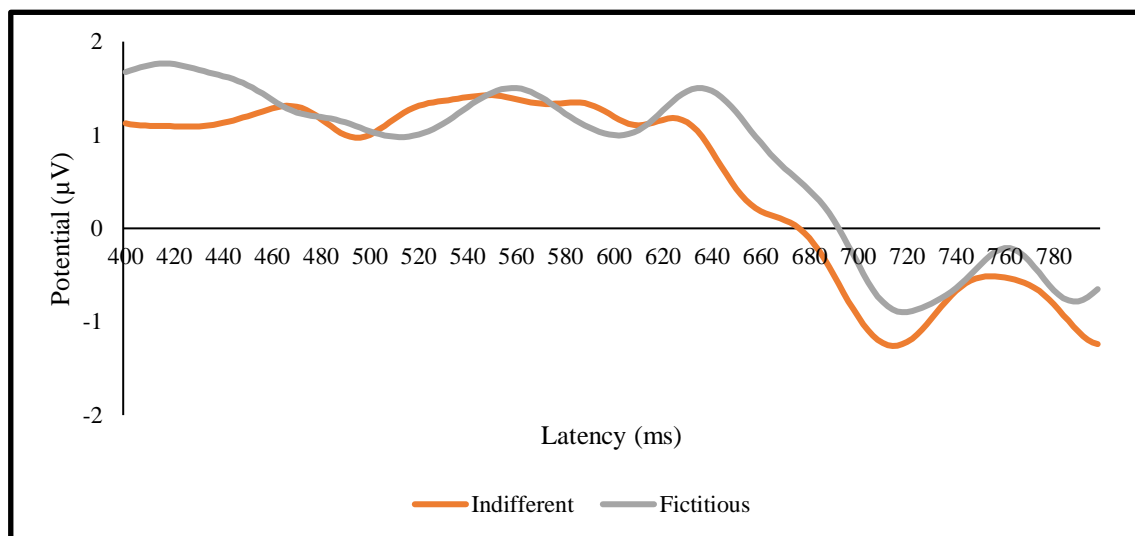


Figure 34 Average potential measured, for the indifferent and fictitious categories, in the E62 electrode

No statistical effect was observed between all condition pairs in the E62 electrode site.

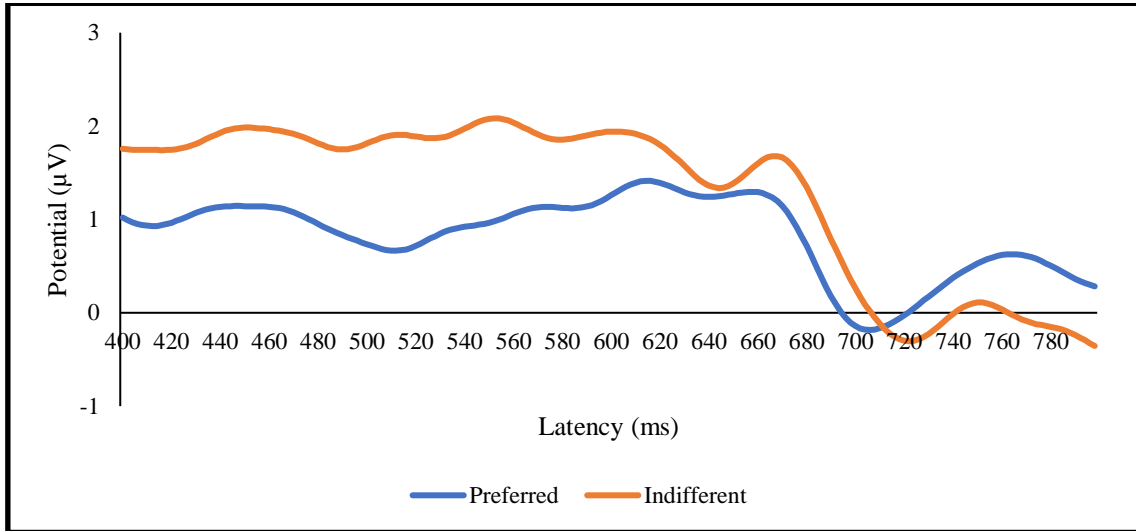


Figure 35 Average potential measured, for the preferred and indifferent categories, in the E92 electrode

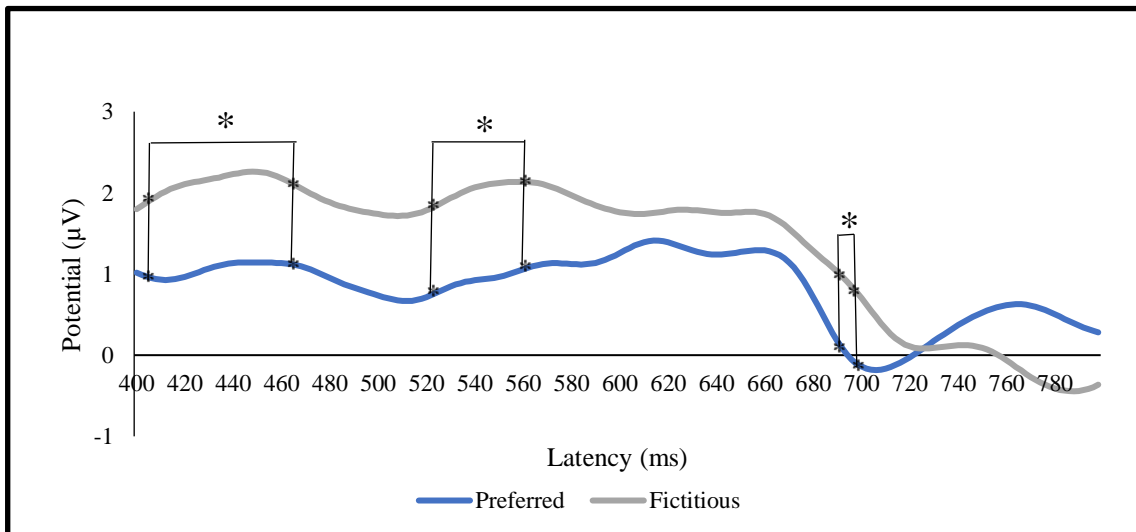


Figure 36 Average potential measured, for the preferred and fictitious categories, in the E92 electrode

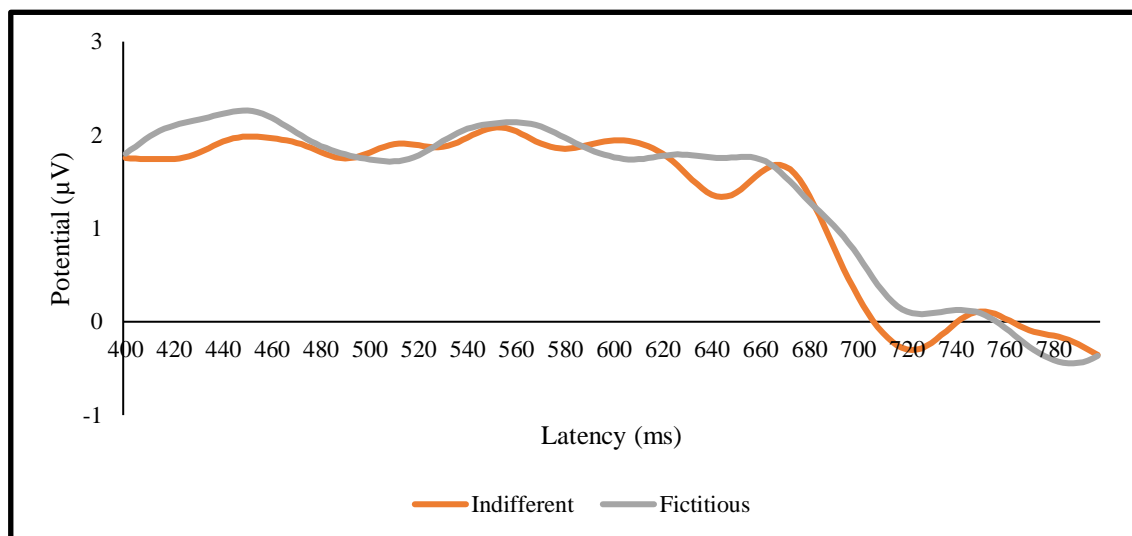


Figure 37 Average potential measured, for the indifferent and fictitious categories, in the E92 electrode

No statistical effect was obtained between preferred and indifferent brands, and between indifferent and fictitious brands in the E92 electrode.

For the preferred and fictitious brands, at E92 electrode site, the statistical effect started occurred at three different latency intervals. The earlier one started at 406 ms ($t = -2,160$; $df = 19$; two tailed; $p = 0,044$) until 466 ms ($t = -2,184$; $df = 19$; two tailed; $p = 0,042$). Maximum statistical effect occurred at 418 ms ($t = -2,616$; $df = 19$; two tailed; $p = 0,017$). The middle interval with statistical effect started at 524 ms ($t = -2,157$; $df = 19$; two tailed; $p = 0,044$) and ended at 562 ms ($t = -2,111$; $df = 19$; two tailed; $p = 0,048$). The maximal statistical effect in this second interval occurred at 542 ms ($t = -2,877$; $df = 19$; two tailed; $p = 0,010$). The last interval with statistical effect occurred between 692 ms ($t = -2,189$; $df = 19$; two tailed; $p = 0,041$) and 698 ms ($t = -2,198$; $df = 19$; two tailed; $p = 0,040$). The maximal statistical effect in this interval occurred at 694 ms ($t = -2,246$; $df = 19$; two tailed, $p = 0,034$).

3. Analysis of neural sources of brand valuation

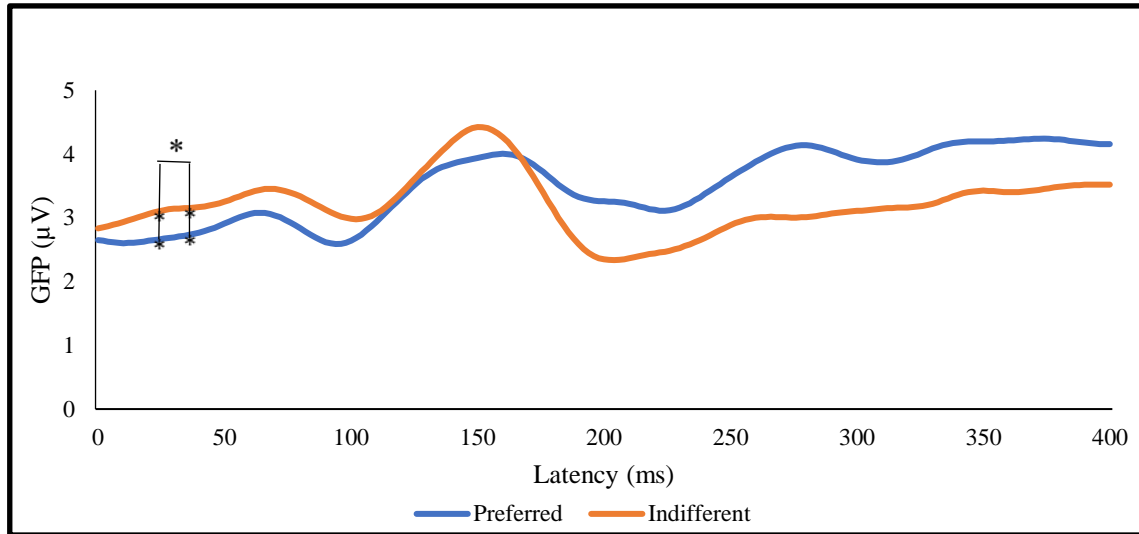


Figure 38 Average GFP for the preferred and indifferent categories

The significant statistical effect between the GFP elicited by preferred and indifferent brand logos occurred between the 24 ms ($t = -2,261$; $df = 19$; two tailed; $p = 0,036$) and the 36 ms ($t = -2,178$; $df = 19$; two tailed; $p = 0,042$) of latency. The maximum statistical effect between both brand categories occurred at 30 ms ($t = -2,438$; $df = 19$; two tailed; $p = 0,025$).

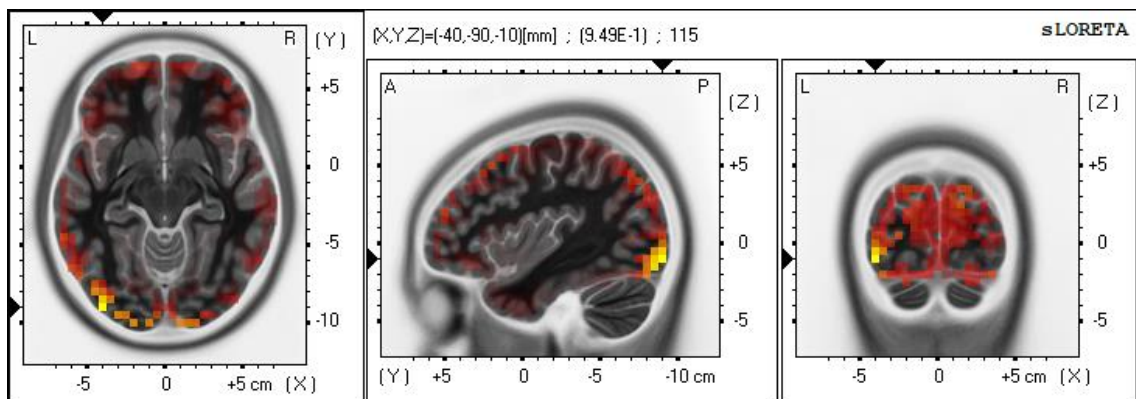


Figure 39 Average eLORETA image of neural source for preferred brand logos at 28 ms.

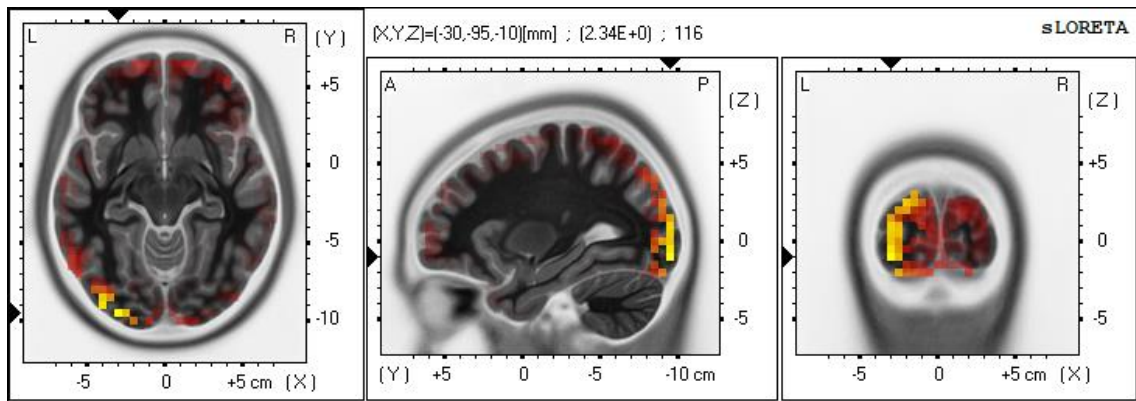


Figure 40 Average eLORETA image of the brain source for preferred brand logos at 30 ms.

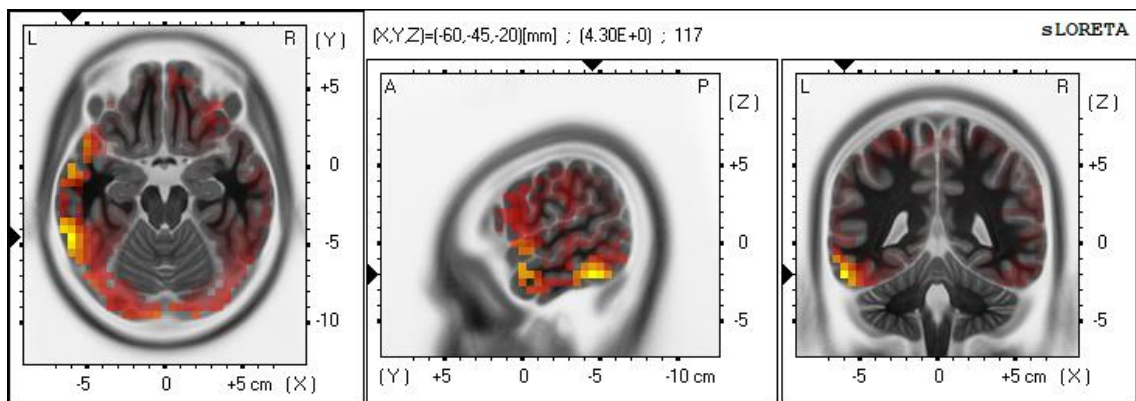


Figure 41 Average eLORETA image of the brain source for preferred brand logos at 32 ms.

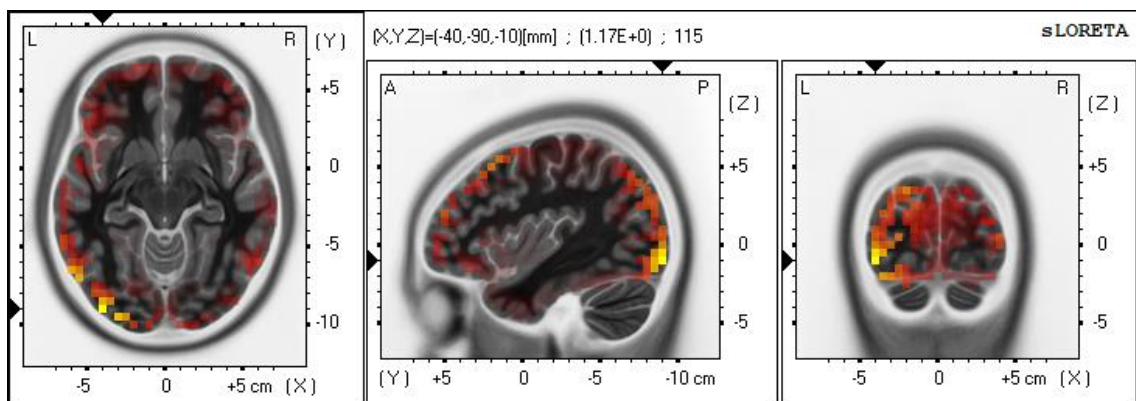


Figure 42 Average eLORETA image of neural source for indifferent brand logos at 28 ms.

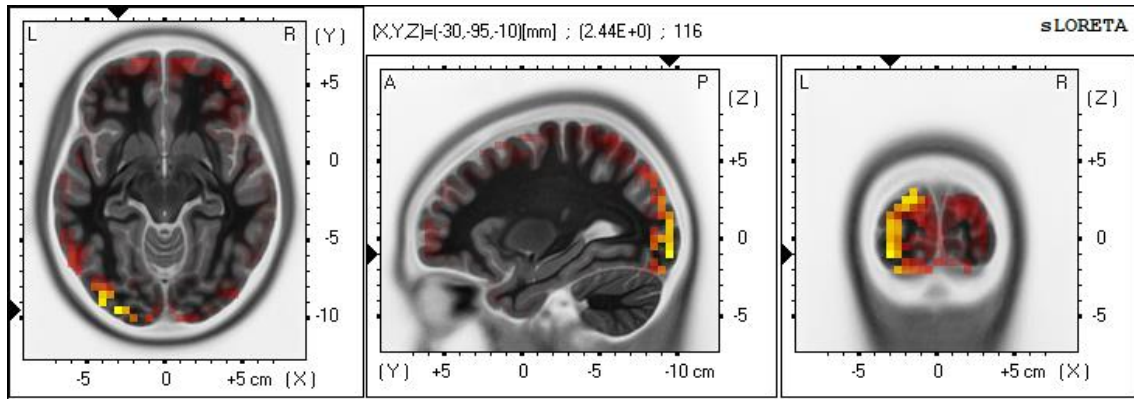


Figure 43 Average eLORETA image of the brain source for indifferent brand logos at 30 ms.

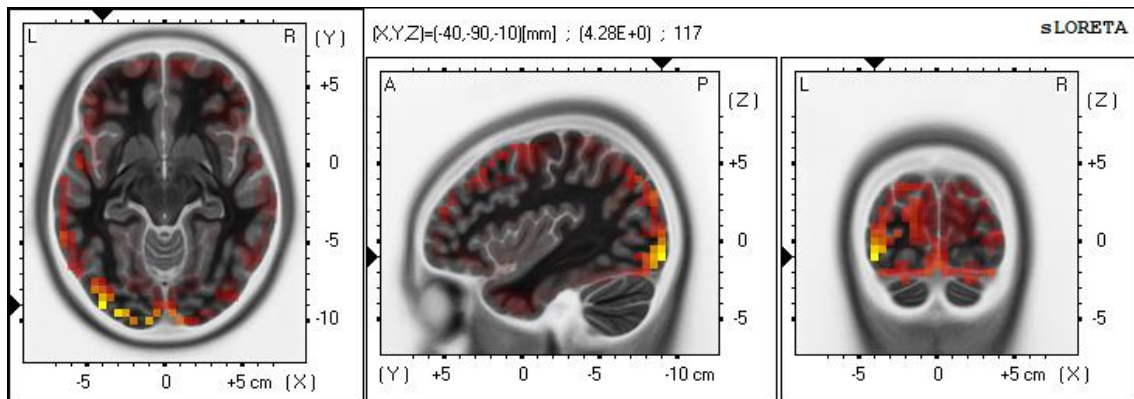


Figure 44 Average eLORETA image of the brain source for indifferent brand logos at 32 ms.

The neural source of the activity elicited by the preferred brands, between the 28 ms of latency and the 30 ms was the left inferior occipital gyrus, demonstrating a lorGFP value of 0,949 μV , at 28 ms, and 2,34 μV at 30 ms. At 32 ms, the preferred brands elicited the highest activity in the left middle temporal gyrus, with the lorGFP having, as its value, 4,30 μV .

The neural source of the activity elicited by the indifferent brands, between the 28 ms of latency and the 32 ms was the left inferior occipital gyrus, demonstrating a lorGFP value of 1,17 μV , at 28 ms, 2,34 μV at 30 ms, and at 32 ms, a value of 4,28 μV .

The paired t-test produced between these two experimental conditions obtained the following results: at 28 ms ($t = -0,596$), at 30 ms ($t = -0,246$), and at 32 ms (for the left middle temporal gyrus: $t = 0,915$; for the left inferior occipital gyrus: $t = -0,0702$).

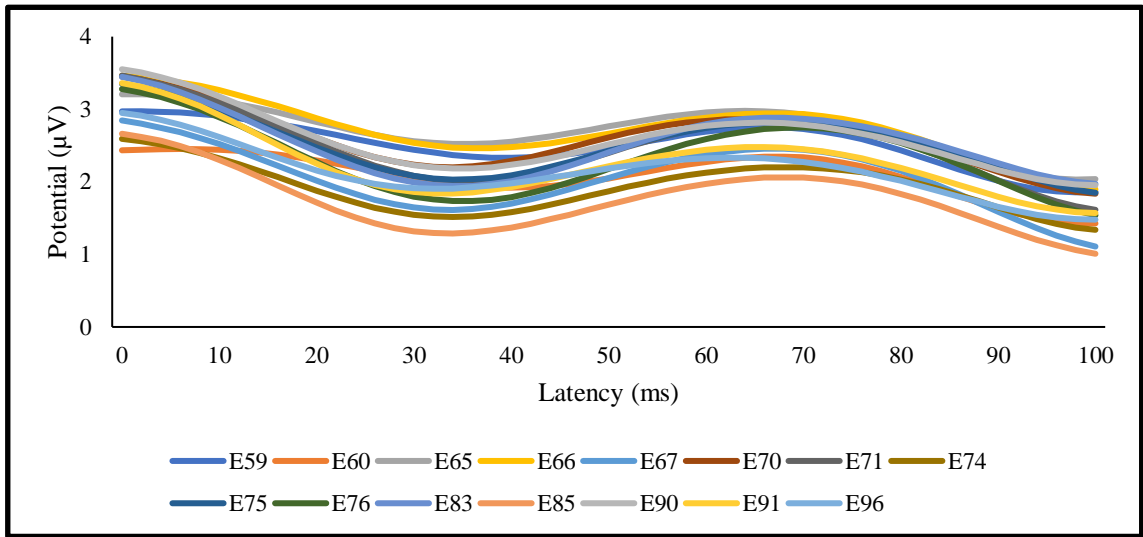


Figure 45 Average potential registered in the occipital electrodes for the “preferred” brand logos, from 0 ms to 100 ms of latency.

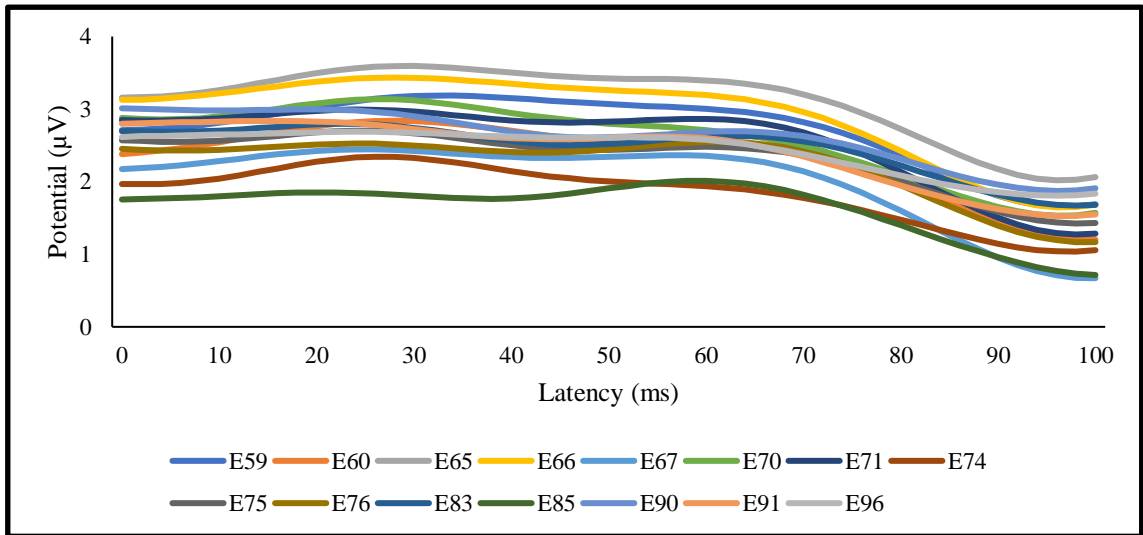


Figure 46 Average potential registered in the occipital electrodes for the “indifferent” brand logos, from 0 ms to 100 ms of latency.

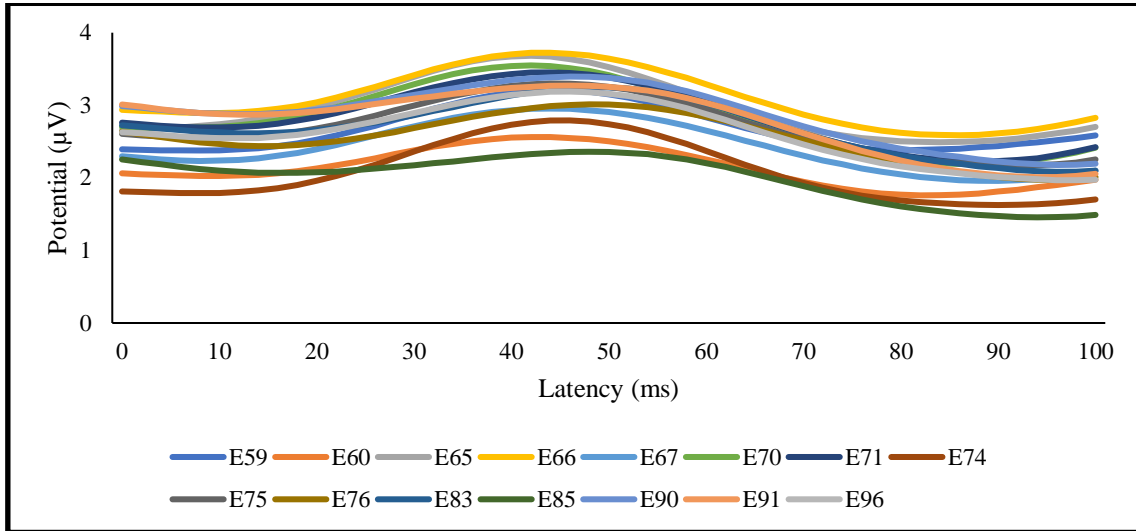


Figure 47 Average potential registered in the occipital electrodes for the “fictitious” brand logos, from 0 ms to 100 ms of latency.

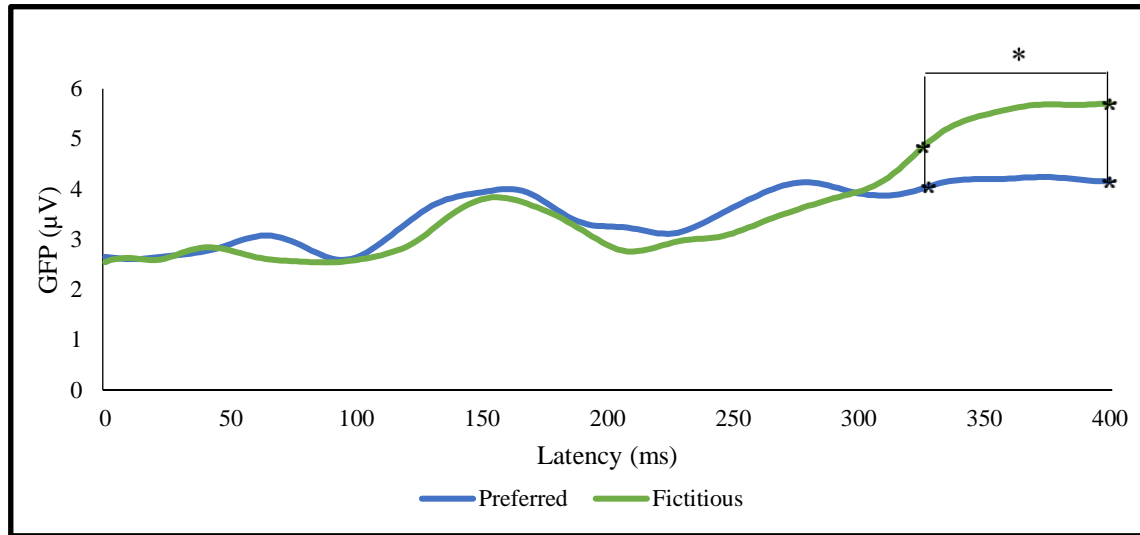


Figure 48 Average GFP for the preferred and fictitious categories

The significant statistical effect between the GFP elicited by preferred and fictitious brand logos occurred between the 326 ms ($t = 2,307$; $df = 19$; two tailed; $p = 0,032$) and the 400 ms ($t = -2,125$; $df = 19$; two tailed; $p = 0,047$) of latency. The maximum statistical effect between both brand categories occurred at 378 ms ($t = 4,992$; $df = 19$; two tailed; $p = 0,00008$).

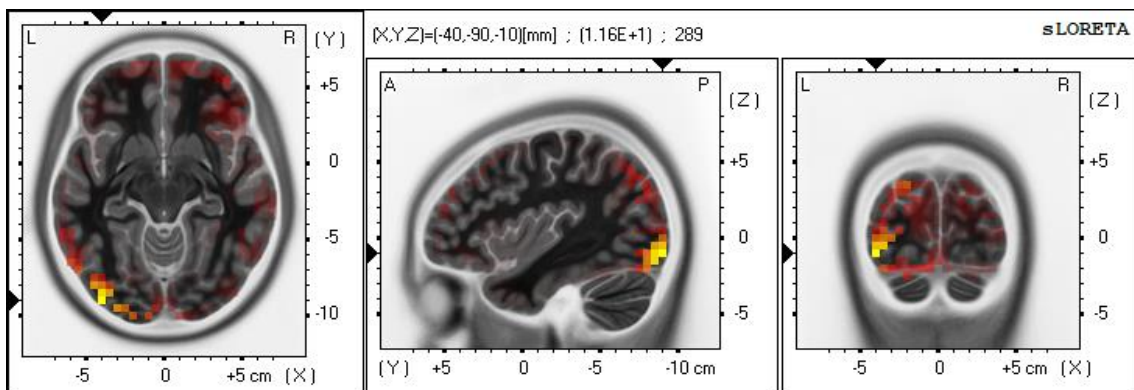


Figure 49 Average eLORETA image of the brain source for preferred brand logos at 376 ms.

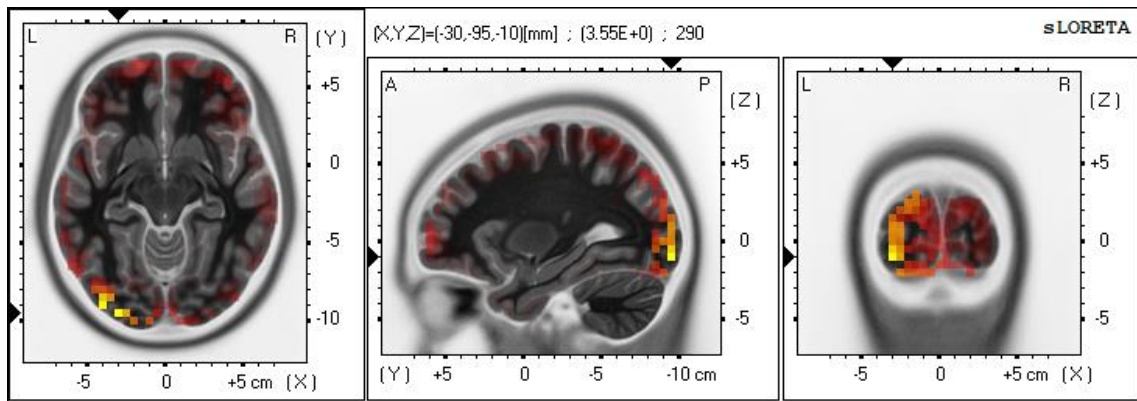


Figure 50 Average eLORETA image of the brain source for preferred brand logos at 378 ms.

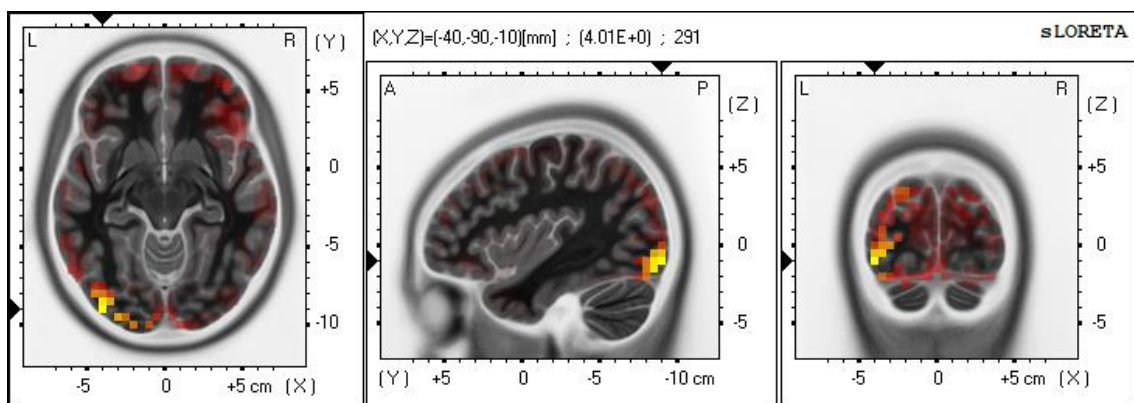


Figure 51 Average eLORETA image of the brain source for preferred brand logos at 380 ms.

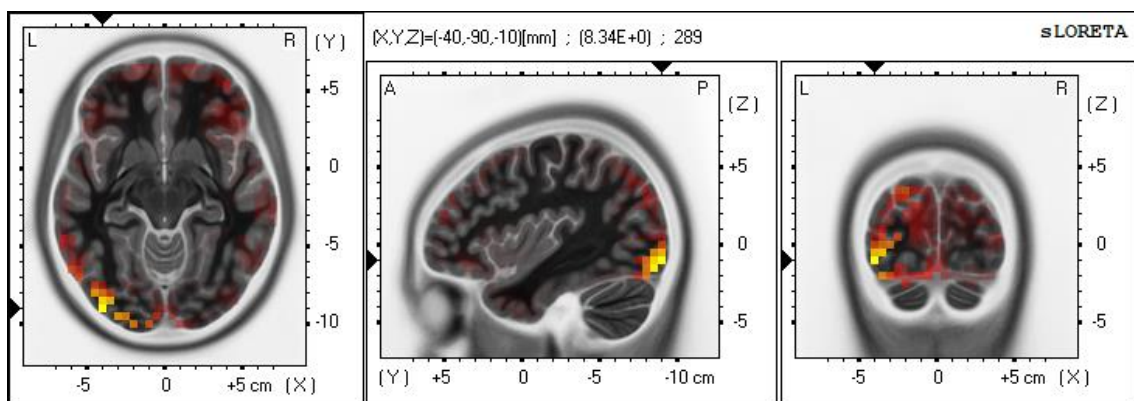


Figure 52 Average eLORETA image of the brain source for fictitious brand logos at 376 ms.

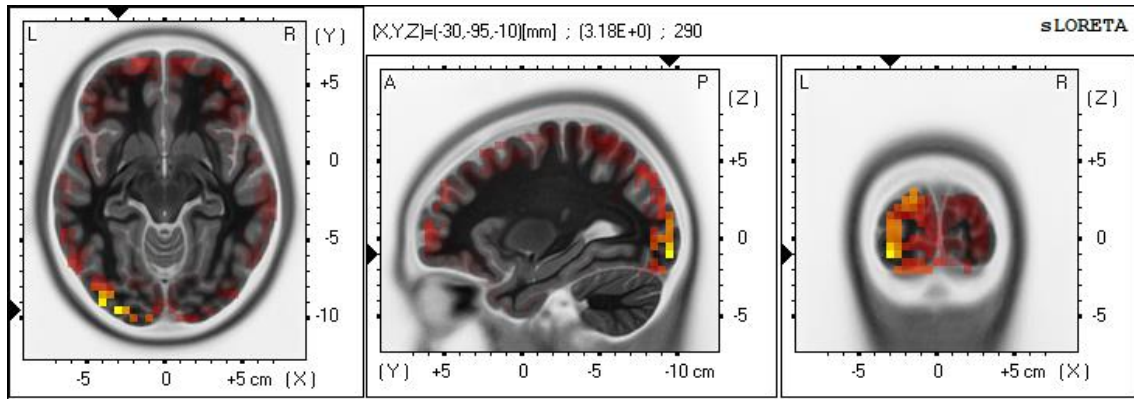


Figure 53 Average eLORETA image of the brain source for fictitious brand logos at 378 ms.

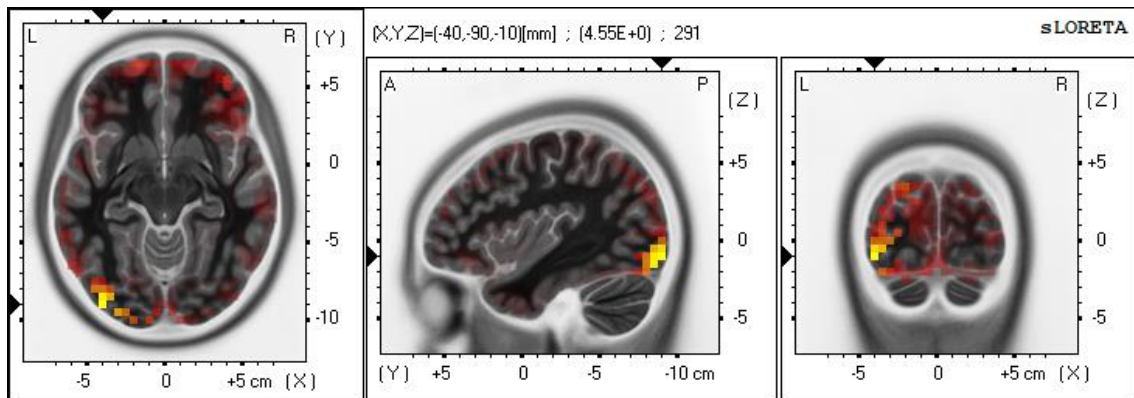


Figure 54 Average eLORETA image of the brain source for fictitious brand logos at 380 ms.

The neural source of the activity elicited by the preferred brands, between the 376 ms of latency and the 380 ms was the left inferior occipital gyrus, demonstrating a lorGFP value $11,6 \mu\text{V}$, at 376 ms, $3,55 \mu\text{V}$ at 378 ms, and $4,01 \mu\text{V}$ at 380 ms.

The neural source of the activity elicited by the fictitious brands, between the 376 ms of latency and the 380 ms was the left inferior occipital gyrus, demonstrating a lorGFP value of $8,34 \mu\text{V}$, at 376 ms, $3,18 \mu\text{V}$ at 378 ms, and at 380 ms, a value of $4,55 \mu\text{V}$.

The paired t-test produced between these two experimental conditions obtained the following results: at 376 ms ($t = 1,36$), at 378 ms ($t = 0,686$), and at 380 ms ($t = -0,522$).

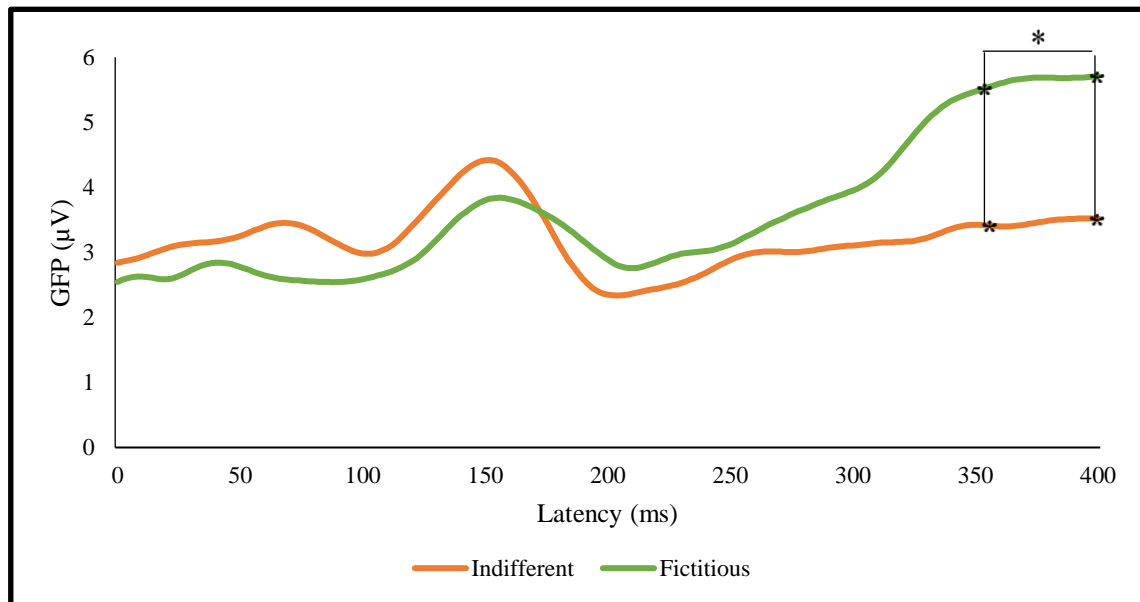


Figure 55 Average GFP for the indifferent and fictitious categories

The significant statistical effect between the GFP elicited by indifferent and fictitious brand logos occurred between the 354 ms ($t = -2,115$; $df = 19$; two tailed; $p = 0,048$) and the 400 ms ($t = -2,125$; $df = 19$; two tailed; $p = 0,047$) of latency. The maximum statistical effect between both brand categories occurred at 372 ms ($t = -2,474$; $df = 19$; two tailed; $p = 0,023$).

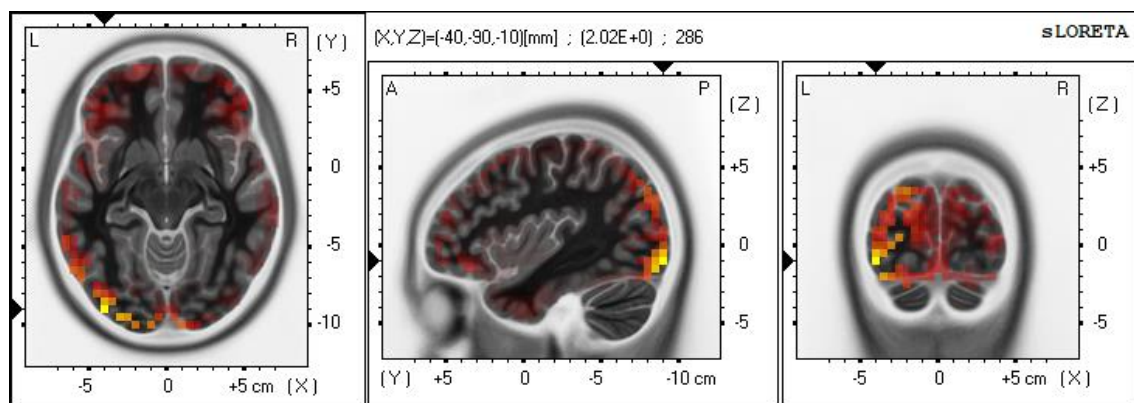


Figure 56 Average eLORETA image of the brain source for indifferent brand logos at 370 ms.

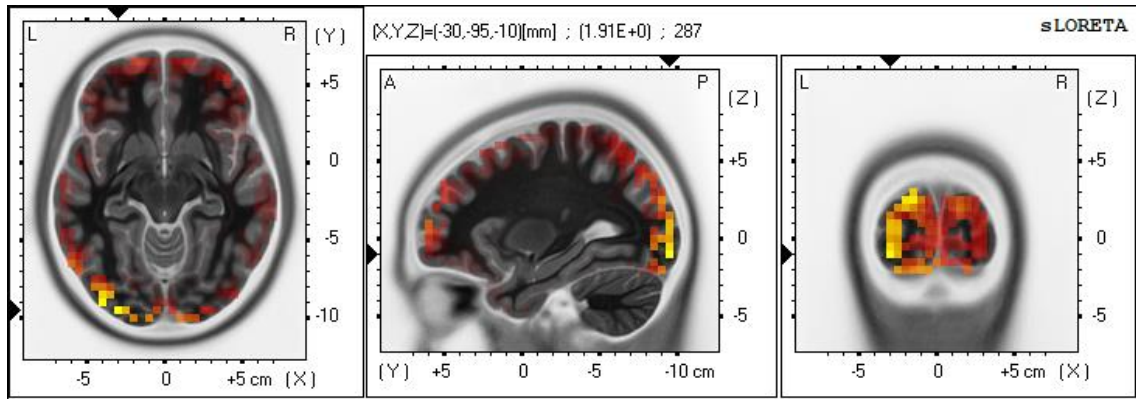


Figure 57 Average eLORETA image of the brain source for indifferent brand logos at 372 ms.

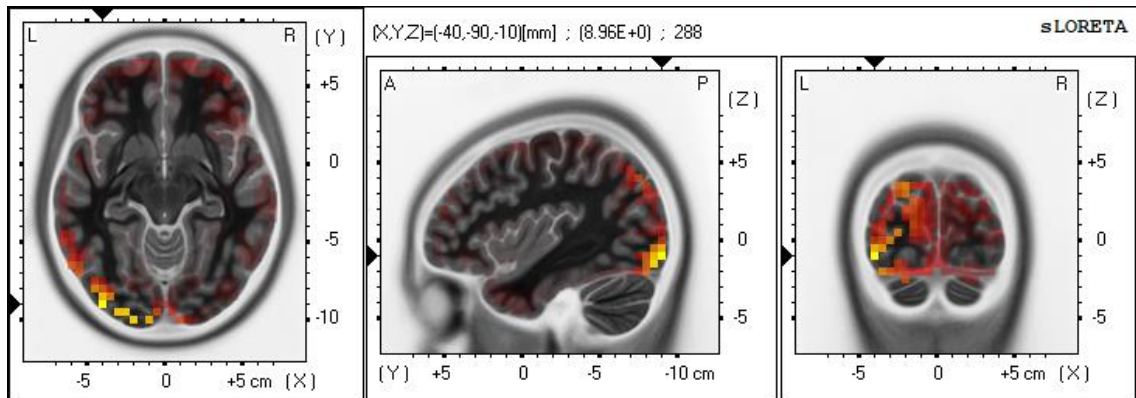


Figure 58 Average eLORETA image of the brain source for indifferent brand logos at 374 ms.

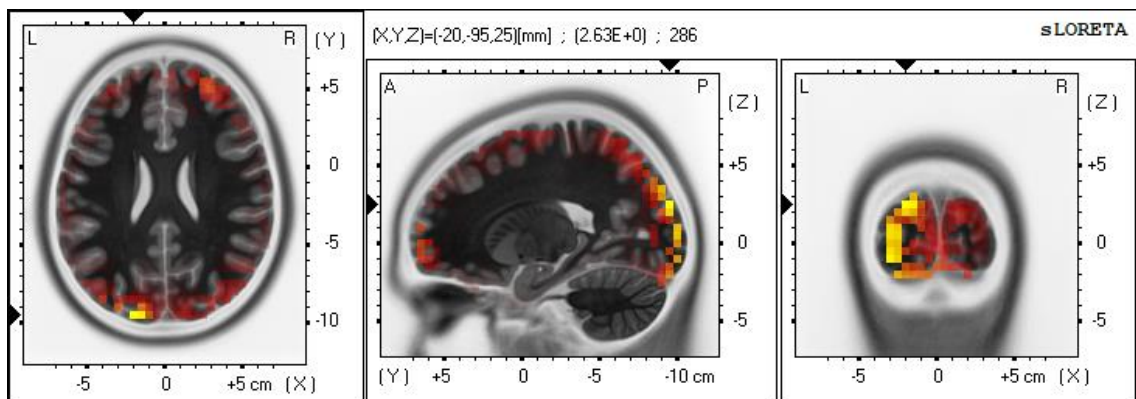


Figure 59 Average eLORETA image of the brain source for fictitious brand logos at 370 ms.

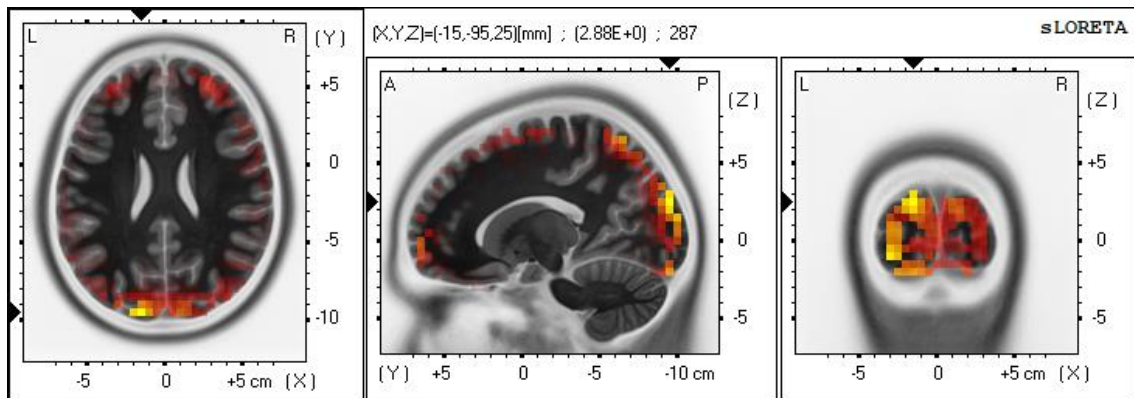


Figure 60 Average eLORETA image of the brain source for fictitious brand logos at 372 ms.

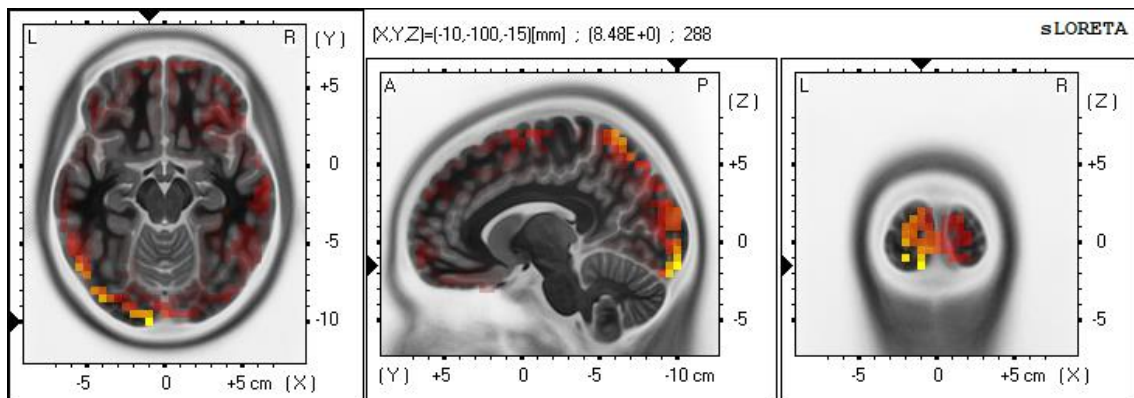


Figure 61 Average eLORETA image of the brain source for fictitious brand logos at 374 ms.

The neural source of the activity elicited by the indifferent brands, between the 370 ms of latency and the 374 ms was the left inferior occipital gyrus, demonstrating a lorGFP value 2,02 μV , at 370 ms, 1,91 μV at 372 ms, and 8,96 μV at 372 ms.

The neural source of the activity elicited by the fictitious brands, at 370 ms, was the left cuneus, with a lorGFP value of 2,63 μV , and at 372 ms, with a lorGFP value of 2,88 μV . At 374 ms, the neural source was the left lingual gyrus, with a lorGFP value of 8,48 μV

The paired t-test produced between these two experimental conditions obtained the following results: at 370 ms (at left inferior occipital gyrus: $t = -1,00$; at left cuneus: $t = -1,86$), at 378 ms (at the left inferior occipital gyrus: $t = -1,86$; at left cuneus: $t = -1,67$), and at 380 ms (at left inferior occipital gyrus: $t = 0,549$; at left lingual gyrus: $t = 0,121$).

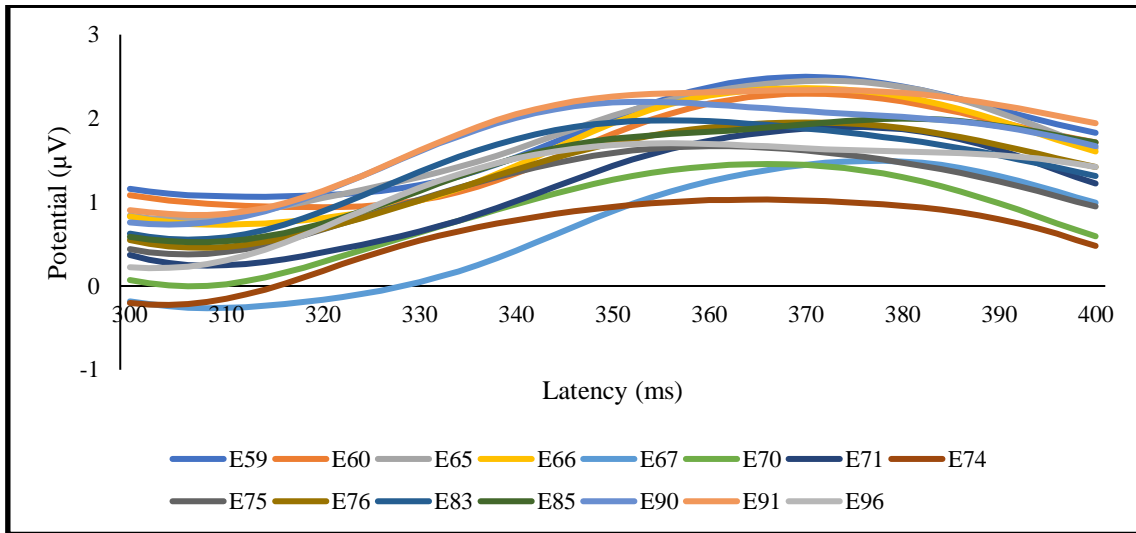


Figure 62 Average potential registered in the occipital electrodes for the “preferred” brand logos from 300 ms to 400 ms of latency.

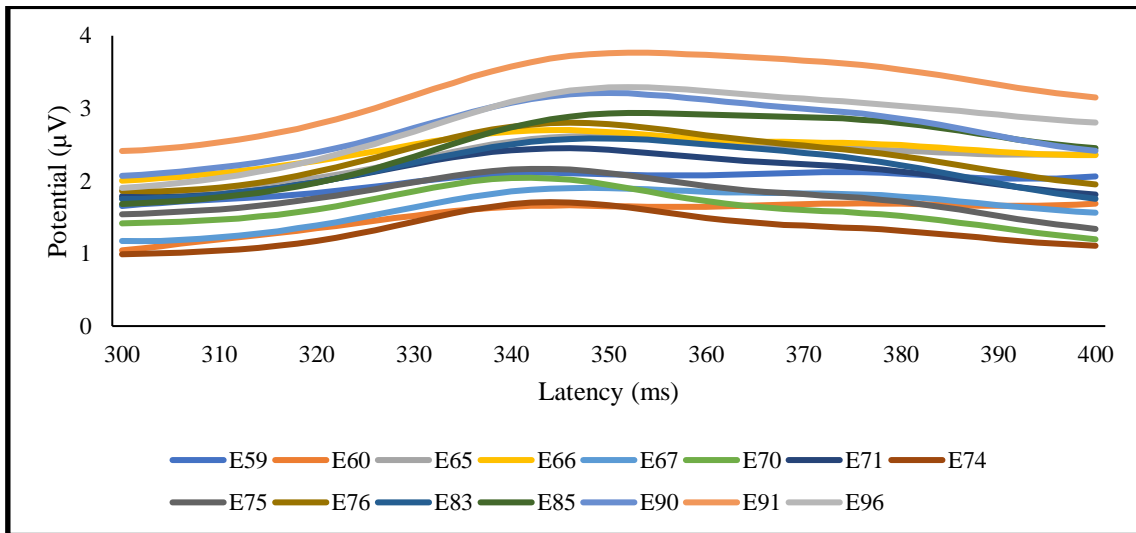


Figure 63 Average potential registered in the occipital electrodes for the “indifferent” brand logos from 300 ms to 400 ms of latency.

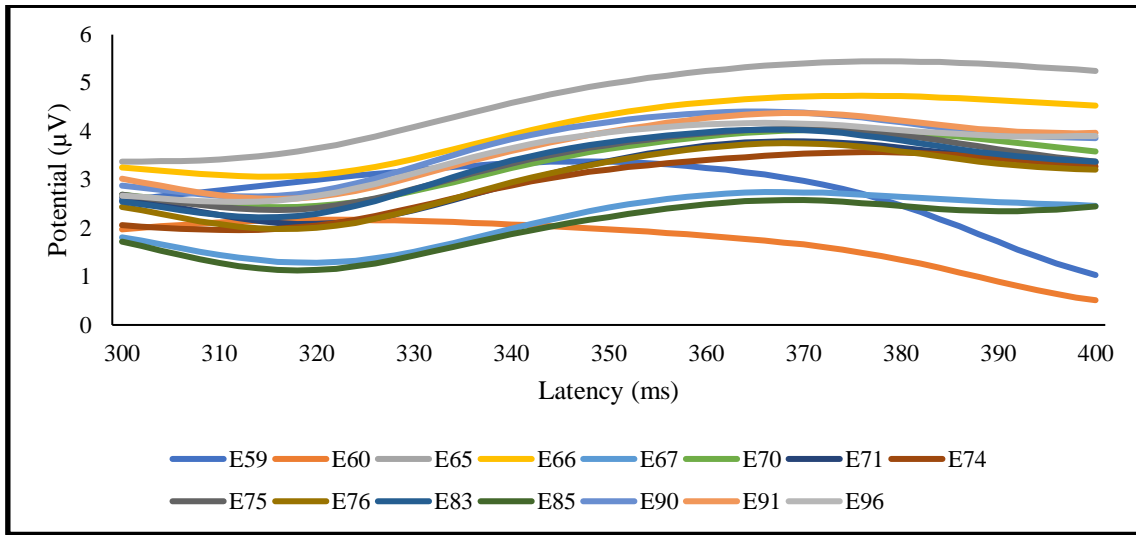


Figure 64 Average potential registered in the occipital electrodes for the “fictitious” brand logos from 300 ms to 400 ms of latency.

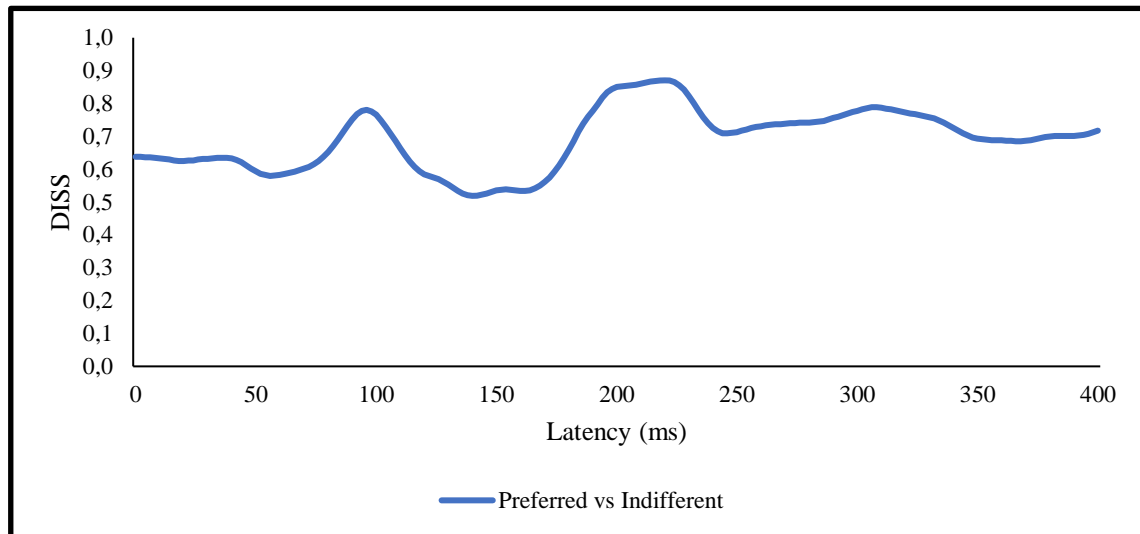


Figure 65 Global dissimilarity values for the preferred and the indifferent categories

The DISS calculated between the preferred and indifferent categories reached its maximum value (DISS = 0,87) at 220 ms of latency, and the minimum value (DISS = 0,52) at 140 ms. In the interval in which a statistical effect was determined between the GFP of both categories, the value of DISS varied between 0,63 (at 24 ms) and 0,64 (at 36 ms). When the maximum statistical effect was observed (30 ms), the value of DISS was 0,63.

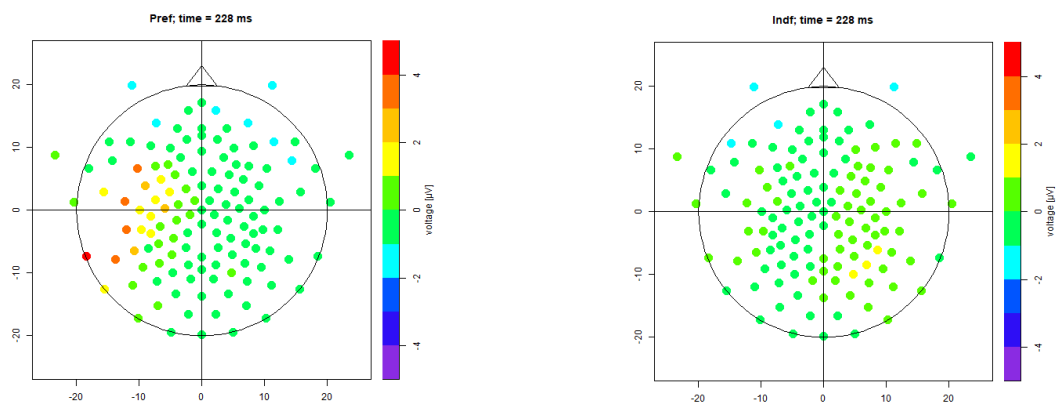


Figure 66 Brain topographic map at 220 ms (max. DISS), for the preferred and for the indifferent categories

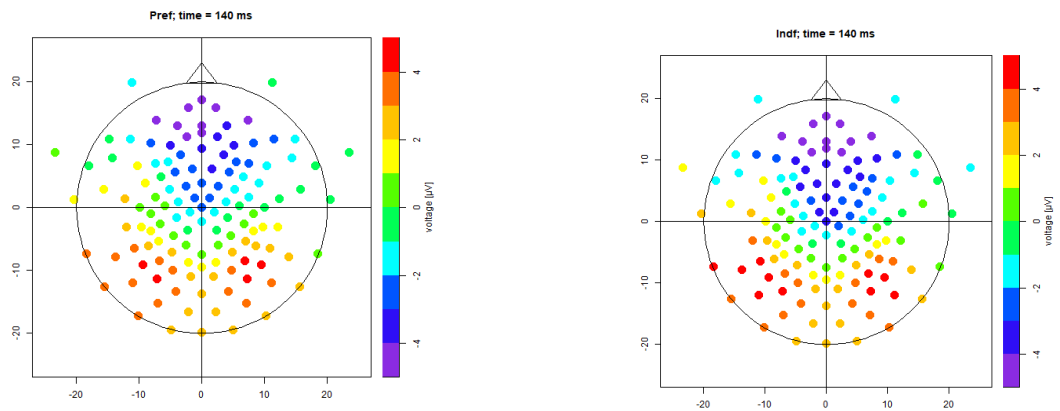


Figure 67 Brain topographic map at 140 ms (min. DISS), for the preferred and for the indifferent categories

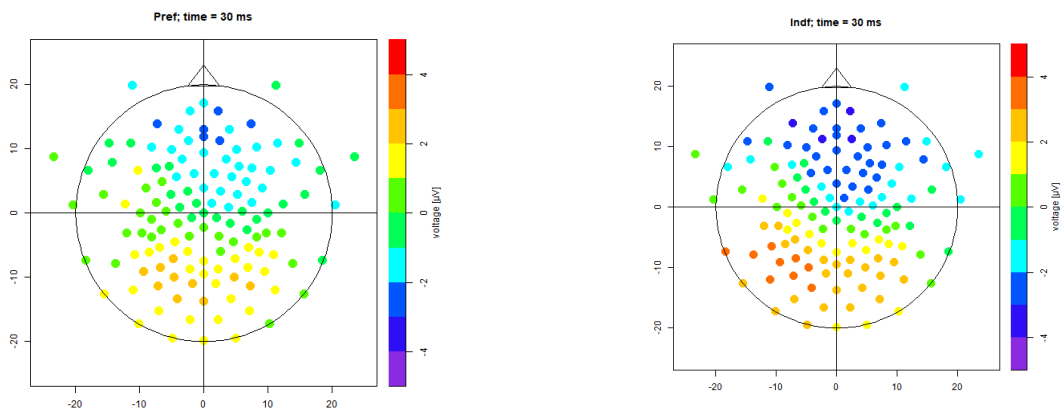


Figure 68 Brain topographic map at 30 ms (max. statistical effect), for the preferred and for the indifferent categories

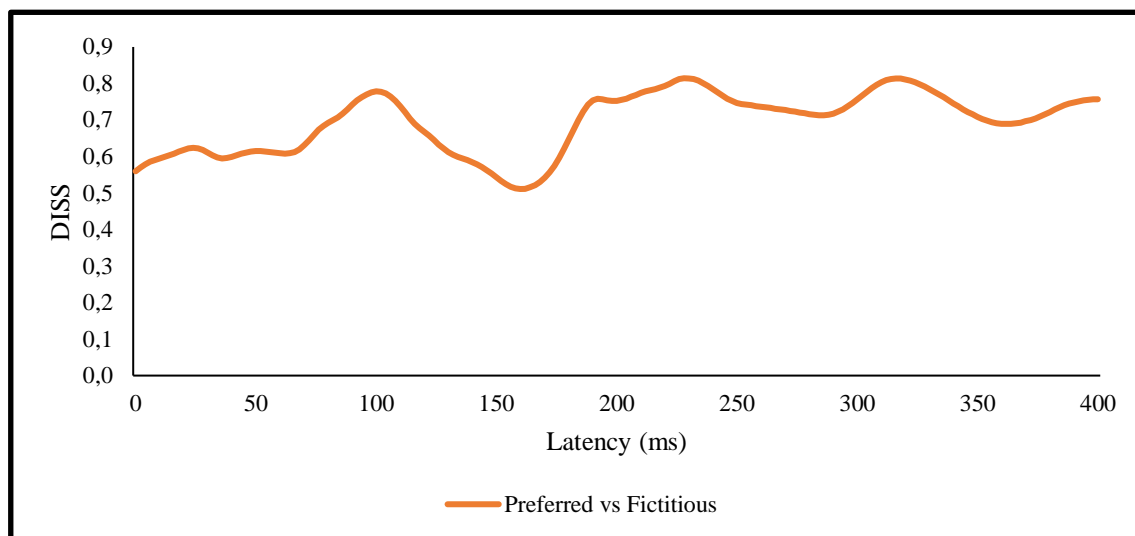


Figure 69 Global dissimilarity values for the preferred and the fictitious categories

The DISS calculated between preferred and fictitious categories reached its maximum value (DISS = 0,81) at 228 ms of latency, and the minimum value (DISS = 0,51) at 160 ms. In the interval in which a statistical effect was determined between the GFP of both categories, the value of DISS varied between 0,80 (at 326 ms) and 0,76 (at 400 ms). When the maximum statistical effect was observed (378 ms), the value of DISS was 0,72.

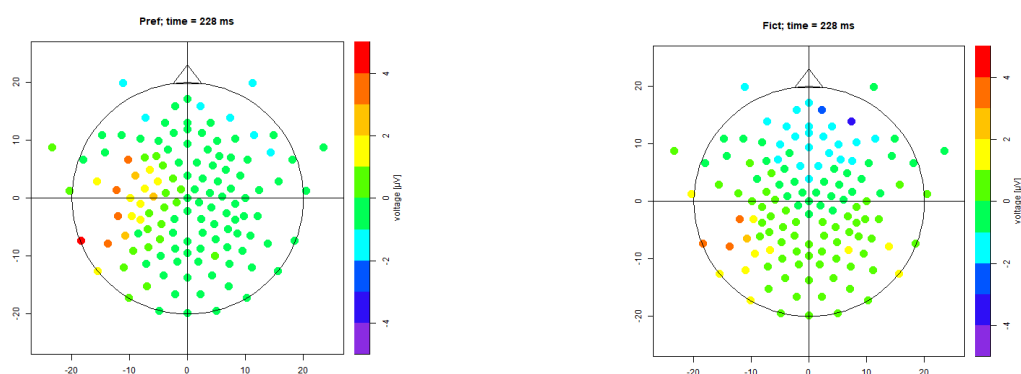


Figure 70 Brain topographic map at 228 ms (max. DISS), for the preferred and for the fictitious categories

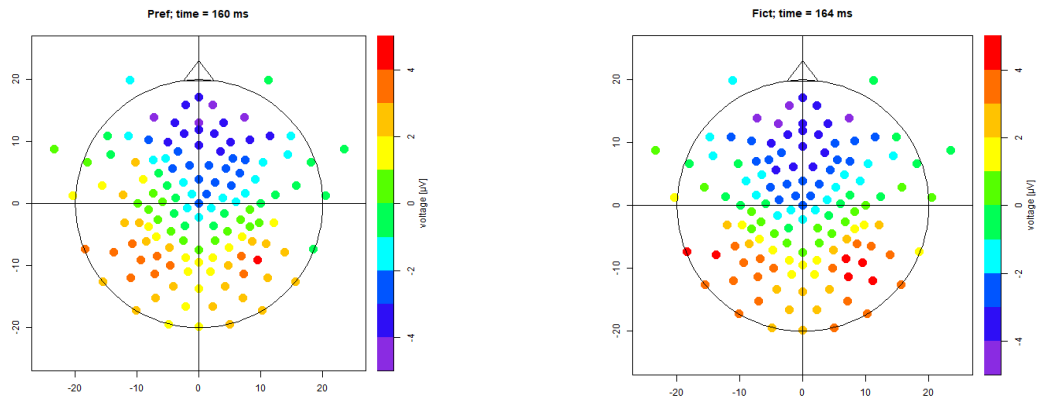


Figure 71 Brain topographic map at 160 ms (min. DISS), for the preferred and for the fictitious categories

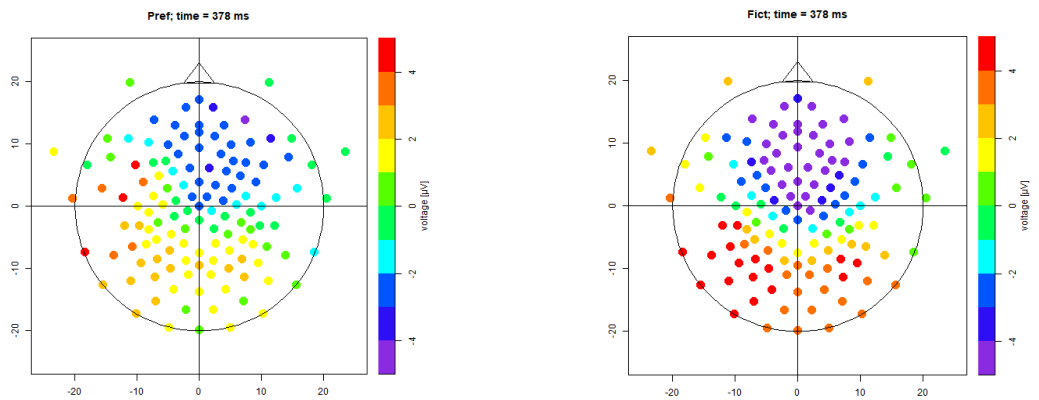


Figure 72 Brain topographic map at 378 ms (max. statistical effect), for the preferred and for the fictitious categories

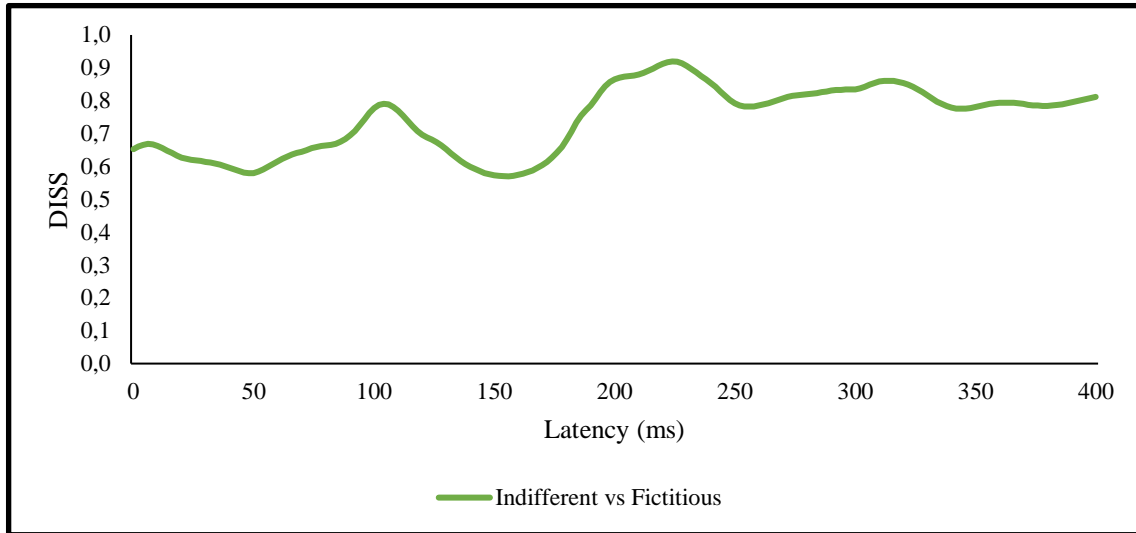


Figure 73 Global dissimilarity values for the indifferent and the fictitious categories

The DISS calculated between preferred and fictitious categories reached its maximum value (DISS = 0,92) at 224 ms of latency, and the minimum value (DISS = 0,57) at 154 ms. In the interval in which a statistical effect was determined between the GFP of both categories, the value of DISS varied between 0,79 (at 356 ms) and 0,81 (at 400 ms). When the maximum statistical effect was observed (372 ms), the value of DISS was 0,79.

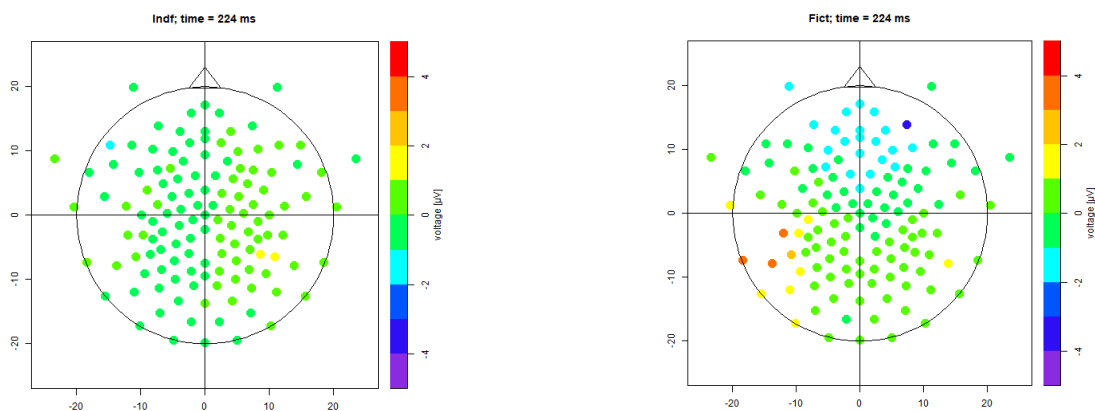


Figure 74 Brain topographic map at 224 ms (max. DISS), for the indifferent and for the fictitious categories

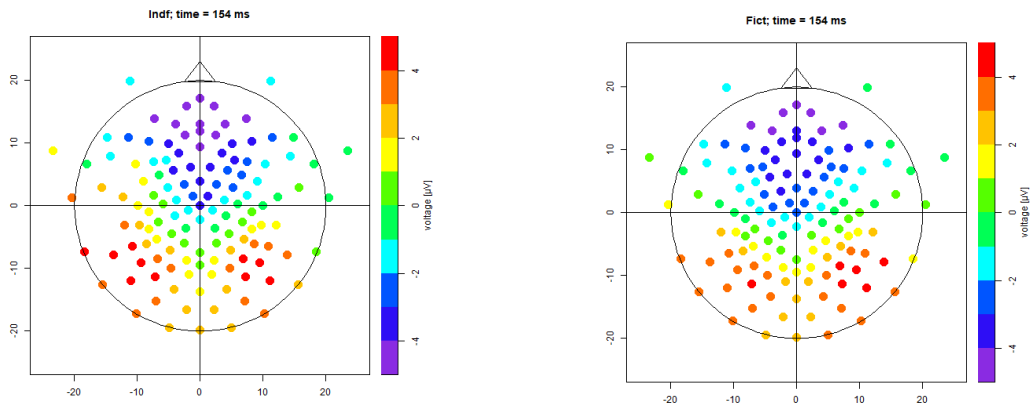


Figure 75 Brain topographic map at 154 ms (min. DISS), for the indifferent and for the fictitious categories

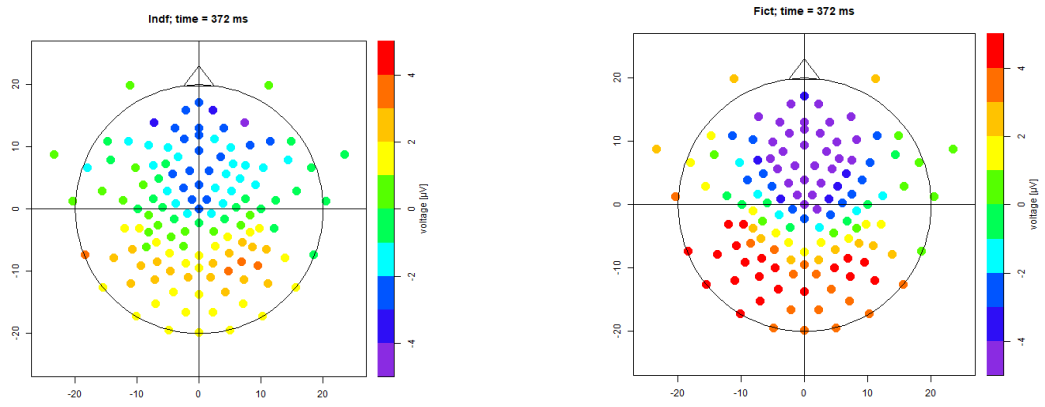


Figure 76 Brain topographic map at 372 ms (max. statistical DISS), for the indifferent and for the fictitious categories

Discussion

1. Event-related potentials associated with the expression of preference

For evaluating the cognitive process of brand preference, we have referenced four event-related potentials that were directly associated with this specific cognitive process. They were the N100, the N200, the P300, and the Late Positive Potential (LPP).

To verify the behaviour of brain activity concerning the N100 ERP, we analysed the potentials registered for the three main occipital electrodes of the system that we use. The results we obtained agree with some of the results that were reported in Nazari et al. (2019), however, it may contradict its conclusion. When we verify the potential registered in the left occipital electrode (E70 / O1), central occipital electrode (E75 / Oz), and right occipital electrode (E83 / O2), we could verify that both preferred and indifferent brand logos elicit greater negativity, around the 100 ms, when compared with fictitious brand logos. However, when comparing the preferred and the indifferent brand logos, the potential registered presented higher negativity for the indifferent ones, although this potential discrepancy evoked between the two categories is very small. Another result that differed between our experiment and Nazari et al. (2019) experiment was the latency of this component. In our experiment, the peak latencies of preferred and indifferent brand logos were later than the peak latency of the fictitious brand logos, contradicting the results presented by Nazari et al. (2019), where the familiar brand logos presented an earlier peak latency than the unfamiliar ones, represented, in our work, by the fictitious brand logos. Our experiment also could not replicate the extent of amplitude decrease such as the ones described in Nazari et al. (2019) presenting only a slight decrease between the three categories studied. Our results may then contradict the results of Nazari et al. (2019), since they associated the N100 with the expression of preference, since they verified that the majority of the expressed preference was associated with brands presented in the familiar set of brand logos. However, considering our results, we could contest that claim and add another hypothesis for the interpretation of the N100 ERP. We could claim that the N100t may express an electrophysiological marker of familiarity in relation to a brand logo instead of expressing the personal preference of a subject for a specific brand logo.

Other ERPs that we studied in this experiment, which were associated with the construction of preference for a certain brand, were the N200, or more properly, the N2b,

associated with conscious attention to visual stimuli, and the P300. Generally, both are directly correlated, and preferably visualized in the left frontal electrode (E24 / F3), the central frontal electrode (E11 / Fz), and the right frontal electrode (E124 / F4). In the study of Q. Ma et al. (2019) increased negativity, around the 200 ms, was elicited by non-preferred brand logos when compared with the potential registered for the preferred brand logos. In our results, we could not verify this same variation in the potential registered in the same electrodes, having even been verified positivities for all three experimental conditions. Taking into account the main aim for the Q. Ma et al. (2019) study, which was the influence of ethnicity in the development of preference, the N200 ERP may be related to cultural biases towards brands evaluation, a hypothesis that could not be verified in our work, taking into account the experimental protocol that we used, whose participants all belonged to the same ethnicity, this being a possible reason for not being able to replicate the same results as Q. Ma et al. (2019).

Concerning the P300, we verified the potential registered for the same three frontal electrodes then we compared the results reported in Khushaba et al. (2015) and Gajewski et al. (2016). In this case, it was possible to verify a positivity, around 300 ms, for the preferred and fictitious brand logos, being that the indifferent brand logos did not elicit the same component. However, comparing the amplitudes of the potential registered, we could verify that the preferred brands elicited a higher positivity when compared with the potential registered for the fictitious brand logos in all three electrodes, and higher than the potential registered the left frontal electrode. These results replicate the ones presented in Khushaba et al. (2015) and in Gajewski et al. (2016) since they both report higher amplitudes for the P300 ERP when soliciting a decision between a preferred and a non-preferred option. This could mean that the measurement of the P300 component in frontal sites can be an interesting neurophysiological marker to verify brand valuation.

Concerning the late positive potential, we used the results of Bosshard et al. (2016) as a reference. To verify, we analysed the potential registered in the three main parietal electrodes, the left parietal electrode (E52 / P3), the central parietal electrode (E62 / Pz), and the right parietal electrode (E92 / P4) after the 400 ms of latency. The results obtained by Bosshard et al. (2016) were not replicated in our experiment. Both in terms of the amplitude of the ERPs for the different categories evaluated and for the laterality of the ERP verified by Bosshard et al. (2016). In this work, the preferred brands exhibit higher

positivity for the liked brands than for the disliked brands. In our work, we didn't classify any brand as disliked, this is, no brand was negatively evaluated, so we did not have a complete replica, but we had the indifferent brands, which had a lower value for each of the subjects, and the fictitious brands, which should not have any value for the subjects. So, it would be expected that the preferred brand logos should elicit the effect described above when compared with the indifferent and fictitious brand logos. However, only in the potential registered in the E62 (Pz) electrode was possible to observe higher amplitudes for the preferred brands when compared with the potential elicited by indifferent. For the remaining of the referred electrodes, this ERP modulation present in Bosshard et al. (2016) was not verified. Another distinction between the results of Bosshard et al. (2016) study and our study was the absence of the right dominant effect on the LPP, since the values of potential registered in the respective electrodes were higher for the E52 (P3) than the potential registered in E92 (94) electrode, thus demonstrating higher participation of the left hemisphere, rather than the right one. An additional distinction between the results of both studies is the onset time of the ERP, since Bosshard et al. (2016) presented the LPP onset around the 1000 ms, while in our experiment the onset was around the 400 ms, thus, the cause presented by Bosshard, that this late onset of LPP was associated with the higher cognitive complexity involved in the interpretation and valuation of brands may be put on check with the results of our experiment. Since the conclusion presented by Bosshard et al. (2016) was the functions of the LPP as an indicator of the motivation that a subject has to purchase from a certain brand. This difference may be explained by the different protocols used, since our study focused on the categorization of brand logos, while Bosshard et al. (2016) focused on purchase decisions involving different brand categories. This last one seems to involve more complex cognitive processes than a categorization task, hence the disparity in latencies may be understandable.

2. Source of the brain activity related to the expression of preference

The main interest in the area of neuroeconomics and neuromarketing in the study of preference is it is related to enhancing the attractiveness that a brand presents to a subject so that he feels more enticed to buy products or services that they present. Thus, the main focus has been understanding the decision-making process and the involvement of emotions in this cognitive process. Bearing in mind that these have been the backbone of the different hypotheses associated with the development of preference, the commonly described neural sources are mainly located at prefrontal brain structures. These structures are normally associated with rational processing, decision-making, and emotion processing. As it was described in McClure et al. (2004) and Koenigs and Tranel (2008), the ventromedial prefrontal cortex seems to have an essential role in the personal definition of preference. A piece of interesting information that these studies presented is that this structure seems to be essential in the decision-making processes in which the individual has significant knowledge about all the options available before making the decision. This seems to demonstrate that the role of this brain structure, for this cognitive function, is to aggregate information/arguments to support a future decision. However, this may not mean that the valuation process, through which personal preference is developed, is mainly centered on the higher cognitive brain structures, such as the ventromedial prefrontal cortex. Our results seem to support this hypothesis. When we look at the brain sources that were determined in this experiment, we could pinpoint the source of brand categorization in the posterior regions of the brain, more specifically, the occipital gyrus. The areas that were elicited when comparing the three different brand logos categories are regions usually associated with visual processing. The interesting information provided by the distinction between the GFP elicited by the preferred and the indifferent brand logo is its latency, conciliated with its source. Since there seems to be a distinction between preferred and indifferent brands between 24 and 36 ms, and that both stimuli category elicited activity in the same brain structure, the left inferior occipital gyrus, we may hypothesise that the valuation process starts much earlier in the processing of visual stimuli. When we compare the GFP elicited by preferred brand logos and fictitious brand logos, we can observe, that the distinction may occur later in the cognitive process, and the incongruity created by the fictitious brands may be responsible for this distinction occurring at a more advanced

moment in the process, as more cognitive tools may be needed to make a concrete assessment of the preferred brands. The same is possible to be considered between the indifferent and the fictitious brand logos categories since the distinction between both seems to happen at the same latency as the distinction between preferred and fictitious. All these results seem to provide an interesting contribution for the process of preference construction, seeming to displace the cognition involved to earlier moments of processing and to more associative structures of the brain, allowing us to consider the possibility that specific sensory information of the stimulus and the familiarity that it elicits in the subject have a vital function for the personal construction of preference.

This location influence can also be confirmed by the information provided by the global dissimilarity values and the brain map topography. The difference between brand logos categories may not reside on each one having specific neural circuits, responsible for conduct the semantic information that the stimulus elicits on the subject, but it may reside in different activity thresholds, in visual and visual associative areas, that trigger specific information about past experience regarding the stimulus, contributing to a quick discrimination of a preferred brand when it is mixed with less preferred ones. The fact that DISS values are not at their relative maximum when there is a statistically significant difference between the GFP of all categories studied, supports this same conclusion.

Conclusions and Future Perspectives

At the beginning of this research project, a scientific question was asked about the participation of visual and visual-associative areas, such as the fusiform gyrus, in the cognitive process of discriminating stimuli, such as brands and brand logos, according to personal preference. The answer to that emerges from the analysis of the potential registered, over the trial period, on the two regions of interest, IC2, and IC7, which had shown their scientific relevance in the work of Marques dos Santos et al. (2014). Confirming the participation of both regions in the cognitive discrimination between more and less personally affective brand logos demonstrates the important role that these visual processing areas may have in this cognitive process. Another conclusion obtained through the analysis of the timing of the activations in both regions of interest demonstrate that these seem to have an extensive role, both in early stages of cognition, associated with the sensorial processing of the brand logos, and in later stages of cognition, associated with semantic processing, moments in which it is possible that the preference, or the absence of it, is being consolidated about the brand under analysis.

To better comprehend the participation of both regions of interest, and, in specific, the role of the fusiform gyri in the cognitive process of discrimination by preference, a new experiment could be run, comparing these same brand logo categories with other visual stimuli with better-known processes involving the fusiform gyri, such as human faces and objects. This experiment was already planned, as it is presented in Part A of this dissertation.

The other objective of this work was to evaluate the time profile of the cognitive process of preference construction. Interesting results were obtained since there was a clear distinction between brand logos categories at different times of cognition. The most interesting of the results was the one obtained through the comparison of preferred and indifferent brand logos. This distinction, occurring in the early stages of cognition and having as its setting at the inferior occipital gyrus introduce new questions about this cognitive process. Since both brand logos categories contain known brands, while the fictitious category has the unknown brands, the first two only differ in personal appreciation that each subject has concerning each one of the brands, a possible familiarity effect can be a reason for the early window of difference between both categories. When observing these results contrasted with the results obtained with the comparison of these two categories with the fictitious brand logos, the significant difference occurs in much

later latencies, probably demonstrating the requirement for more complex cognitive processes, conceivably to solve the incongruity effect that the visual stimuli may present to the individual.

To better comprehend these results, a novel experiment, such as the one described in Part A of this dissertation, in which, it would be possible to determine the impact that familiarity and recollection can have in this clear time distinction between brand logo categories. This would be accessed using specific, and individually confirmed, known, and unknown visual stimuli of three distinct categories: human faces, objects, and brand logos.

In short, the results obtained through this experiment demonstrated interesting new possibilities, forwarding the cognitive processes associated with the personal valuation of brands for earlier moments of cognition and more posterior regions of the brain rather than the most commonly associated anterior regions for explicit decisions such as preference statement.

References

- Allan, K., L. Wilding, E., & Rugg, M. D. (1998). Electrophysiological evidence for dissociable processes contributing to recollection. *Acta Psychologica*, *98*(2), 231-252. doi:10.1016/S0001-6918(97)00044-9
- Bentin, S., Allison, T., Puce, A., Perez, E., & McCarthy, G. (1996). Electrophysiological Studies of Face Perception in Humans. *Journal of Cognitive Neuroscience*, *8*(6), 551-565. doi:10.1162/jocn.1996.8.6.551
- Bodamer, J. (1947). Die Prosop-Agnosie. *Archiv für Psychiatrie und Nervenkrankheiten*, *179*(1), 6-53. doi:10.1007/BF00352849
- Bosshard, S. S., Bourke, J. D., Kunaharan, S., Koller, M., & Walla, P. (2016). Established liked versus disliked brands: Brain activity, implicit associations and explicit responses. *Cogent Psychology*, *3*(1). doi:10.1080/23311908.2016.1176691
- Bradley, M. M., & Lang, P. J. (2017). International Affective Picture System. In V. Zeigler-Hill & T. K. Shackelford (Eds.), *Encyclopedia of Personality and Individual Differences* (pp. 1-4). Cham: Springer International Publishing.
- Bridger, E. K., Bader, R., Kriukova, O., Unger, K., & Mecklinger, A. (2012). The FN400 is functionally distinct from the N400. *NeuroImage*, *63*(3), 1334-1342. doi:10.1016/j.neuroimage.2012.07.047
- Cacioppo, J. T., Crites, S. L., & Gardner, W. L. (1996). Attitudes to the Right: Evaluative Processing is Associated with Lateralized Late Positive Event-Related Brain Potentials. *Personality and Social Psychology Bulletin*, *22*(12), 1205-1219. doi:10.1177/01461672962212002
- Camarrone, F., & Van Hulle, M. M. (2019). Measuring brand association strength with EEG: A single-trial N400 ERP study. *PLOS ONE*, *14*(6), e0217125. doi:10.1371/journal.pone.0217125
- Chang, S., Kim, C.-Y., & Cho, Y. S. (2017). Sequential effects in preference decision: Prior preference assimilates current preference. *PLOS ONE*, *12*(8), e0182442. doi:10.1371/journal.pone.0182442
- Chatterjee, S., & Heath, T. B. (1996). Conflict and Loss Aversion in Multiattribute Choice: The Effects of Trade-Off Size and Reference Dependence on Decision Difficulty. *Organizational Behavior and Human Decision Processes*, *67*(2), 144-155. doi:10.1006/obhd.1996.0070
- Coch, D., & Mitra, P. (2010). Word and pseudoword superiority effects reflected in the ERP waveform. *Brain Research*, *1329*, 159-174. doi:10.1016/j.brainres.2010.02.084
- Delorme, A., & Makeig, S. (2004). EEGLAB: an open source toolbox for analysis of single-trial EEG dynamics including independent component analysis. *Journal of Neuroscience Methods*, *134*(1), 9-21. doi:10.1016/j.jneumeth.2003.10.009
- Deppe, M., Schwindt, W., Kugel, H., Plassmann, H., & Kenning, P. (2005). Nonlinear responses within the medial prefrontal cortex reveal when specific implicit information influences economic decision making. *J Neuroimaging*, *15*(2), 171-182. doi:10.1177/1051228405275074
- Downar, J., Crawley, A. P., Mikulis, D. J., & Davis, K. D. (2001). The Effect of Task Relevance on the Cortical Response to Changes in Visual and Auditory Stimuli: An Event-Related fMRI Study. *NeuroImage*, *14*(6), 1256-1267. doi:10.1006/nimg.2001.0946
- Downar, J., Crawley, A. P., Mikulis, D. J., & Davis, K. D. (2002). A cortical network sensitive to stimulus salience in a neutral behavioral context across multiple sensory modalities. *J Neurophysiol*, *87*(1), 615-620. doi:10.1152/jn.00636.2001
- Eimer, M. (2000). The face-specific N170 component reflects late stages in the structural encoding of faces. *Neuroreport*, *11*(10), 2319-2324. doi:10.1097/00001756-200007140-00050
- Epstein, R., Harris, A., Stanley, D., & Kanwisher, N. (1999). The Parahippocampal Place Area: Recognition, Navigation, or Encoding? *Neuron*, *23*(1), 115-125. doi:10.1016/S0896-6273(00)80758-8

- Evans, L. H., & Wilding, E. L. (2012). Recollection and Familiarity Make Independent Contributions to Memory Judgments. *The Journal of Neuroscience*, *32*(21), 7253. doi:10.1523/JNEUROSCI.6396-11.2012
- Feng, R., Ma, W., Liu, R., Zhang, M., Zheng, Z., Qing, T., . . . Qian, C. (2019). How Preferred Brands Relate to the Self: The Effect of Brand Preference, Product Involvement, and Information Valence on Brand-Related Memory. *Frontiers in Psychology*, *10*(783). doi:10.3389/fpsyg.2019.00783
- Franklin, M. S., Dien, J., Neely, J. H., Huber, E., & Waterson, L. D. (2007). Semantic priming modulates the N400, N300, and N400RP. *Clinical Neurophysiology*, *118*(5), 1053-1068. doi:10.1016/j.clinph.2007.01.012
- Friedman, D., & Johnson Jr, R. (2000). Event-related potential (ERP) studies of memory encoding and retrieval: A selective review. *Microscopy Research and Technique*, *51*(1), 6-28. doi:10.1002/1097-0029(20001001)51:1<::AID-JEMT2>3.0.CO;2-R
- Gajewski, P. D., Drizinsky, J., Zülch, J., & Falkenstein, M. (2016). ERP Correlates of Simulated Purchase Decisions. *Frontiers in Neuroscience*, *10*(360). doi:10.3389/fnins.2016.00360
- Gao, C., Conte, S., Richards, J. E., Xie, W., & Hanayik, T. (2019). The neural sources of N170: Understanding timing of activation in face-selective areas. *Psychophysiology*, *56*(6), e13336-e13336. doi:10.1111/psyp.13336
- Gauthier, I., Skudlarski, P., Gore, J. C., & Anderson, A. W. (2000). Expertise for cars and birds recruits brain areas involved in face recognition. *Nature Neuroscience*, *3*(2), 191-197. doi:10.1038/72140
- Gonzalez, F., Relova, J. L., Prieto, A., Peleteiro, M., & Romero, M. C. (2006). Hemifield dependence of responses to colour in human fusiform gyrus. *Vision Research*, *46*(16), 2499-2504. doi:10.1016/j.visres.2006.01.033
- Gray, H. (1918). *Anatomy of the Human Body* (20 ed.). Philadelphia and New York: Lea and Febiger.
- Hamm, J. P., Johnson, B. W., & Kirk, I. J. (2002). Comparison of the N300 and N400 ERPs to picture stimuli in congruent and incongruent contexts. *Clinical Neurophysiology*, *113*(8), 1339-1350. doi:10.1016/S1388-2457(02)00161-X
- Hanson, S. J., Matsuka, T., & Haxby, J. V. (2004). Combinatorial codes in ventral temporal lobe for object recognition: Haxby (2001) revisited: is there a "face" area? *NeuroImage*, *23*(1), 156-166. doi:10.1016/j.neuroimage.2004.05.020
- Holmes, A. P., Blair, R. C., Watson, J. D. G., & Ford, I. (1996). Nonparametric analysis of statistic images from functional mapping experiments. *Journal of Cerebral Blood Flow and Metabolism*, *16*(1), 7-22. doi:10.1097/00004647-199601000-00002
- Horst, J. S., & Hout, M. C. (2016). The Novel Object and Unusual Name (NOUN) Database: A collection of novel images for use in experimental research. *Behavior Research Methods*, *48*(4), 1393-1409. doi:10.3758/s13428-015-0647-3
- Huschke, E. (1854). *Schaedel, Hirn und Seele des Menschen und der Thiere nach Alter, Geschlecht und Race, dargestellt nach neuen Methoden und Untersuchungen*. Jena: Mauke.
- Itier, R. J., Latinus, M., & Taylor, M. J. (2006). Face, eye and object early processing: What is the face specificity? *NeuroImage*, *29*(2), 667-676. doi:10.1016/j.neuroimage.2005.07.041
- Jonas, J., Rössion, B., Brissart, H., Frismand, S., Jacques, C., Hossu, G., . . . Maillard, L. (2015). Beyond the core face-processing network: Intracerebral stimulation of a face-selective area in the right anterior fusiform gyrus elicits transient prosopagnosia. *Cortex*, *72*, 140-155. doi:10.1016/j.cortex.2015.05.026
- Kanwisher, N., McDermott, J., & Chun, M. M. (1997). The fusiform face area: a module in human extrastriate cortex specialized for face perception. *The Journal of neuroscience : the official journal of the Society for Neuroscience*, *17*(11), 4302-4311. doi:10.1523/JNEUROSCI.17-11-04302.1997

- Kanwisher, N., McDermott, J., & Chun, M. M. (1997). The Fusiform Face Area: A Module in Human Extrastriate Cortex Specialized for Face Perception. *The Journal of Neuroscience*, *17*(11), 4302. doi:10.1523/JNEUROSCI.17-11-04302.1997
- Khushaba, R. N., Greenacre, L., Al-Timemy, A., & Al-Jumaily, A. (2015). Event-related Potentials of Consumer Preferences. *Procedia Computer Science*, *76*, 68-73. doi:10.1016/j.procs.2015.12.277
- Koenigs, M., & Tranel, D. (2008). Prefrontal cortex damage abolishes brand-cued changes in cola preference. *Social cognitive and affective neuroscience*, *3*(1), 1-6. doi:10.1093/scan/nsm032
- Leynes, P. A., Bruett, H., Krizan, J., & Veloso, A. (2017). What psychological process is reflected in the FN400 event-related potential component? *Brain and Cognition*, *113*, 142-154. doi:10.1016/j.bandc.2017.02.004
- Li, B., Wang, W., Gao, C., & Guo, C. (2016). Masked repetition priming hinders subsequent recollection but not familiarity: A behavioral and event-related potential study. *Cognitive, Affective, & Behavioral Neuroscience*, *16*(5), 789-801. doi:10.3758/s13415-016-0431-6
- Lin, M.-H., Cross, S. N. N., Jones, W. J., & Childers, T. L. (2018). Applying EEG in consumer neuroscience. *European Journal of Marketing*, *52*(1/2), 66-91. doi:10.1108/EJM-12-2016-0805
- Lu, G., & Hou, G. (2019). Effects of Semantic Congruence on Sign Identification: An ERP Study. *Human Factors*, *62*(5), 800-811. doi:10.1177/0018720819854880
- Ma, D. S., Correll, J., & Wittenbrink, B. (2015). The Chicago face database: A free stimulus set of faces and norming data. *Behavior Research Methods*, *47*(4), 1122-1135. doi:10.3758/s13428-014-0532-5
- Ma, Q., Abdeljelil, H. m. M., & Hu, L. (2019). The Influence of the Consumer Ethnocentrism and Cultural Familiarity on Brand Preference: Evidence of Event-Related Potential (ERP). *Frontiers in Human Neuroscience*, *13*(220). doi:10.3389/fnhum.2019.00220
- Marques dos Santos, J., Moutinho, L., & Castelo-Branco, M. (2014). 'Mind Reading': Hitting Cognition by Using ANNs to Analyze fMRI Data in a Paradigm Exempted from Motor Responses. Paper presented at the ICINCO 2014, Vienna, Austria.
- Maurer, U., Brandeis, D., & McCandliss, B. D. (2005). Fast, visual specialization for reading in English revealed by the topography of the N170 ERP response. *Behavioral and Brain Functions*, *1*(1), 13. doi:10.1186/1744-9081-1-13
- Maurer, U., Zevin, J. D., & McCandliss, B. D. (2008). Left-lateralized N170 effects of visual expertise in reading: evidence from Japanese syllabic and logographic scripts. *Journal of Cognitive Neuroscience*, *20*(10), 1878-1891. doi:10.1162/jocn.2008.20125
- McClure, S. M., Li, J., Tomlin, D., Cypert, K. S., Montague, L. M., & Montague, P. R. (2004). Neural Correlates of Behavioral Preference for Culturally Familiar Drinks. *Neuron*, *44*(2), 379-387. doi:10.1016/j.neuron.2004.09.019
- Mehrabian, A. (1995). Framework for a comprehensive description and measurement of emotional states. *Genetic, Social, and General Psychology Monographs*, *121*(3), 339-361.
- Mickes, L., Wais, P. E., & Wixted, J. T. (2009). Recollection is a continuous process: implications for dual-process theories of recognition memory. *Psychol Sci*, *20*(4), 509-515. doi:10.1111/j.1467-9280.2009.02324.x
- Molinaro, N., Conrad, M., Barber, H. A., & Carreiras, M. (2010). On the functional nature of the N400: Contrasting effects related to visual word recognition and contextual semantic integration. *Cognitive Neuroscience*, *1*(1), 1-7. doi:10.1080/17588920903373952
- Morris, J. D. (1995). Observations: SAM: The self-assessment manikin: An efficient cross-cultural measurement of emotional response. *Journal of Advertising Research*, *35*(6), 63-68.
- Murray, M. M., Brunet, D., & Michel, C. M. (2008). Topographic ERP Analyses: A Step-by-Step Tutorial Review. *Brain Topography*, *20*(4), 249-264. doi:10.1007/s10548-008-0054-5

- Nazari, M. A., Fadardi, J., Doborjeh, Z., Oghaz, T., Saeedi, M. T., & Yazdi, S. (2019). Event-related potential Evidence for Pre-comprehension Processing of Consumers to Marketing Logos. *Caspian Journal of Neurological Sciences*, *5*, 16-22. doi:10.32598/CJNS.5.16.16
- Nichols, T. E., & Holmes, A. P. (2002). Nonparametric permutation tests for functional neuroimaging: a primer with examples. *Hum Brain Mapp*, *15*(1), 1-25. doi:10.1002/hbm.1058
- O'Hara, D., Dale, R., Piiroinen, P. T., & Connolly, F. (2013). Local dynamics in decision making: The evolution of preference within and across decisions. *Scientific Reports*, *3*, 2210. doi:10.1038/srep02210
- Olivares, E. I., Iglesias, J., Saavedra, C., Trujillo-Barreto, N. J., & Valdés-Sosa, M. (2015). Brain Signals of Face Processing as Revealed by Event-Related Potentials. *Behavioural Neurology*, *2015*, 514361. doi:10.1155/2015/514361
- Pascual-Marqui, R. (2007). Discrete, 3D distributed, linear imaging methods of electric neuronal activity. Part 1: Exact, zero error localization. *Math. Physics Biol. Physics Neurons Cogn.*, *0710*.
- Pascual-Marqui, R. D., Michel, C. M., & Lehmann, D. (1994). Low resolution electromagnetic tomography: a new method for localizing electrical activity in the brain. *Int J Psychophysiol*, *18*(1), 49-65. doi:10.1016/0167-8760(84)90014-x
- Petit, J.-P., Midgley, K. J., Holcomb, P. J., & Grainger, J. (2006). On the time course of letter perception: A masked priming ERP investigation. *Psychonomic Bulletin & Review*, *13*(4), 674-681. doi:10.3758/BF03193980
- Plassmann, H., Ramsøy, T. Z., & Milosavljevic, M. (2012). Branding the brain: A critical review and outlook. *Journal of Consumer Psychology*, *22*(1), 18-36. doi:10.1016/j.jcps.2011.11.010
- Puce, A., Allison, T., Asgari, M., Gore, J. C., & McCarthy, G. (1996). Differential Sensitivity of Human Visual Cortex to Faces, Letterstrings, and Textures: A Functional Magnetic Resonance Imaging Study. *The Journal of Neuroscience*, *16*(16), 5205. doi:10.1523/JNEUROSCI.16-16-05205.1996
- R Development Core Team. (2010). R: A language and environment for statistical computing. Vienna, Austria: R Foundation for Statistical Computing. Retrieved from <https://www.R-project.org/>
- Ratcliff, R., Philiastides, M. G., & Sajda, P. (2009). Quality of evidence for perceptual decision making is indexed by trial-to-trial variability of the EEG. *Proceedings of the National Academy of Sciences*, *106*(16), 6539. doi:10.1073/pnas.0812589106
- Russell, J., & Mehrabian, A. (1977). Evidence for a Three-Factor Theory of Emotions. *Journal of Research in Personality*, *11*, 273-294. doi:10.1016/0092-6566(77)90037-X
- Russell, J. A., & Mehrabian, A. (1977). Evidence for a three-factor theory of emotions. *Journal of Research in Personality*, *11*(3), 273-294. doi:10.1016/0092-6566(77)90037-X
- Skrandies, W. (1990). Global field power and topographic similarity. *Brain Topography*, *3*(1), 137-141. doi:10.1007/BF01128870
- Speer, N. K., & Curran, T. (2007). ERP correlates of familiarity and recollection processes in visual associative recognition. *Brain Research*, *1174*, 97-109. doi:10.1016/j.brainres.2007.08.024
- Stróžak, P., Abedzadeh, D., & Curran, T. (2016). Separating the FN400 and N400 potentials across recognition memory experiments. *Brain Research*, *1635*, 41-60. doi:10.1016/j.brainres.2016.01.015
- Swait, J., & Adamowicz, W. (2001). Choice Environment, Market Complexity, and Consumer Behavior: A Theoretical and Empirical Approach for Incorporating Decision Complexity into Models of Consumer Choice. *Organizational Behavior and Human Decision Processes*, *86*(2), 141-167.

- Talairach, J., & Tournoux, P. (1988). *Co-planar stereotaxic atlas of the human brain: 3-Dimensional proportional system: An approach to cerebral imaging*. New York: Thieme Medical Publishers, Inc.
- Tanaka, J. W., & Curran, T. (2001). A Neural Basis for Expert Object Recognition. *Psychological Science, 12*(1), 43-47. doi:10.1111/1467-9280.00308
- Thierry, G., Pegna, A., Dodds, C., Roberts, M., Basan, S., & Downing, P. (2006). An event-related potential component sensitive to images of the human body. *NeuroImage, 32*, 871-879. doi:10.1016/j.neuroimage.2006.03.060
- Towle, V. L., Bolaños, J., Suarez, D., Tan, K., Grzeszczuk, R., Levin, D. N., . . . Spire, J. P. (1993). The spatial location of EEG electrodes: locating the best-fitting sphere relative to cortical anatomy. *Electroencephalogr Clin Neurophysiol, 86*(1), 1-6. doi:10.1016/0013-4694(93)90061-y
- Vlaev, I., Chater, N., Stewart, N., & Brown, G. D. (2011). Does the brain calculate value? *Trends in Cognitive Sciences, 15*(11), 546-554. doi:10.1016/j.tics.2011.09.008
- Voss, J. L., & Federmeier, K. D. (2011). FN400 potentials are functionally identical to N400 potentials and reflect semantic processing during recognition testing. *Psychophysiology, 48*(4), 532-546. doi:10.1111/j.1469-8986.2010.01085.x
- Warren, C., McGraw, A. P., & Van Boven, L. (2010). Values and preferences: defining preference construction. *Wiley Interdisciplinary Reviews: Cognitive Science, 2*(2), 193-205. doi:10.1002/wcs.98
- Weiner, K. S., & Zilles, K. (2016). The anatomical and functional specialization of the fusiform gyrus. *Neuropsychologia, 83*, 48-62. doi:10.1016/j.neuropsychologia.2015.06.033
- Wimmer, G. E., & Shohamy, D. (2012). Preference by Association: How Memory Mechanisms in the Hippocampus Bias Decisions. *Science, 338*(6104), 270. doi:10.1126/science.1223252
- Wixted, J. T. (2007). Dual-process theory and signal-detection theory of recognition memory. *Psychol Rev, 114*(1), 152-176. doi:10.1037/0033-295x.114.1.152
- Wong, A. C. N., Gauthier, I., Woroch, B., Debusse, C., & Curran, T. (2005). An early electrophysiological response associated with expertise in letter perception. *Cognitive, Affective, & Behavioral Neuroscience, 5*(3), 306-318. doi:10.3758/CABN.5.3.306

Appendix A – Visual stimuli

Part A
Known Brand Logos







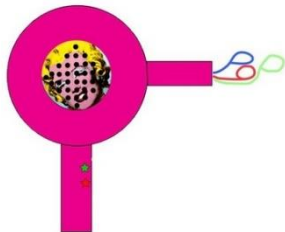
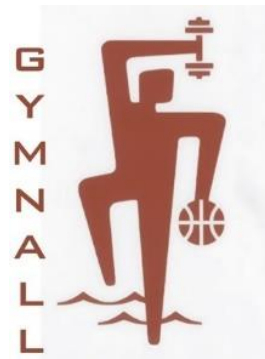




ZARA

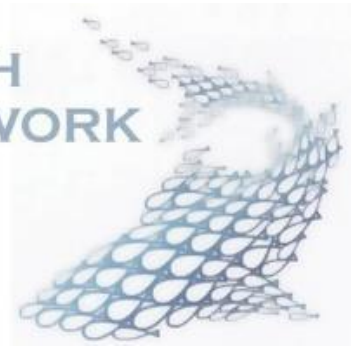
Unknown Brand Logos



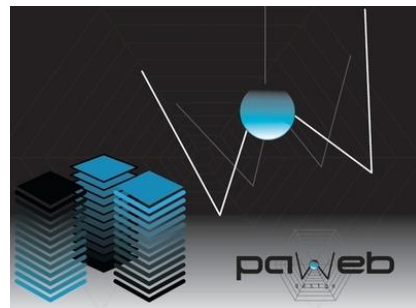




PHISH
NETWORK



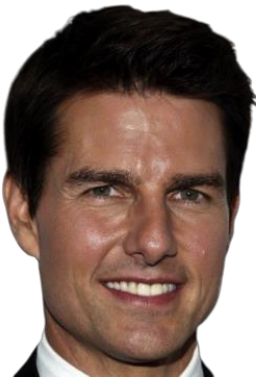
power-drink







Known faces



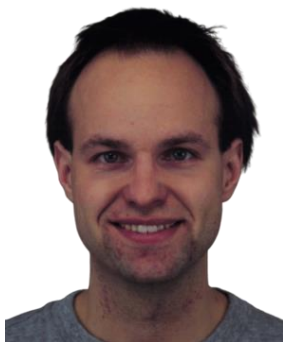
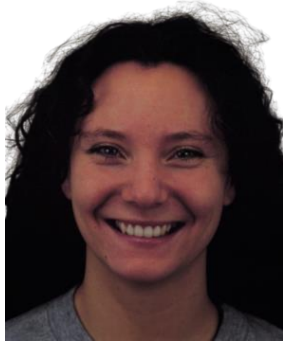






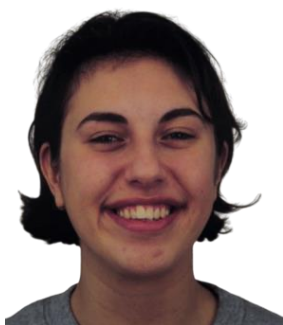
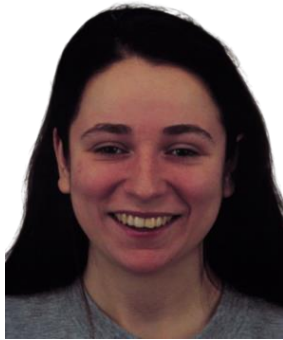


Unknown Faces











Known objects











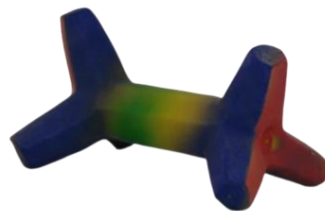


Unknown objects











Part B
Brand logos





BOSS
HUGO BOSS



BRITISH AIRWAYS 



C.117

CK
Calvin Klein













MANGO



Massimo Dutti



mazda





OYSHO





Pepe Jeans.
LONDON




pierre cardin
PARIS



POLO
RALPH LAUREN



PRIMARK®

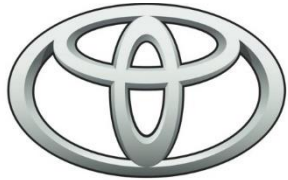








Timberland



TOYOTA



VERSACE

VISA





ZARA

Appendix B – Statistical Analysis

Statistical analysis of the lorGFP elicited in IC2 and IC7

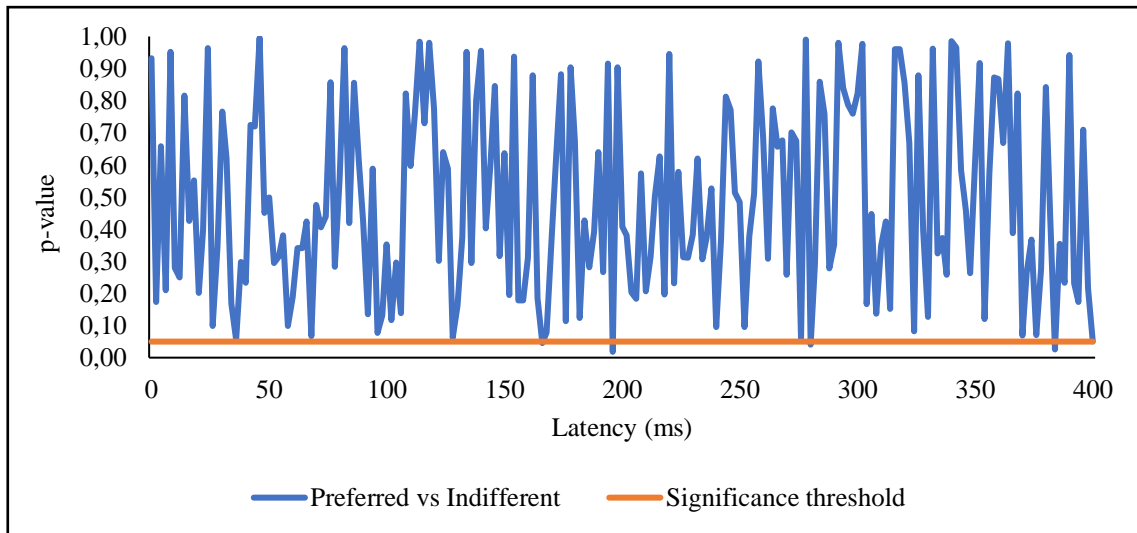


Figure 77 Paired t-test results for the statistical analysis of lorGFP elicited by the “preferred” brand logos versus the lorGFP elicited by the “indifferent” brand logos in region of IC2.

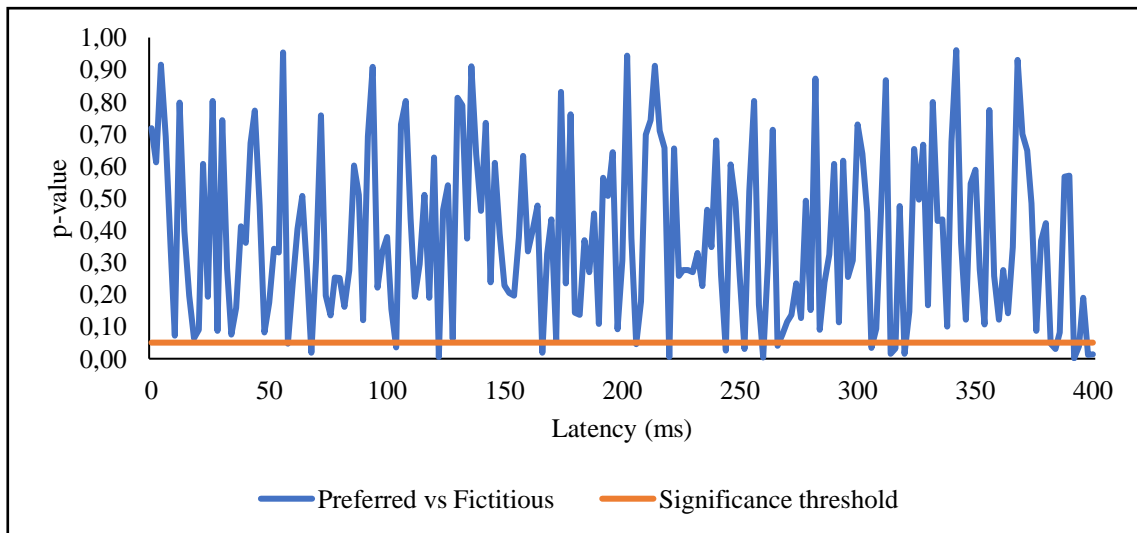


Figure 78 Paired t-test results for the statistical analysis of lorGFP elicited by the “preferred” brand logos versus the lorGFP elicited by the “fictitious” brand logos in region of IC2.

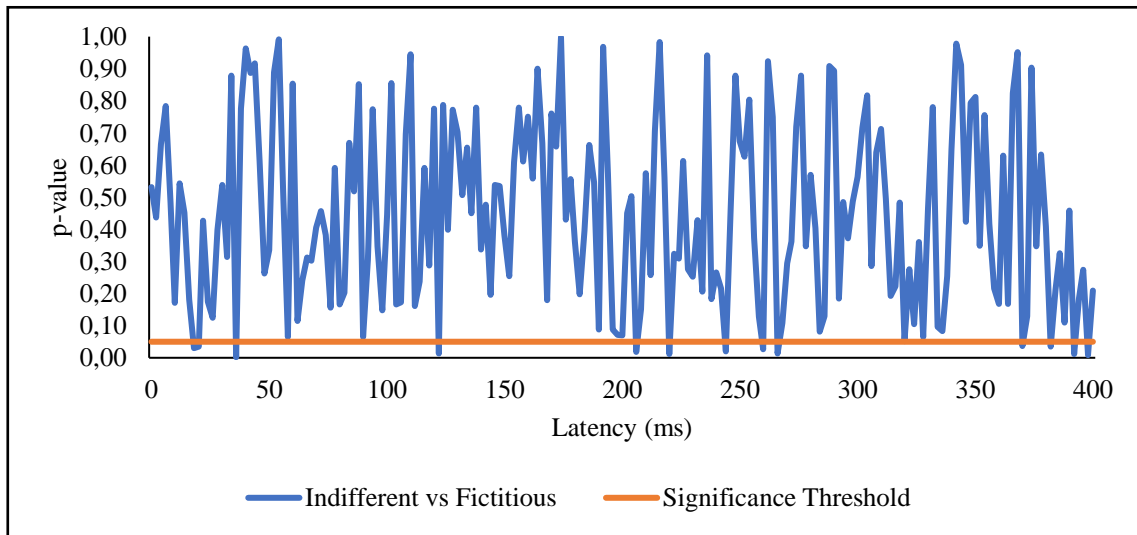


Figure 79 Paired t-test results for the statistical analysis of lorGFP elicited by the “indifferent” brand logos versus the lorGFP elicited by the “fictitious” brand logos in region of IC2. The value of α was set to 0,05.

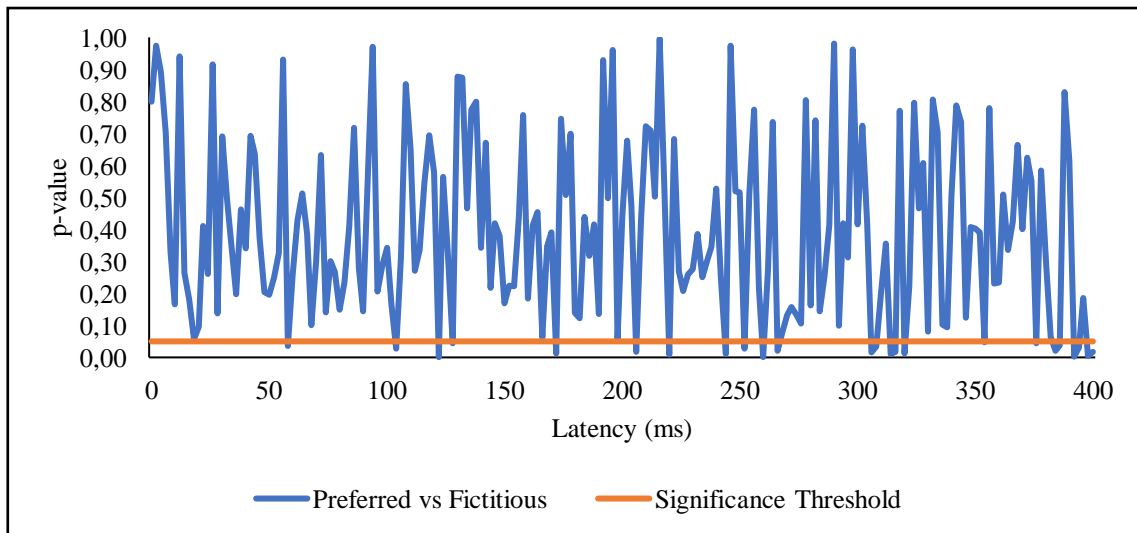


Figure 80 Paired t-test results for the lorGFP elicited by the “preferred” brand logos versus the lorGFP elicited by the “indifferent” brand logos in the region of IC7.

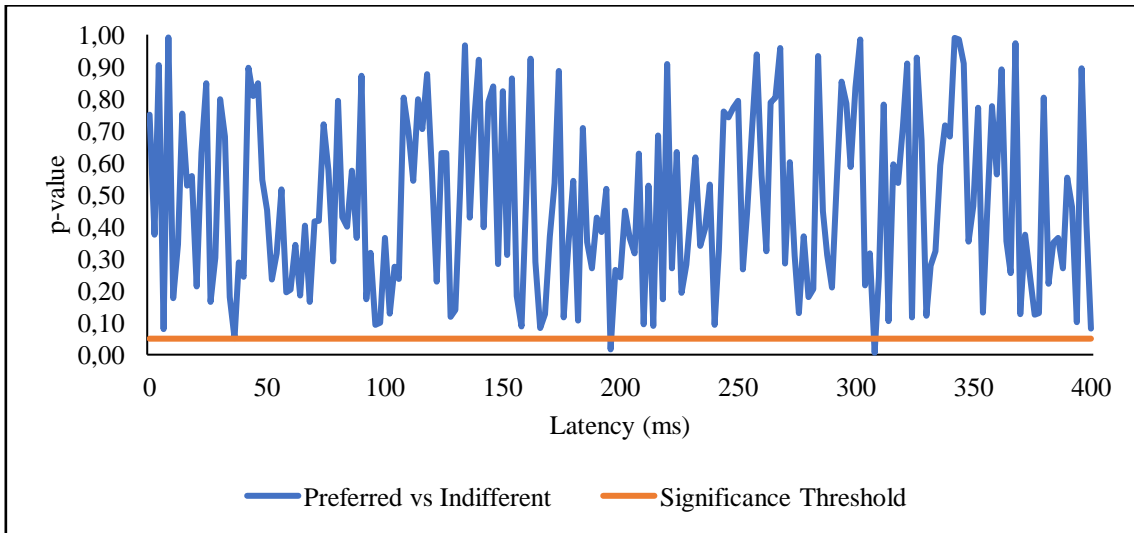


Figure 81 Paired t-test results for the lorGFP elicited by the “preferred” brand logos versus the lorGFP elicited by the “fictitious” brand logos in the region of IC7.

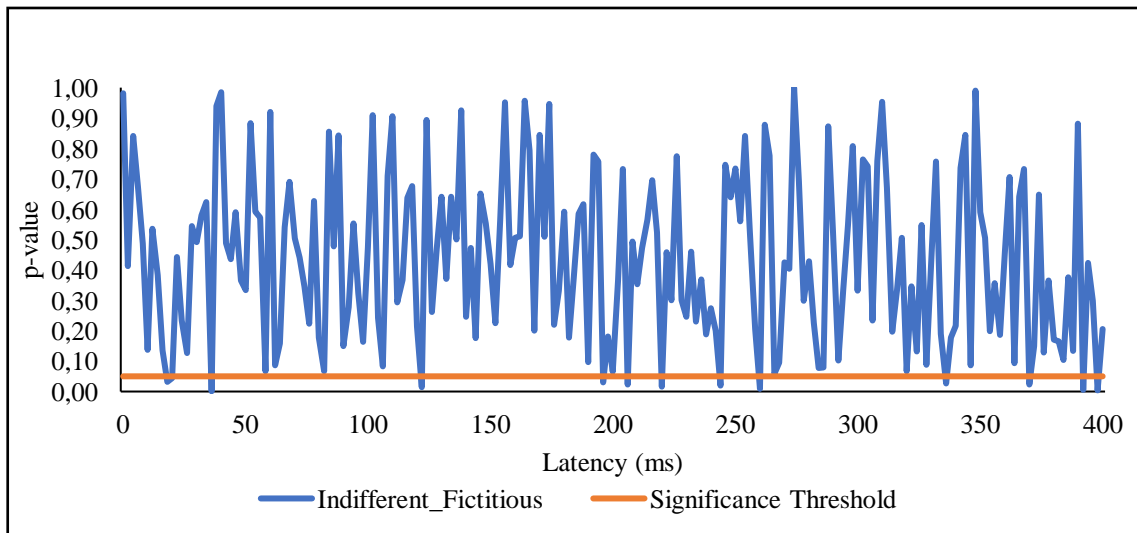


Figure 82 Paired t-test results for the lorGFP elicited by the “indifferent” brand logos versus the lorGFP elicited by the “fictitious” brand logos in the region of IC7.

Statistical analysis of the GFP

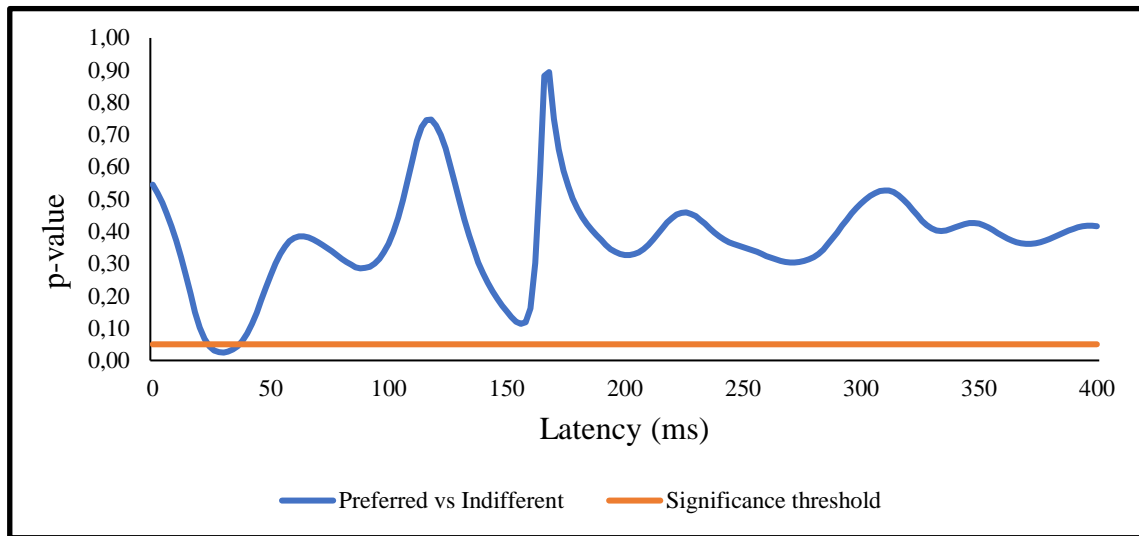


Figure 83 Paired t-test results for the GFP elicited by the “preferred” brands versus the GFP elicited by the “indifferent” brands.

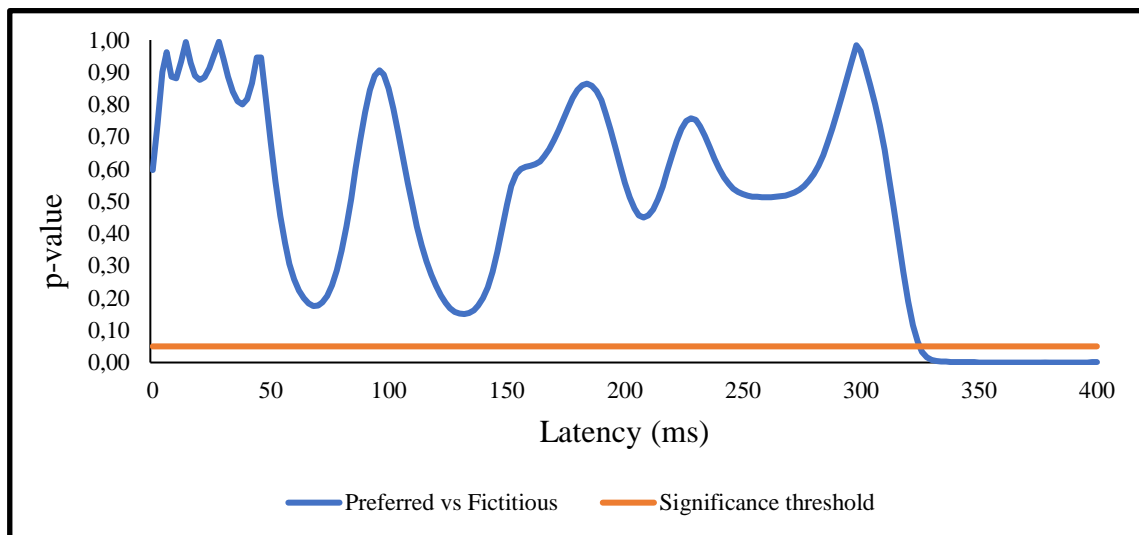


Figure 84 Paired t-test results for the GFP elicited by the “preferred” brands versus the GFP elicited by the “fictitious” brands.

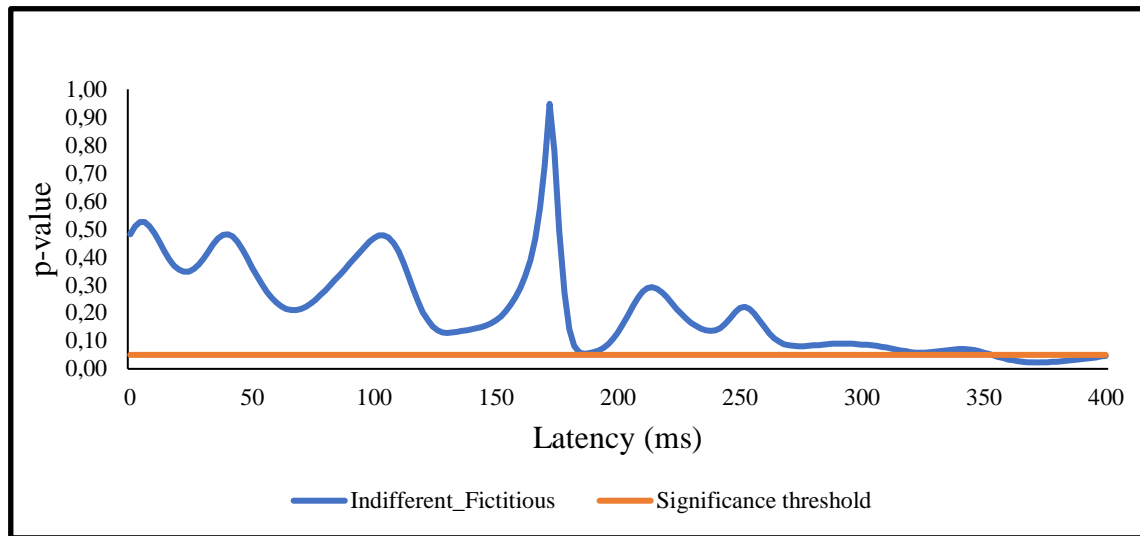


Figure 85 Paired t-test results for the GFP elicited by the “indifferent” brands versus the GFP elicited by the “fictitious” brands.

eLORETA Paired t-test

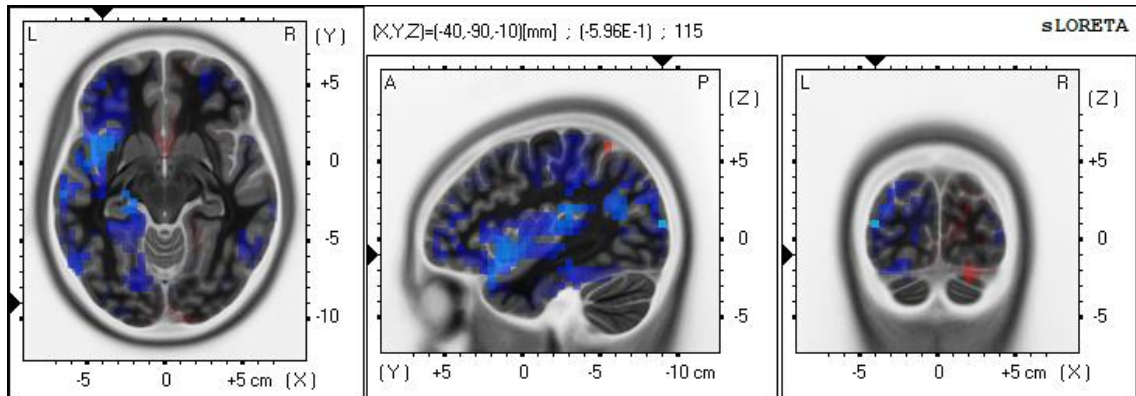


Figure 87 Paired t-test map produced in eLORETA for “Preferred vs Indifferent” at 28 ms. t-value (left inferior occipital gyrus) = -0,596.

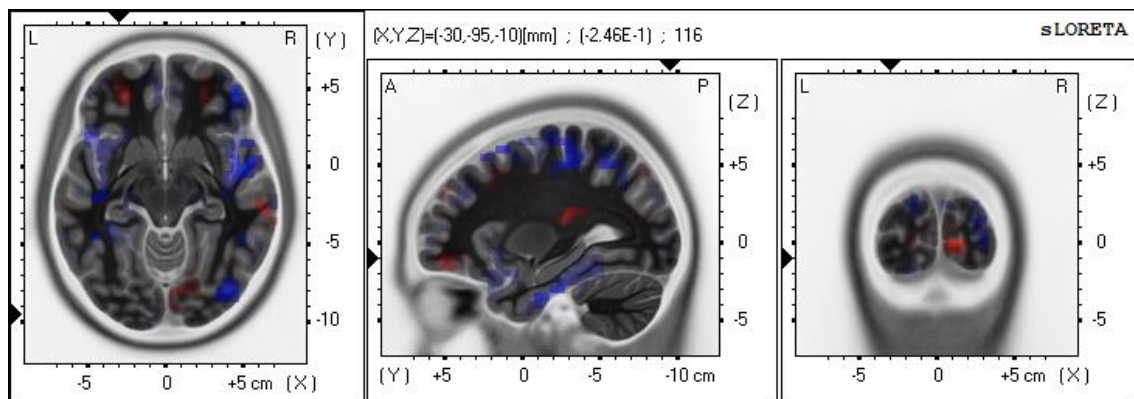


Figure 86 Paired t-test map produced in eLORETA for “Preferred vs Indifferent” at 30 ms. t-value (left inferior occipital gyrus) = -0,246.

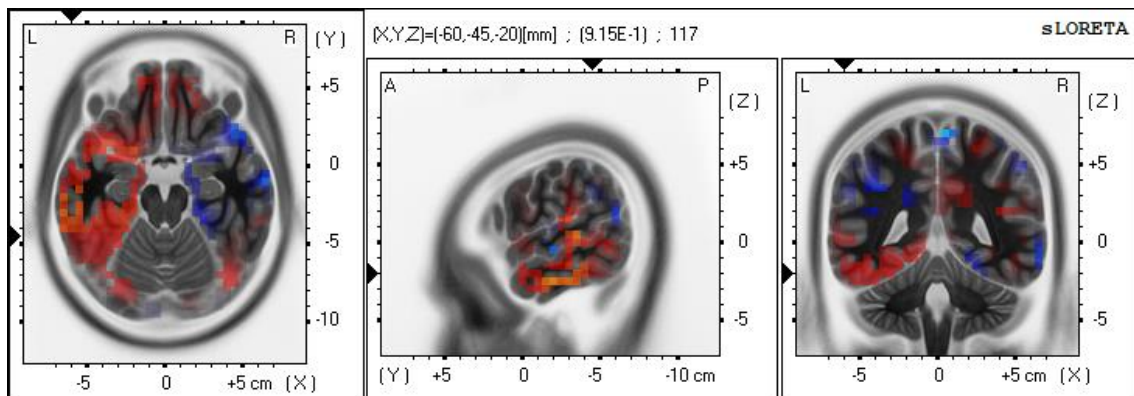


Figure 88 Paired t-test map produced in eLORETA for “Preferred vs Indifferent” at 32 ms. t-value (left middle temporal gyrus) = 0,915.

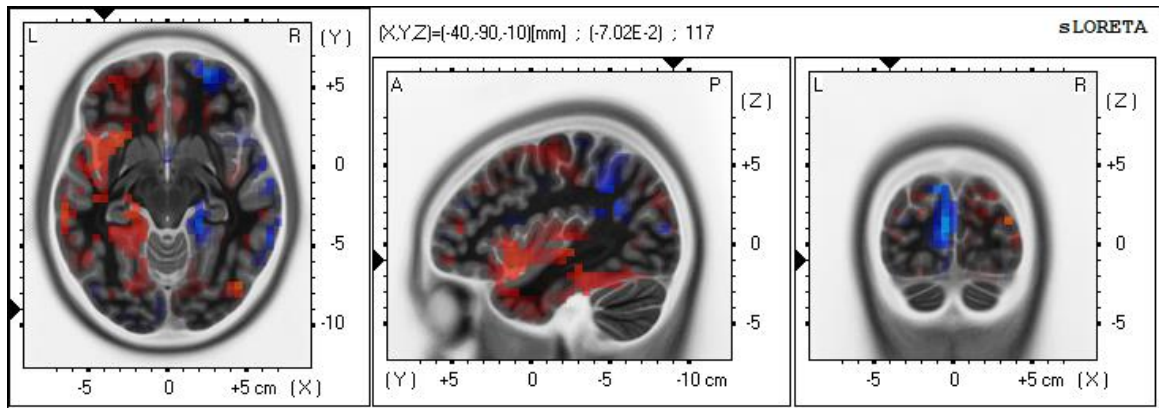


Figure 89 Paired t-test map produced in eLORETA for “Preferred vs Indifferent” at 32 ms. t-value (left middle temporal gyrus) = -0,0702.

Max T-Value

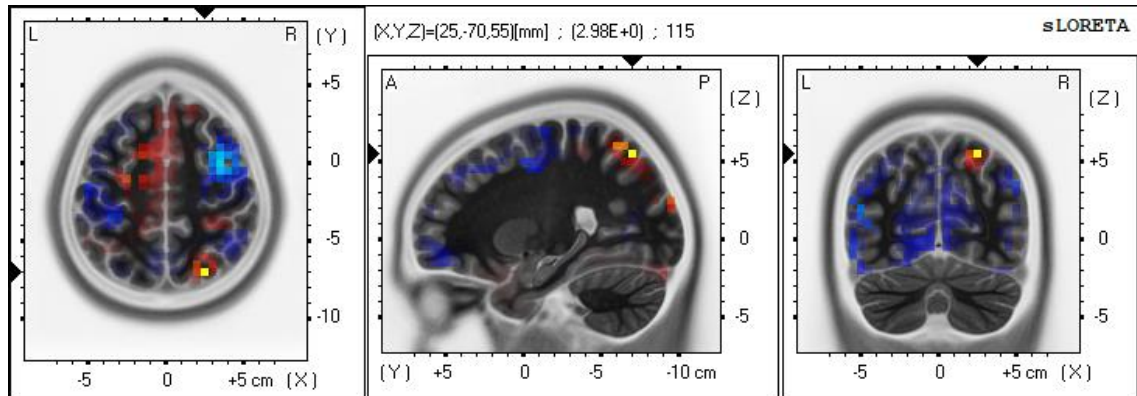


Figure 90 Paired t-test map produced in eLORETA for “Preferred vs Indifferent” at 28 ms. The maximum t-value was 2,98 at the superior parietal lobule.

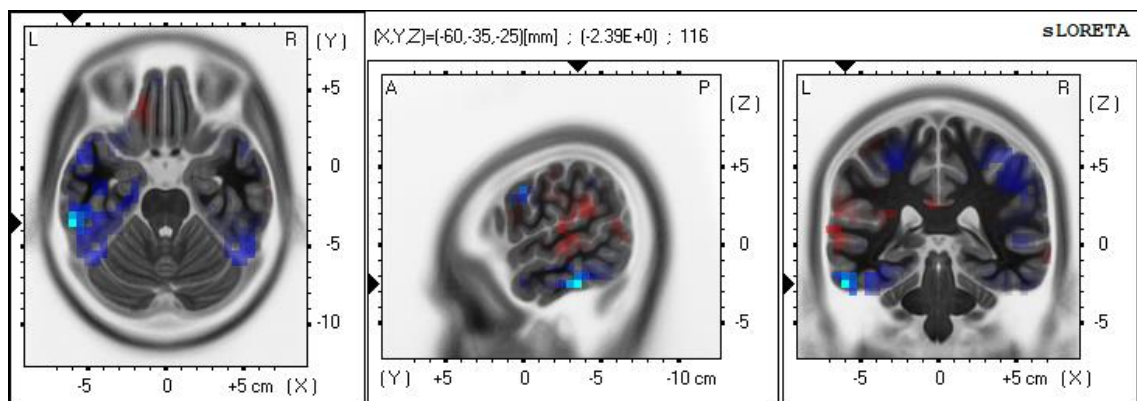


Figure 91 Paired t-test map produced in eLORETA for “Preferred vs Indifferent” at 30 ms. The maximum t-value was -2,39 at the inferior temporal gyrus.

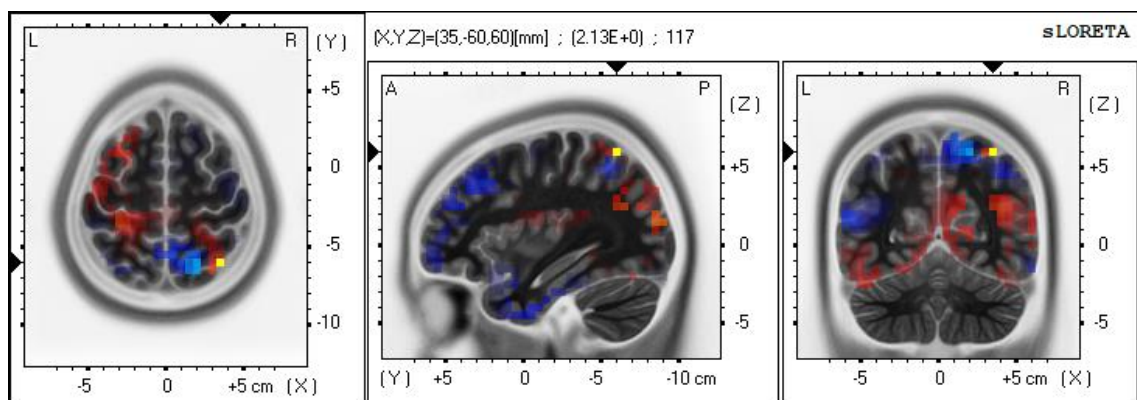


Figure 92 Paired t-test map produced in eLORETA for “Preferred vs Indifferent” at 32 ms. The maximum t-value was 2,13 at the superior parietal lobule.

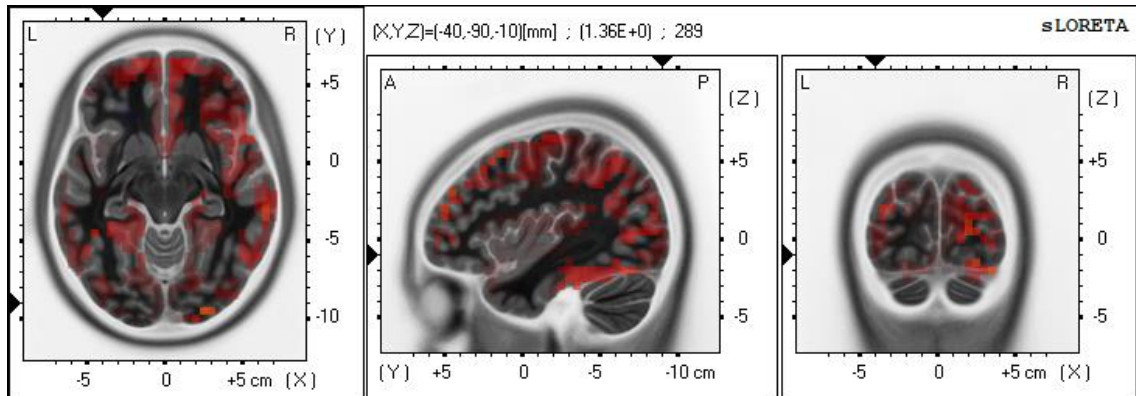


Figure 94 Paired t-test map produced in eLORETA for “Preferred vs Fictitious” at 376 ms. t-value (left inferior occipital gyrus) = 1,360.

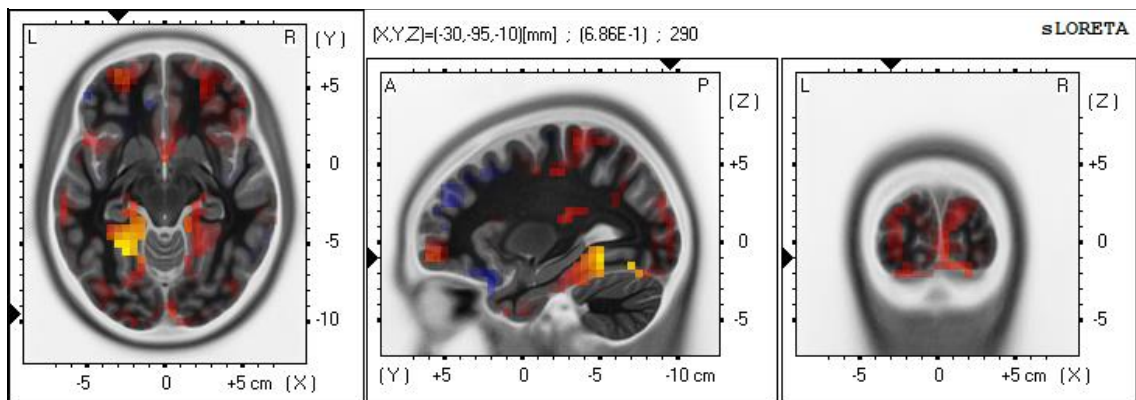


Figure 93 Paired t-test map produced in eLORETA for “Preferred vs Fictitious” at 378 ms. t-value (left inferior occipital gyrus) = 0,686.

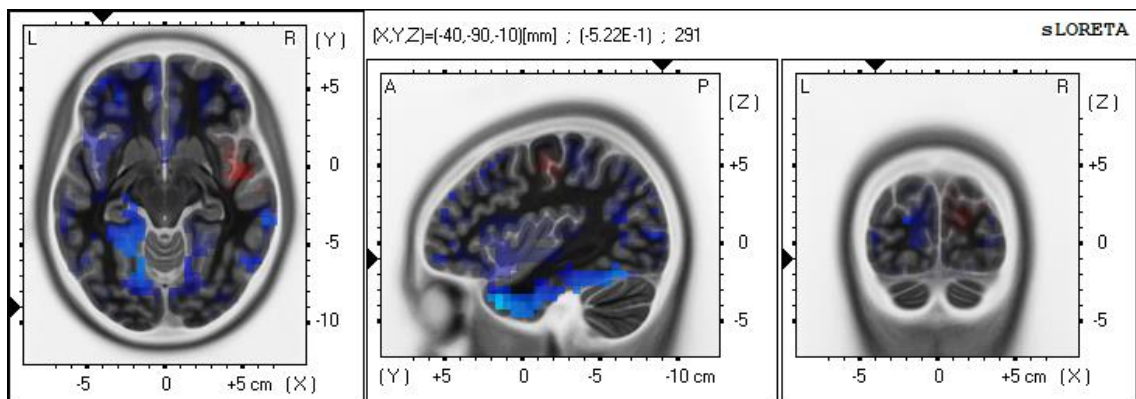


Figure 95 Paired t-test map produced in eLORETA for “Preferred vs Fictitious” at 380 ms. t-value (left inferior occipital gyrus) = -0,522.

Max T-Value

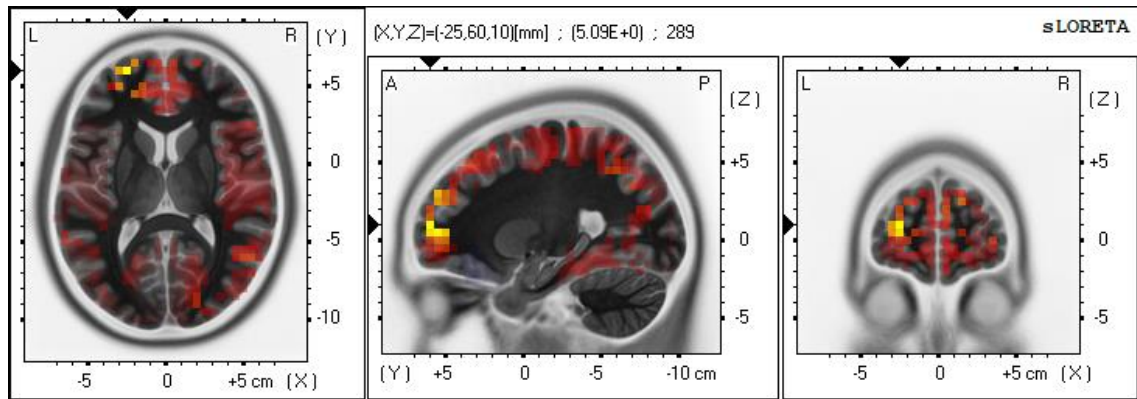


Figure 96 Paired t-test map produced in eLORETA for "Preferred vs Fictitious" at 376 ms. The maximum t-value was 5,09 at the superior frontal gyrus.

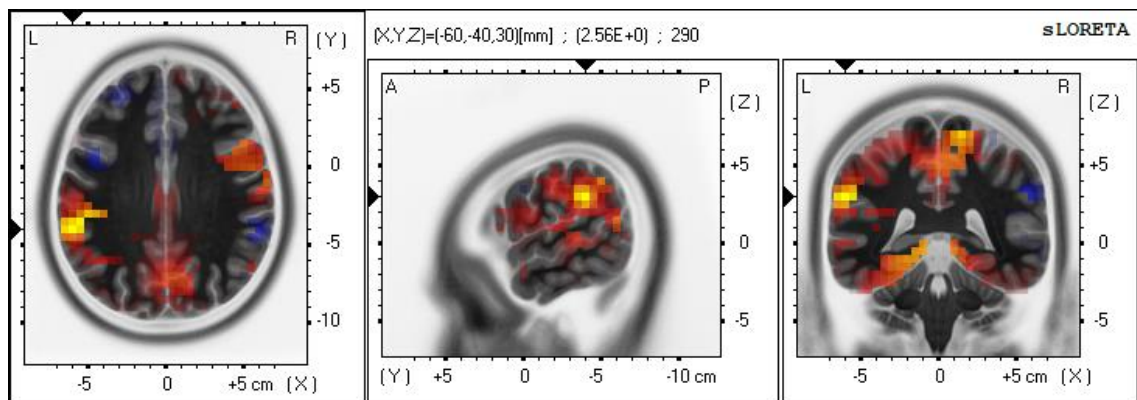


Figure 97 Paired t-test map produced in eLORETA for "Preferred vs Fictitious" at 378 ms. The maximum t-value was 2,56 at the inferior parietal lobule.

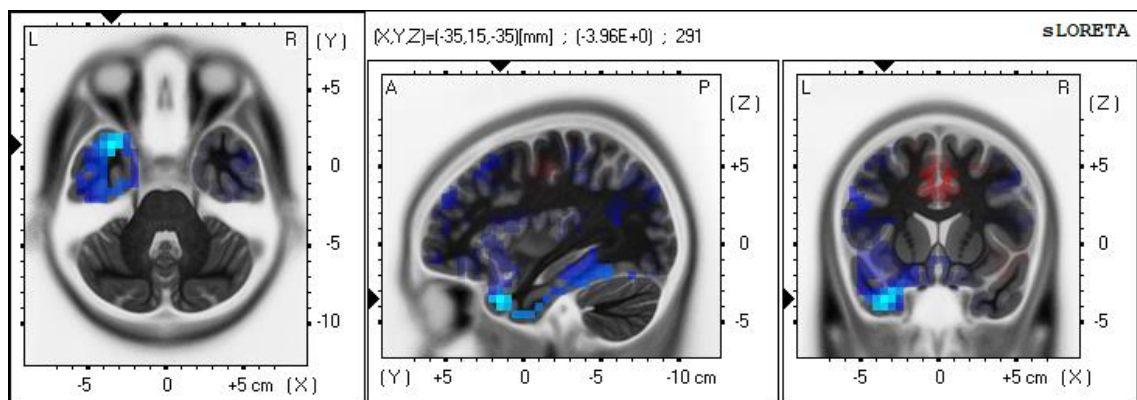


Figure 98 Paired t-test map produced in eLORETA for "Preferred vs Fictitious" at 380 ms. The maximum t-value was -3,96 at the superior temporal gyrus.

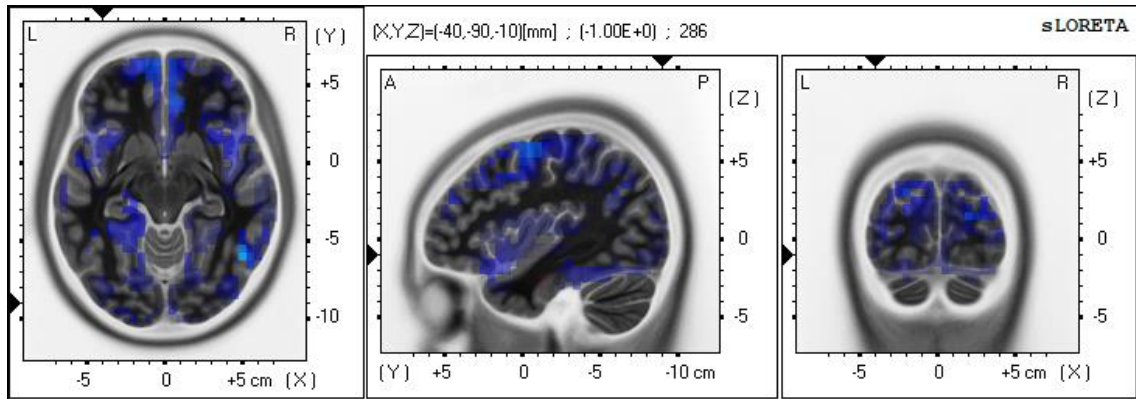


Figure 99 Paired t-test map produced in eLORETA for “Indifferent vs Fictitious” at 370 ms. t-value (left inferior occipital gyrus) = -1,00.

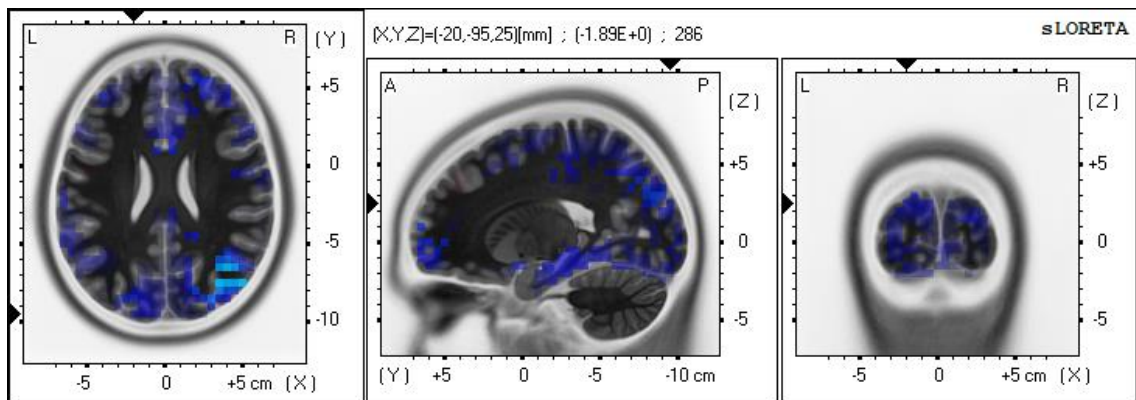


Figure 100 Paired t-test map produced in eLORETA for “Indifferent vs Fictitious” at 370 ms. t-value (left inferior occipital gyrus) = -1,89.

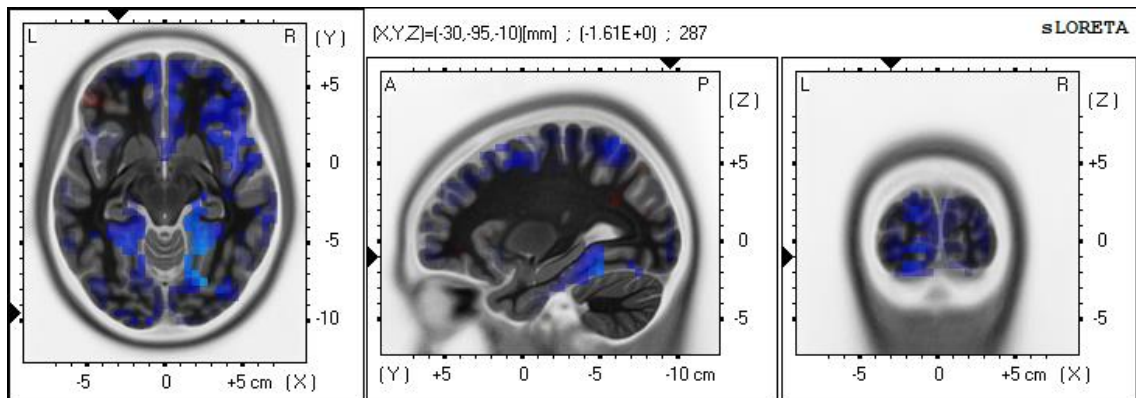


Figure 101 Paired t-test map produced in eLORETA for “Indifferent vs Fictitious” at 372 ms. t-value (left inferior occipital gyrus) = -1,61.

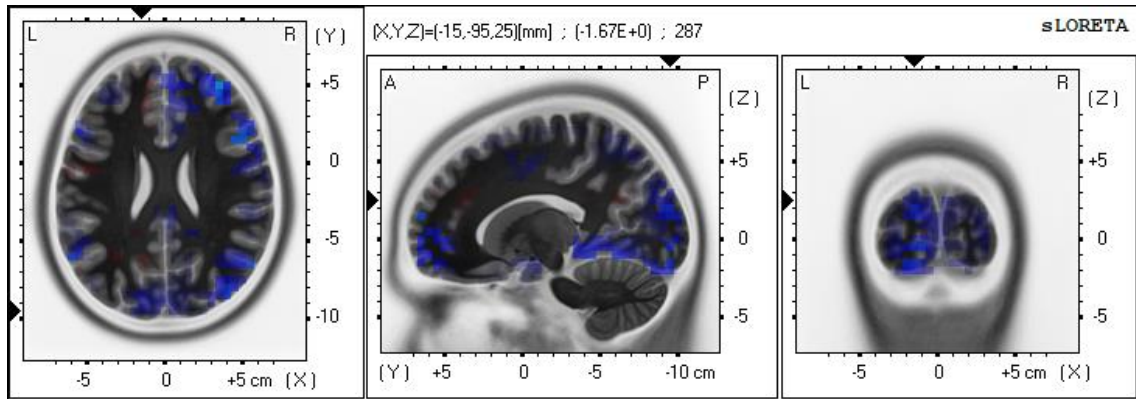


Figure 102 Paired t-test map produced in eLORETA software for “Indifferent vs Fictitious” at 372 ms. t-value (left cuneus) = -1,67.

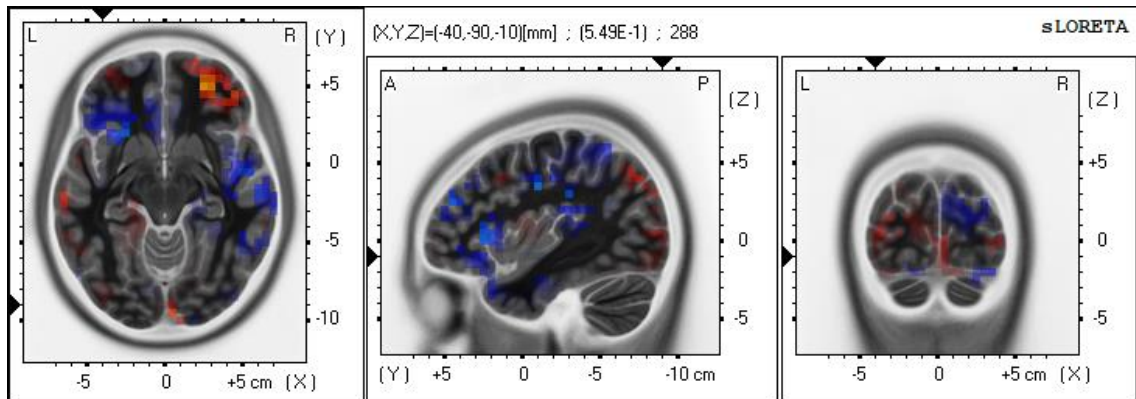


Figure 103 Paired t-test map produced in eLORETA for “Indifferent vs Fictitious” at 374 ms. t-value (left inferior occipital gyrus) = 0,549.

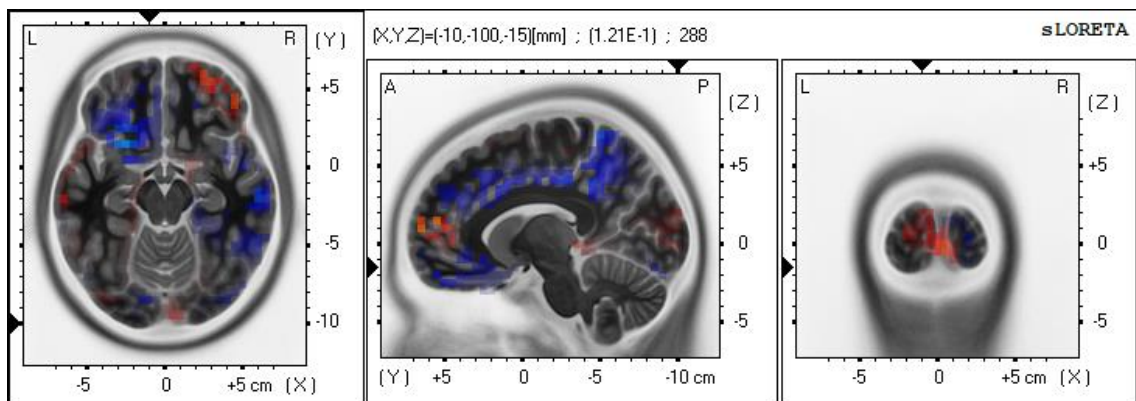


Figure 104 Paired t-test map produced in eLORETA for “Indifferent vs Fictitious” at 374 ms. t-value (left lingual gyrus) = 0,121.

Max T-Value:

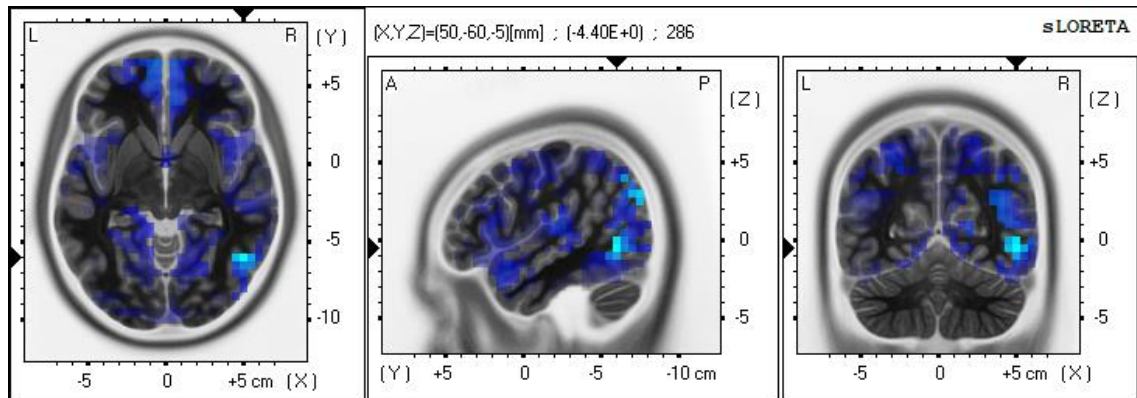


Figure 106 Paired t-test map produced in eLORETA for “Indifferent vs Fictitious” at 370 ms. The maximum t-value was -4,40 at the right inferior temporal gyrus.

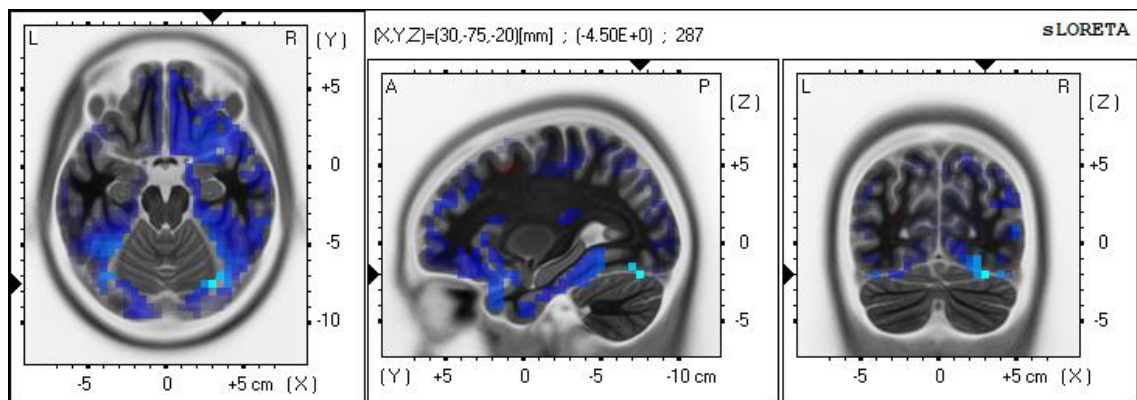


Figure 105 Paired t-test map produced in eLORETA for “Indifferent vs Fictitious” at 372 ms. Maximum t-value was -4,50 at right fusiform gyrus.

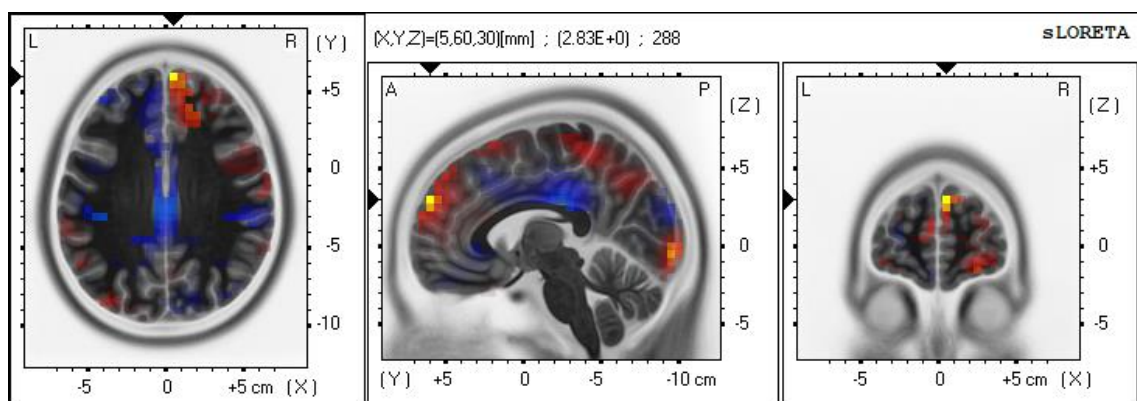


Figure 107 Paired t-test map produced in eLORETA for “Indifferent vs Fictitious” at 374 ms. The maximum t-value was 2,98 at the superior frontal gyrus.

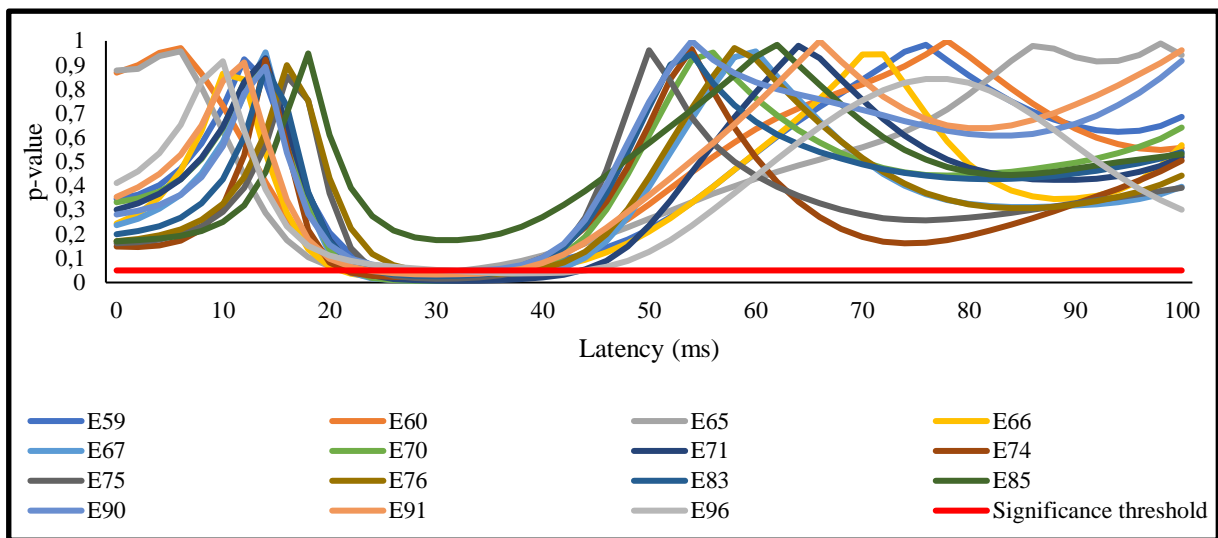


Figure 108 Paired t-test results for the statistical analysis of the potential registered in occipital electrodes when comparing the “preferred” brand logos brain activity with the “indifferent” brand logos brain activity, between 0 and 100 ms .

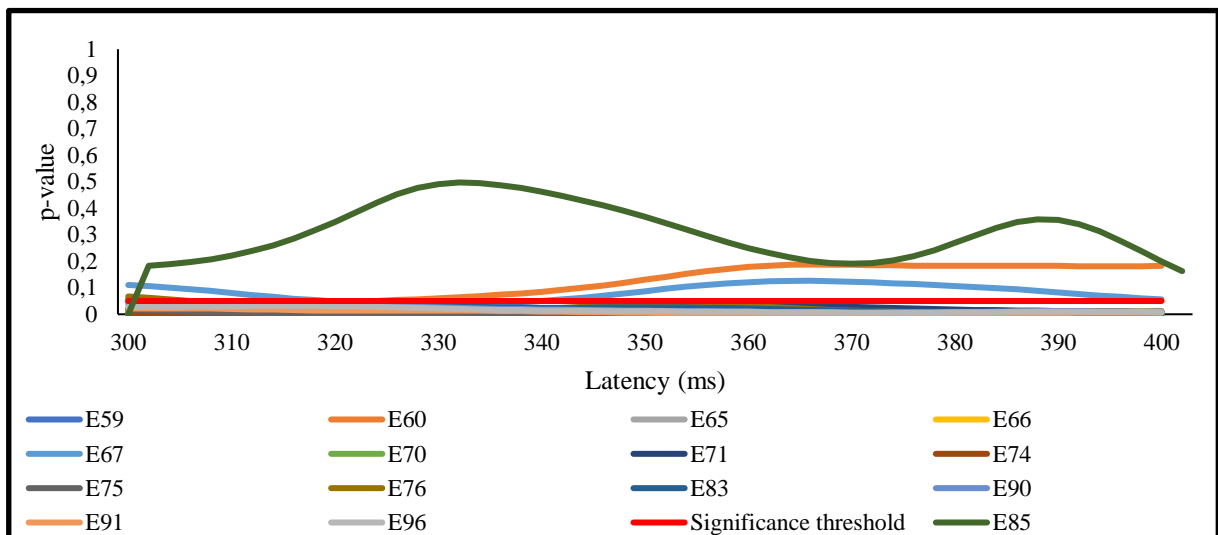


Figure 109 Paired t-test results for the statistical analysis of the potential registered in occipital electrodes when comparing the “preferred” brand logos brain activity with the “fictitious” brand logos brain activity, between 300 and 400 ms.

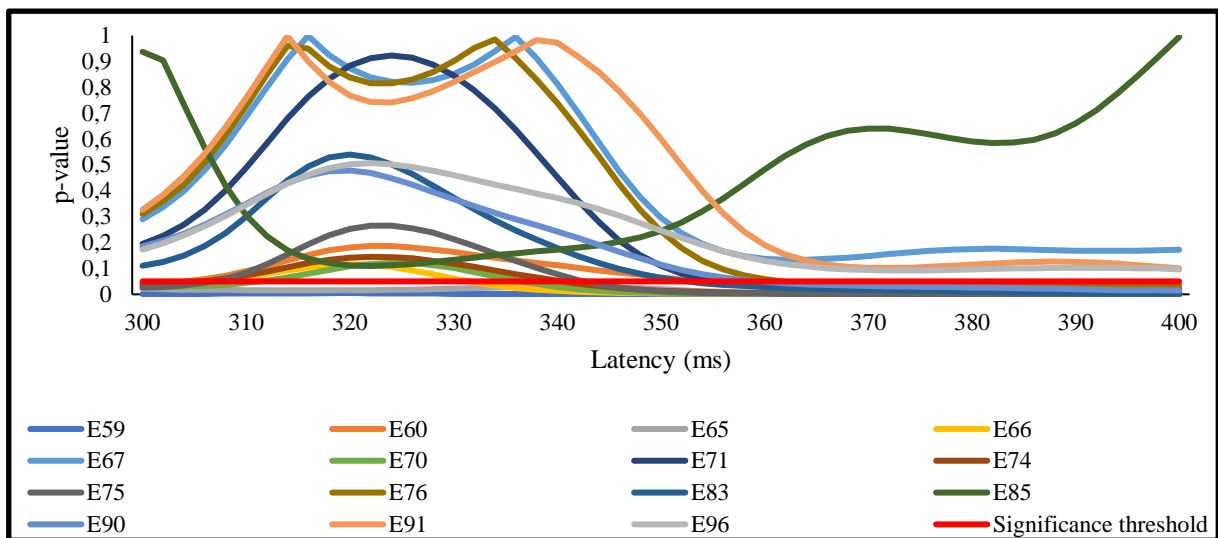


Figure 110 Paired t-test results for the statistical analysis of the potential registered in occipital electrodes when comparing the “indifferent” brand logos brain activity with the “fictitious” brand logos brain activity, between 300 and 400 ms.

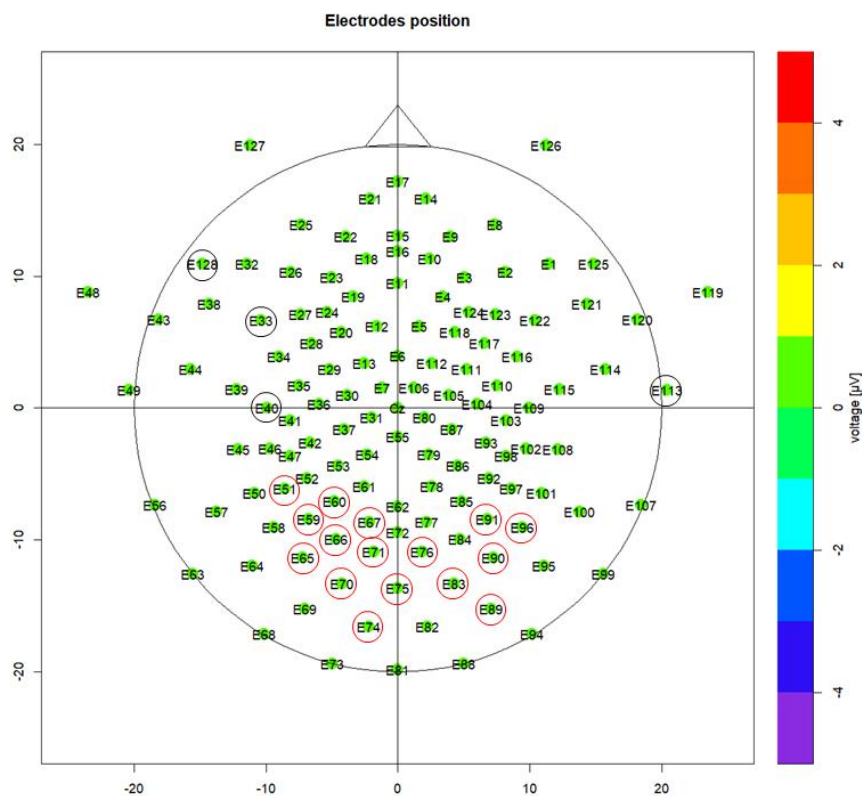


Figure 111 Topographic map highlighting the electrodes, circled in red, that presented significant statistical effect between preferred and indifferent brand logos, starting at 24 ms and ending at 36 ms

Appendix C – IC2 coordinates

X-MNI	Y-MNI	Z-MNI	Structure	X-MNI	Y-MNI	Z-MNI	Structure
40	-80	30	Angular Gyrus	-50	-70	-20	Fusiform Gyrus
-10	50	0	Anterior Cingulate	-50	-60	-20	Fusiform Gyrus
0	-35	25	Cingulate Gyrus	-45	-70	-20	Fusiform Gyrus
0	-35	30	Cingulate Gyrus	-45	-65	-20	Fusiform Gyrus
0	-30	30	Cingulate Gyrus	-30	-85	-20	Fusiform Gyrus
5	-35	30	Cingulate Gyrus	-30	-80	-20	Fusiform Gyrus
-5	-40	40	Cingulate Gyrus	-30	-75	-20	Fusiform Gyrus
10	-95	0	Cuneus	-30	-45	-20	Fusiform Gyrus
15	-95	0	Cuneus	-30	-40	-20	Fusiform Gyrus
-20	-85	10	Cuneus	-30	-35	-20	Fusiform Gyrus
-20	-85	10	Cuneus	-25	-75	-20	Fusiform Gyrus
-25	-80	15	Cuneus	-20	-85	-20	Fusiform Gyrus
-20	-90	15	Cuneus	-20	-80	-20	Fusiform Gyrus
-20	-80	15	Cuneus	25	-85	-20	Fusiform Gyrus
-15	-85	15	Cuneus	30	-85	-20	Fusiform Gyrus
-25	-95	20	Cuneus	30	-40	-20	Fusiform Gyrus
-25	-80	20	Cuneus	30	-35	-20	Fusiform Gyrus
-20	-95	20	Cuneus	35	-35	-20	Fusiform Gyrus
-20	-90	20	Cuneus	-30	-50	-15	Fusiform Gyrus
-15	-90	20	Cuneus	-25	-70	-15	Fusiform Gyrus
30	-90	20	Cuneus	-25	-60	-15	Fusiform Gyrus
-30	-90	25	Cuneus	-25	-55	-15	Fusiform Gyrus
-25	-85	25	Cuneus	-25	-50	-15	Fusiform Gyrus
-20	-95	25	Cuneus	-20	-70	-15	Fusiform Gyrus
-15	-95	25	Cuneus	-20	-65	-15	Fusiform Gyrus
-15	-90	25	Cuneus	-20	-60	-15	Fusiform Gyrus
15	-90	25	Cuneus	25	-65	-15	Fusiform Gyrus
25	-95	25	Cuneus	25	-60	-15	Fusiform Gyrus
30	-90	25	Cuneus	30	-70	-15	Fusiform Gyrus
30	-85	25	Cuneus	30	-50	-15	Fusiform Gyrus
-30	-90	30	Cuneus	45	-55	-15	Fusiform Gyrus
-30	-85	30	Cuneus	-55	15	15	Inferior Frontal Gyrus
-25	-90	30	Cuneus	-45	-80	-10	Inferior Occipital Gyrus
-25	-85	30	Cuneus	-40	-90	-5	Inferior Occipital Gyrus
-20	-90	30	Cuneus	-40	-85	-5	Inferior Occipital Gyrus
-20	-85	30	Cuneus	-50	-35	40	Inferior Parietal Lobule
-20	-80	30	Cuneus	35	-50	45	Inferior Parietal Lobule
-15	-95	30	Cuneus	-50	-70	-5	Inferior Temporal Gyrus
25	-90	30	Cuneus	-45	-70	-5	Inferior Temporal Gyrus
30	-85	30	Cuneus	-25	-80	-15	Lingual Gyrus
-25	-90	35	Cuneus	-20	-80	-15	Lingual Gyrus
-20	-90	35	Cuneus	-20	-75	-15	Lingual Gyrus
-60	-15	-30	Fusiform Gyrus	-15	-85	-15	Lingual Gyrus
-30	-40	-25	Fusiform Gyrus	-15	-80	-15	Lingual Gyrus
-30	-35	-25	Fusiform Gyrus	15	-80	-15	Lingual Gyrus
30	-35	-25	Fusiform Gyrus	20	-80	-15	Lingual Gyrus
25	-80	-15	Lingual Gyrus	-35	-90	15	Middle Occipital Gyrus
25	-75	-15	Lingual Gyrus	-35	-85	15	Middle Occipital Gyrus
-25	-75	-10	Lingual Gyrus	-30	-95	15	Middle Occipital Gyrus
-20	-80	-10	Lingual Gyrus	-30	-90	15	Middle Occipital Gyrus

-20	-75	-10	Lingual Gyrus	-30	-85	15	Middle Occipital Gyrus
-20	-70	-10	Lingual Gyrus	-30	-80	15	Middle Occipital Gyrus
-15	-75	-10	Lingual Gyrus	-25	-95	15	Middle Occipital Gyrus
25	-75	-10	Lingual Gyrus	-15	-90	15	Middle Occipital Gyrus
10	-90	0	Lingual Gyrus	30	-95	15	Middle Occipital Gyrus
-40	40	15	Middle Frontal Gyrus	30	-90	15	Middle Occipital Gyrus
-50	-70	-15	Middle Occipital Gyrus	30	-85	15	Middle Occipital Gyrus
-45	-80	-15	Middle Occipital Gyrus	30	-80	15	Middle Occipital Gyrus
30	-85	-15	Middle Occipital Gyrus	35	-90	15	Middle Occipital Gyrus
50	-65	-15	Middle Occipital Gyrus	35	-85	15	Middle Occipital Gyrus
-45	-75	-10	Middle Occipital Gyrus	-30	-80	20	Middle Occipital Gyrus
-35	-90	-5	Middle Occipital Gyrus	30	-80	20	Middle Occipital Gyrus
-40	-90	0	Middle Occipital Gyrus	-45	-65	-5	Middle Temporal Gyrus
-35	-90	0	Middle Occipital Gyrus	45	-75	10	Middle Temporal Gyrus
-30	-90	0	Middle Occipital Gyrus	50	-80	10	Middle Temporal Gyrus
-30	-85	0	Middle Occipital Gyrus	-40	-85	15	Middle Temporal Gyrus
-40	-90	5	Middle Occipital Gyrus	40	-85	15	Middle Temporal Gyrus
-35	-90	5	Middle Occipital Gyrus	45	-85	15	Middle Temporal Gyrus
-35	-85	5	Middle Occipital Gyrus	-40	-85	20	Middle Temporal Gyrus
-30	-95	5	Middle Occipital Gyrus	-35	-85	20	Middle Temporal Gyrus
-30	-85	5	Middle Occipital Gyrus	35	-85	20	Middle Temporal Gyrus
-25	-95	5	Middle Occipital Gyrus	45	-80	20	Middle Temporal Gyrus
-25	-90	5	Middle Occipital Gyrus	40	-75	25	Middle Temporal Gyrus
35	-90	5	Middle Occipital Gyrus	35	-25	-30	Parahippocampal Gyrus
35	-85	5	Middle Occipital Gyrus	-30	-30	-25	Parahippocampal Gyrus
40	-90	5	Middle Occipital Gyrus	30	-30	-25	Parahippocampal Gyrus
40	-85	5	Middle Occipital Gyrus	-30	-30	-20	Parahippocampal Gyrus
40	-80	5	Middle Occipital Gyrus	35	-30	-20	Parahippocampal Gyrus
40	-75	5	Middle Occipital Gyrus	-30	-45	-15	Parahippocampal Gyrus
45	-85	5	Middle Occipital Gyrus	-25	-45	-15	Parahippocampal Gyrus
45	-80	5	Middle Occipital Gyrus	30	-45	-15	Parahippocampal Gyrus
45	-75	5	Middle Occipital Gyrus	-30	-50	-10	Parahippocampal Gyrus
-40	-90	10	Middle Occipital Gyrus	-25	-55	-10	Parahippocampal Gyrus
-40	-85	10	Middle Occipital Gyrus	-25	-50	-10	Parahippocampal Gyrus
-35	-90	10	Middle Occipital Gyrus	-20	-50	-10	Parahippocampal Gyrus
-35	-85	10	Middle Occipital Gyrus	30	-50	-10	Parahippocampal Gyrus
-30	-95	10	Middle Occipital Gyrus	20	-30	-5	Parahippocampal Gyrus
-25	-95	10	Middle Occipital Gyrus	-55	-30	40	Postcentral Gyrus
-30	-95	10	Middle Occipital Gyrus	-50	-5	15	Precentral Gyrus
-25	-95	10	Middle Occipital Gyrus	-25	-75	20	Precuneus
35	-85	10	Middle Occipital Gyrus	-20	-80	25	Precuneus
40	-85	10	Middle Occipital Gyrus	-20	-65	30	Precuneus
40	-80	10	Middle Occipital Gyrus	-25	-85	35	Precuneus
-20	-85	40	Precuneus	25	-70	50	Superior Parietal Lobule
-15	-85	40	Precuneus	25	-65	50	Superior Parietal Lobule
-15	-75	40	Precuneus	-20	-75	55	Superior Parietal Lobule
30	-80	40	Precuneus	-20	-70	55	Superior Parietal Lobule
-20	-80	45	Precuneus	-20	-65	55	Superior Parietal Lobule
-20	-75	45	Precuneus	-15	-70	55	Superior Parietal Lobule
-20	-70	45	Precuneus	-10	-70	55	Superior Parietal Lobule
-20	-65	45	Precuneus	20	-70	55	Superior Parietal Lobule

-20	-60	45	Precuneus	-25	-60	60	Superior Parietal Lobule
-15	-80	45	Precuneus	-20	-65	60	Superior Parietal Lobule
-15	-60	45	Precuneus	25	-70	50	Superior Parietal Lobule
-10	-80	45	Precuneus	25	-65	50	Superior Parietal Lobule
-5	-80	45	Precuneus	-20	-75	55	Superior Parietal Lobule
20	-70	45	Precuneus	-20	-70	55	Superior Parietal Lobule
-20	-70	50	Precuneus	-20	-65	55	Superior Parietal Lobule
-20	-65	50	Precuneus				
-15	-70	50	Precuneus				
-15	-55	50	Precuneus				
-10	-80	50	Precuneus				
-5	-80	50	Precuneus				
15	-75	50	Precuneus				
20	-75	50	Precuneus				
20	-70	50	Precuneus				
25	-75	50	Precuneus				
-20	-60	55	Precuneus				
-10	50	30	Superior Frontal Gyrus				
-5	15	55	Superior Frontal Gyrus				
-35	-90	20	Superior Occipital Gyrus				
-30	-90	20	Superior Occipital Gyrus				
40	-85	20	Superior Occipital Gyrus				
-40	-85	25	Superior Occipital Gyrus				
-30	-85	25	Superior Occipital Gyrus				
35	-85	25	Superior Occipital Gyrus				
35	-80	25	Superior Occipital Gyrus				
35	-75	25	Superior Occipital Gyrus				
40	-85	25	Superior Occipital Gyrus				
40	-80	25	Superior Occipital Gyrus				
35	-85	30	Superior Occipital Gyrus				
35	-80	30	Superior Occipital Gyrus				
-25	-65	45	Superior Parietal Lobule				
-25	-60	45	Superior Parietal Lobule				
-25	-55	45	Superior Parietal Lobule				
25	-70	45	Superior Parietal Lobule				
25	-65	45	Superior Parietal Lobule				
-30	-65	50	Superior Parietal Lobule				
-30	-60	50	Superior Parietal Lobule				
-25	-65	50	Superior Parietal Lobule				

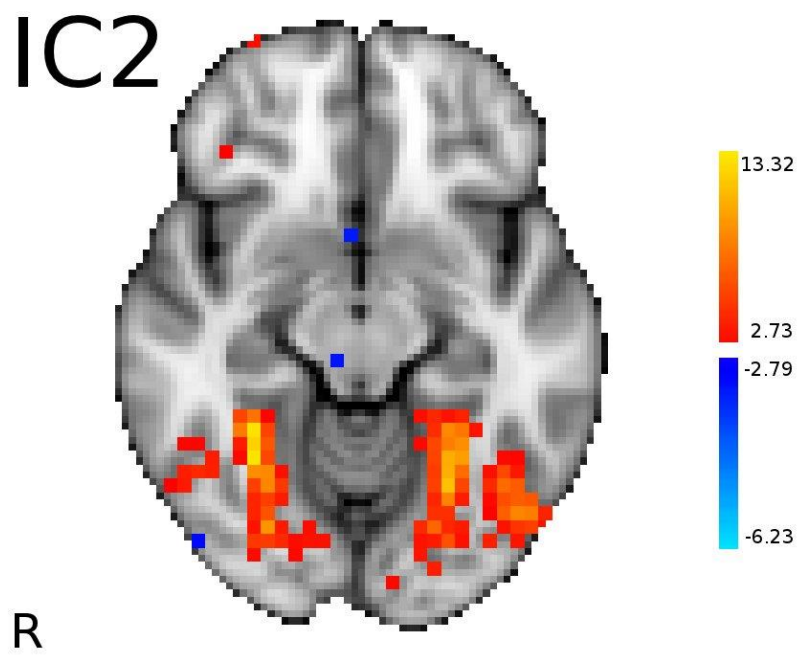


Figure 112 IC2 region retrieved from Marques dos Santos, Moutinho, and Castelo-Branco (2014). Axial cut ($z = -12$)

Appendix D - IC7 coordinates

X-MNI	Y-MNI	Z-MNI	Structure	X-MNI	Y-MNI	Z-MNI	Structure
35	-65	35	Angular Gyrus	40	-60	45	Inferior Parietal Lobule
40	-65	35	Angular Gyrus	40	-55	45	Inferior Parietal Lobule
45	-70	35	Angular Gyrus	45	-65	45	Inferior Parietal Lobule
0	-40	25	Cingulate Gyrus	45	-60	45	Inferior Parietal Lobule
0	-40	30	Cingulate Gyrus	50	-40	45	Inferior Parietal Lobule
5	-45	30	Cingulate Gyrus	50	-35	45	Inferior Parietal Lobule
5	-95	25	Cuneus	55	-35	45	Inferior Parietal Lobule
30	15	-10	Extra-Nuclear	35	-50	50	Inferior Parietal Lobule
40	-25	-30	Fusiform Gyrus	45	-50	50	Inferior Parietal Lobule
-50	-60	-25	Fusiform Gyrus	50	-40	50	Inferior Parietal Lobule
-50	-55	-25	Fusiform Gyrus	35	-55	55	Inferior Parietal Lobule
30	-40	-25	Fusiform Gyrus	60	-25	-25	Inferior Temporal Gyrus
50	-50	-25	Fusiform Gyrus	-60	-40	-20	Inferior Temporal Gyrus
-55	-55	-20	Fusiform Gyrus	-50	-55	-20	Inferior Temporal Gyrus
-45	-60	-20	Fusiform Gyrus	55	-55	-20	Inferior Temporal Gyrus
-40	-40	-20	Fusiform Gyrus	55	-50	-20	Inferior Temporal Gyrus
50	-65	-20	Fusiform Gyrus	60	-50	-20	Inferior Temporal Gyrus
50	-60	-20	Fusiform Gyrus	-55	-60	-15	Inferior Temporal Gyrus
55	-60	-20	Fusiform Gyrus	-50	-55	-15	Inferior Temporal Gyrus
-45	-55	-15	Fusiform Gyrus	50	-55	-15	Inferior Temporal Gyrus
-40	-60	-15	Fusiform Gyrus	50	-50	-15	Inferior Temporal Gyrus
50	-60	-15	Fusiform Gyrus	55	-60	-15	Inferior Temporal Gyrus
50	40	5	Inferior Frontal Gyrus	55	-50	-15	Inferior Temporal Gyrus
-45	5	30	Inferior Frontal Gyrus	60	-60	-15	Inferior Temporal Gyrus
50	5	30	Inferior Frontal Gyrus	60	-55	-15	Inferior Temporal Gyrus
50	10	30	Inferior Frontal Gyrus	60	-55	-10	Inferior Temporal Gyrus
55	10	30	Inferior Frontal Gyrus	40	-20	15	Insula
55	10	35	Inferior Frontal Gyrus	40	50	-10	Middle Frontal Gyrus
-45	-35	40	Inferior Parietal Lobule	25	25	45	Middle Frontal Gyrus
35	-65	40	Inferior Parietal Lobule	-55	-65	-15	Middle Occipital Gyrus
35	-50	40	Inferior Parietal Lobule	-50	-65	-15	Middle Occipital Gyrus
40	-70	40	Inferior Parietal Lobule	55	-65	-15	Middle Occipital Gyrus
40	-60	40	Inferior Parietal Lobule	-55	-65	-10	Middle Occipital Gyrus
40	-55	40	Inferior Parietal Lobule	50	-60	-10	Middle Occipital Gyrus
40	-50	40	Inferior Parietal Lobule	55	-65	-10	Middle Occipital Gyrus
40	-45	40	Inferior Parietal Lobule	60	-45	-20	Middle Temporal Gyrus
45	-70	40	Inferior Parietal Lobule	55	-55	-15	Middle Temporal Gyrus
45	-50	40	Inferior Parietal Lobule	60	-50	-15	Middle Temporal Gyrus
45	-45	40	Inferior Parietal Lobule	65	-40	-15	Middle Temporal Gyrus
50	-65	40	Inferior Parietal Lobule	-60	-35	0	Middle Temporal Gyrus
50	-60	40	Inferior Parietal Lobule	35	-65	25	Middle Temporal Gyrus
50	-35	40	Inferior Parietal Lobule	45	-75	25	Middle Temporal Gyrus
-45	-45	45	Inferior Parietal Lobule	35	-30	-25	Parahippocampal Gyrus
-35	-50	45	Inferior Parietal Lobule	55	-25	30	Postcentral Gyrus
35	-60	45	Inferior Parietal Lobule	40	-30	35	Postcentral Gyrus
35	-55	45	Inferior Parietal Lobule	-45	-30	40	Postcentral Gyrus
50	-30	40	Postcentral Gyrus	35	-70	45	Superior Parietal Lobule
-55	-30	45	Postcentral Gyrus	35	-65	45	Superior Parietal Lobule
55	-30	45	Postcentral Gyrus	40	-75	45	Superior Parietal Lobule
50	-35	50	Postcentral Gyrus	-30	-70	50	Superior Parietal Lobule

-20	-35	60	Postcentral Gyrus	-25	-70	50	Superior Parietal Lobule
40	-30	60	Postcentral Gyrus	30	-70	50	Superior Parietal Lobule
15	-40	65	Postcentral Gyrus	30	-65	50	Superior Parietal Lobule
-5	-45	25	Posterior Cingulate	30	-60	50	Superior Parietal Lobule
5	-40	25	Posterior Cingulate	35	-70	50	Superior Parietal Lobule
5	-35	25	Posterior Cingulate	35	-60	50	Superior Parietal Lobule
-45	0	30	Precentral Gyrus	35	-55	50	Superior Parietal Lobule
-40	0	30	Precentral Gyrus	40	-65	50	Superior Parietal Lobule
-30	-75	35	Precuneus	40	-60	50	Superior Parietal Lobule
-25	-80	35	Precuneus	45	-65	50	Superior Parietal Lobule
-25	-75	35	Precuneus	-30	-70	55	Superior Parietal Lobule
-25	-70	35	Precuneus	-25	-70	55	Superior Parietal Lobule
-20	-70	35	Precuneus	15	-75	55	Superior Parietal Lobule
30	-75	35	Precuneus	20	-75	55	Superior Parietal Lobule
40	-70	35	Precuneus	30	-70	55	Superior Parietal Lobule
45	-75	35	Precuneus	30	-65	55	Superior Parietal Lobule
-30	-80	40	Precuneus	30	-60	55	Superior Parietal Lobule
-30	-75	40	Precuneus	35	-65	55	Superior Parietal Lobule
-30	-65	40	Precuneus	35	-60	55	Superior Parietal Lobule
-25	-80	40	Precuneus	40	-60	55	Superior Parietal Lobule
-25	-75	40	Precuneus	30	-60	60	Superior Parietal Lobule
30	-75	40	Precuneus	45	-20	10	Superior Temporal Gyrus
35	-80	40	Precuneus	50	-35	15	Superior Temporal Gyrus
35	-70	40	Precuneus	40	-45	35	Supramarginal Gyrus
40	-75	40	Precuneus	45	-45	35	Supramarginal Gyrus
25	-80	45	Precuneus	-20	-5	-30	Uncus
-25	-75	50	Precuneus				
-20	-75	50	Precuneus				
-15	-75	50	Precuneus				
30	-55	50	Precuneus				
40	-5	-10	Sub-Gyral				
-20	30	50	Superior Frontal Gyrus				
-35	-65	45	Superior Parietal Lobule				
-30	-75	45	Superior Parietal Lobule				
-30	-65	45	Superior Parietal Lobule				
-25	-80	45	Superior Parietal Lobule				
-25	-75	45	Superior Parietal Lobule				
-25	-70	45	Superior Parietal Lobule				
25	-75	45	Superior Parietal Lobule				
30	-80	45	Superior Parietal Lobule				
30	-75	45	Superior Parietal Lobule				
30	-60	45	Superior Parietal Lobule				
35	-75	45	Superior Parietal Lobule				

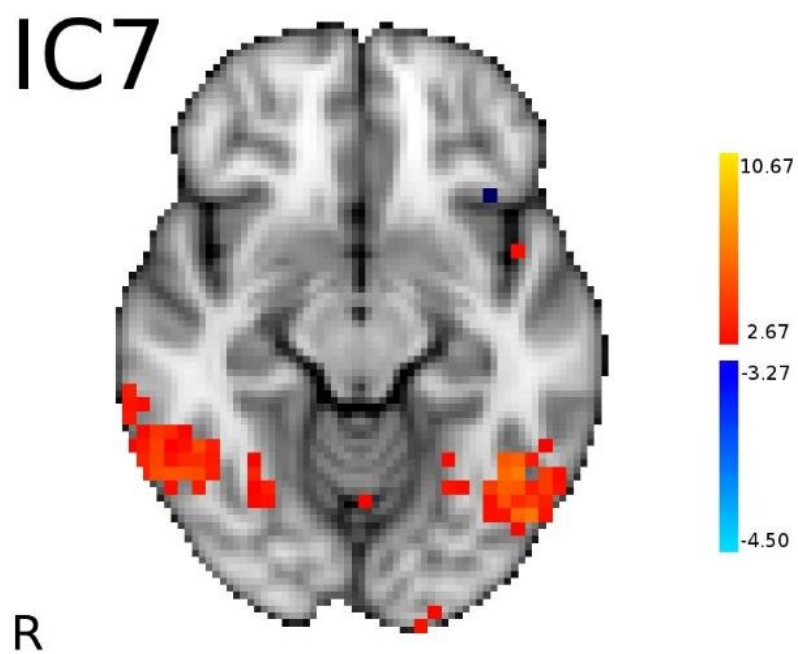


Figure 113 IC7 region retrieved from Marques dos Santos et al. (2014). Axial cut ($z = -12$)

*Appendix E – Hydrocel Geodesic Sensor
Net 128 Channel Map*

